

Centre for Geo-Information

Thesis Report GIRS-2009-12

---

***Computing Sky View Factors from geo-data using a GIS.***  
*MSc-Thesis*

Joseph Steenbergen

June 2009



WAGENINGEN UNIVERSITY  
WAGENINGEN **UR**



# Computing Sky View Factors from geo-data using a GIS

## *MSc Thesis*

J.J.M. Steenbergen

Registration number 81 07 03 798 060

### Supervisors:

Ir. H.J. Stuiver  
Dr. Ir. R.J.A. van Lammeren  
Ir. D. van Dijke

A thesis submitted in partial fulfilment of the degree of Master of Science  
at Wageningen University and Research Centre,  
The Netherlands.

June 4<sup>th</sup>, 2009  
Wageningen, The Netherlands

Thesis code number: GRS-80436  
Thesis Report: GIRS-2009-12  
Wageningen University and Research Centre  
Laboratory of Geo-Information Science and Remote Sensing

## **Preface**

During the summer of 2008 I was offered the possibility to do my thesis research at Meteo Consult. I had the opportunity to contribute to the project called “Preventieve Gladheidsbestrijding op basis van meteorologische, thermal-mapping en GPS data ter plekke” (Prevention of slippery roads based on local meteorological, thermal mapping and GPS data).

I embraced this project as for me this was a way to explore a till then unknown field of work, offering many possibilities of learning new skills. It also offered me the possibility to gain experience outside of the university.

I would like to thank John Stuiver (WUR) and Daniël van Dijke (Meteo Consult) for their excellent supervision, support and patience. I also would like to thank Marcel Wokke for his indispensable mathematical skills and the time and effort it took to validate my results.

Furthermore I would like to thank Ingeborg Zuurendonk for her help with regard to the RGI background of the project and the municipality of Ede (Gerard Westerbroek and Willy Groeneveld) for making geodata available for this research project.

Finally I would like to thank Ron van Lammeren for co-supervising this project and reviewing the concept of this report.

Joseph Steenbergen,

Heiloo, June 2009

## Samenvatting

Meteo Consult is één van de partners binnen het project “Preventieve Gladheidsbestrijding op basis van meteorologische, thermal-mapping en GPS data ter plekke”. Binnen dit project wordt er gezocht naar mogelijkheden om de gladheidspreventie op wegen effectiever te maken. Meteo Consult draagt hier onder andere aan bij door het aanleveren van (en verbeteren van de methode voor) een wegdektemperatuursvoorspelling.

Eén van de parameters in het model voor de wegdektemperatuursvoorspelling is de “Sky View Factor” (SVF). Deze parameter geeft een indicatie van de fractie van de hemelkoepel die zichtbaar is vanaf de locatie van de observator, ofwel de mate waarin het zicht op de hemel wordt beperkt door de omgeving (bomen, gebouwen etc.) voor een gegeven punt.

Tot nu toe werd de SVF bepaald door met een auto uitgerust met een camera en fish-eye lens foto's gericht op het zenit te maken. Op basis van het aantal zichtbare en onzichtbare 'hemel' pixels in deze foto's werd de SVF berekend. Deze methode is erg tijdrovend en daardoor duur. Meteo Consult ging daarom op zoek naar alternatieve methoden.

Geïnspireerd door de ontwikkelingen op GIS gebied, werd besloten de mogelijkheden van het gebruik van GIS en geodata te onderzoeken. Verkennend onderzoek wees uit dat de berekening van de SVF met behulp van een GIS en geodata mogelijk is, alhoewel er een aantal problemen overwonnen moesten worden.

Eén van de grootste problemen was het correct modelleren van bomen. Het merendeel van de loofbomen draagt tijdens de winter geen blad. In de GIS methode wordt het landschap gemodelleerd in een raster. Dit brengt de beperking met zich mee dat complexe 3D structuren zoals kale bomen niet gemodelleerd kunnen worden, het is slechts mogelijk één parameter (in dit geval de terreinhoogte) aan een locatie te koppelen.

Hiervoor is een oplossing gevonden. De twee belangrijkste objecten die het zicht op de hemel belemmeren zijn harde objecten zoals gebouwen en terrein features zoals heuvels, dijken, bergen etc. en zachte objecten zoals bomen e.d. Door de SVF op twee manieren te berekenen, gebaseerd op obstructie alleen door harde objecten enerzijds en door harde én zachte objecten anderzijds, kan bepaald worden welk deel van de obstructie veroorzaakt wordt door enkel bomen. Door hierop een correctiefactor toe te passen kan gecompenseerd worden voor de fractie van de hemelkoepel die zichtbaar is door een kale boom.

De toepassing van deze methode leverde veelbelovende resultaten op. De GIS methode kan echter voorlopig de fotografische methode nog niet vervangen. Hiervoor zijn twee oorzaken aan te wijzen, onvolledigheid van de bron-data en onvolkomenheden in de methode voor de compensatie voor het doorzicht door kale bomen.

De conclusie van dit onderzoek is dat het gebruik van GIS een zeer geschikte aanpak is voor het berekenen van de SVF, mits gebaseerd op nauwkeurige en volledige bron-data en een correct geparametriseerde correctiemethode voor het doorzicht door kale bomen. Gezien de huidige ontwikkelingen op GIS en geodata gebied wordt verwacht dat deze problemen in de toekomst opgelost zullen worden.

Het in 2012 te verschijnen AHN 2 zal een grote verbetering van de nauwkeurigheid van de input data betekenen. Verder wordt verwacht, gezien de ontwikkelingen in 3D GIS, dat op langere termijn de rasterdata vervangen kan worden door vectordata. Hierdoor zal de nauwkeurigheid waarmee de omgeving gemodelleerd kan worden toenemen, hetgeen de ontwikkeling van de GIS SVF methode verder ten goede zal komen.

## Summary

Meteo Consult is involved in a project called “Prevention of slippery roads based on local meteorological, thermal mapping and GPS data”. The aim of this project is to make road slipperiness prevention more effective. Meteo Consult contributes to this goal by providing (and improving the method for) a road surface temperature (RST) forecast.

One of the parameters of the RST forecasting model is the Sky View Factor (SVF). This parameter is a measure of the degree to which the sky is obscured by the surroundings (trees, buildings etc.) for a given point.

So far, the SVF was obtained by using a car equipped with a camera and a fisheye lens, to make a series of photographs pointed at the zenith. These photographs were individually checked for errors after which the SVF was computed based on the number of visible and invisible sky pixels in the photograph. This is a very time consuming and therefore expensive method. This caused Meteo Consult to search for alternative methods.

Inspired by the developments in the GIS sector, the decision was made to explore the possibilities of computing the SVF using a GIS based on geodata. Preliminary research pointed out that a GIS and geodata can indeed be used for the SVF computation, although several hurdles still had to be taken.

One of the major problems was the correct modeling of trees. In winter, deciduous trees generally do not carry leaves. Using the GIS method, the landscape is modeled using a raster dataset. This limits the amount of information that can be held within the dataset. Complex 3D structures such as trees could not be modeled. Only one parameter (in this case terrain height) could be modeled in this raster.

A solution for this problem was found. The two most important types of objects blocking the sky view are ‘hard objects’ such as buildings, hills, mountains etcetera and ‘soft objects’ like for instance trees. By computing the SVF in 2 ways, once based on only ‘hard objects’ and once based on both the hard and the ‘soft objects’, it is possible to determine which fraction of obscured sky is purely obstructed by soft objects. By applying a correction factor to this fraction, compensation for the fraction of sky which is visible through a bare tree is possible.

The application of this method yielded promising results. To the authors knowledge this is the first published method which successfully integrates trees in the GIS SVF computation. The GIS method is not yet ready to replace the photographic method. This is caused by two factors: inaccuracy of the source data and current limitations of the method which is used to compensate for the amount of sky which is visible through bare trees.

The conclusion of this research is that using a GIS and geodata is a suitable approach for computing the SVF, provided that the computations are based on accurate and comprehensive source data and that the compensation method for correcting the amount of sky visible through bare trees is parameterized correctly. Considering the developments in the GIS and geodata fields, both problems are expected to be solved in the future.

In 2012 the AHN 2 will be published. This dataset will offer an increase in source data resolution and accuracy. Given the developments in 3D GIS, in the long term raster data will be replaced with vector data. This will further increase the accuracy of the modeling of the environment, which in turn will benefit the development of the GIS SVF method.

## TABLE OF CONTENTS

PREFACE	I
SAMENVATTING	II
SUMMARY	III
<b>1 INTRODUCTION</b>	<b>1</b>
1.1 BACKGROUND	1
1.2 SKY VIEW FACTOR	2
1.3 SVF COMPUTATION	3
1.4 PROBLEM DEFINITION	6
1.5 RESEARCH OBJECTIVES	7
1.6 REPORT OUTLINE	8
<b>2 METHODOLOGY</b>	<b>9</b>
2.1 RESEARCH AREA	9
2.2 MATERIALS	11
2.2.1 DATASETS	11
2.2.2 SOFTWARE	12
2.3 METHODOLOGY	13
2.3.1 READING DIRECTIONS METHODOLOGY	13
2.3.2 METHODOLOGICAL APPROACH	15
2.3.3 GENERAL DATA PRE-PROCESSING	19
2.3.4 DATASET SPECIFIC PRE-PROCESSING NATIONAL DATASETS	21
2.3.5 IMPROVING THE TREE MODELLING	24
2.3.6 SVF COMPUTATION	26
2.3.7 VALIDATION OF THE RESULTS	29
2.3.8 METHODOLOGICAL DIFFERENCES BETWEEN PRELIMINARY RESEARCH AND THIS RESEARCH.	30
<b>3 RESULTS AND DISCUSSION</b>	<b>31</b>
3.1 USE OF GRASS	31
3.2 LOCAL AVAILABILITY OF SUITABLE DATASETS	31
3.3 COMPUTED SVF	34
3.3.1 SVF WITHOUT TREE FILTER	34
3.3.2 SVF WITH TREE FILTER	39
3.4 VALIDATION OF THE RESULTS	48
3.4.1 VALIDATION USING THE NETWORK MODEL	48
<b>4 CONCLUSION AND RECOMMENDATIONS</b>	<b>51</b>
4.1 CONCLUSION	51
4.2 RECOMMENDATIONS	52
4.2.1 IMPROVEMENT OF THE GIS SVF COMPUTATION	52
4.2.2 TEMPORAL ASPECTS	53
4.2.3 SCIENTIFIC RELEVANCE	53

<b>CITED REFERENCES</b>	<b>54</b>
-------------------------	-----------

---

<b>APPENDICES</b>	<b>56</b>
-------------------	-----------

---

<b>APPENDIX 1: MODEL GRAPHICS.</b>	<b>56</b>
<b>APPENDIX 2: (TDN-) CODE DESCRIPTIONS.</b>	<b>78</b>
<b>APPENDIX 3: EQUATIONS USED TO COMPENSATE FOR TREE TRANSPARENCY.</b>	<b>80</b>
<b>APPENDIX 4: TREE TRANSPARENCY CURVES</b>	<b>81</b>
<b>APPENDIX 5: SCATTERPLOTS GIS SVF AGAINST REFERENCE SVF</b>	<b>82</b>
<b>APPENDIX 6: SVF GRAPHS LINEAR FILTERS</b>	<b>85</b>
<b>APPENDIX 7: SCATTERPLOTS GIS-BASED RST FORECAST AGAINST REFERENCE SVF-BASED RST FORECAST.</b>	<b>87</b>
<b>APPENDIX 8: SCATTERPLOTS RST FORECAST AGAINST MEASURED RST.</b>	<b>88</b>
<b>APPENDIX 9: BUG SOLAR RADIATION GRAPHICS TOOL</b>	<b>89</b>

## OVERVIEW OF TABLES AND FIGURES

### Tables:

TABLE 1: MAXIMUM IMPROVEMENTS OF THE GIS SVF RESULTS CAUSED BY THE APPLICATION OF THE TREE FILTERS. THE RESULTS ARE BASED ON THE SCATTERPLOTS OF THE GIS SVF AGAINST THE REFERENCE SVF AS SHOWN IN TABLE 10, TABLE 11 AND TABLE 12.	43
TABLE 2: $R^2$ VALUES AND TREND LINE EQUATIONS OF THE SVF COMPUTED AT GROUND LEVEL (LEFT) AND $R^2$ VALUES AND TREND LINE EQUATIONS OF THE SVF COMPUTED AT 1.5 M ABOVE GROUND LEVEL (RIGHT). THE SVF COMPUTATIONS ARE BASED ON 2 DIFFERENT MAXIMUM TREE HEIGHTS (17 AND 20 METER [T17 AND T20]) AND 2 DIFFERENT TREE FILTERS (95 % AND 80 % TREE TRANSPARENCY IN THE INNER ANNULUS).	44
TABLE 3: 4 RANDOMLY SELECTED EXAMPLES OF SCATTERPLOTS OF THE SVF COMPUTED AT GROUND LEVEL AGAINST THE SVF COMPUTED AT 1.5 M ABOVE GROUND LEVEL. THE LEFT COLUMN CONTAINS RESULTS SVF RESULTS BASED ON A DEM CONTAINING TREES OF MAXIMUM 20 METER HIGH, THE LEFT COLUMN 17 METER. ). ERRONEOUS VALUES OF WHICH THE CAUSE OF THE ERROR COULD BE EXPLAINED WERE REMOVED FROM THE ANALYSIS (22-33 AND 123-130). $R^2$ VALUE AND EQUATION BASED ON A TREND LINE FORCED THROUGH (0,0).	45
TABLE 4: 4 RANDOMLY SELECTED EXAMPLES OF SCATTERPLOTS SHOWING THE SVF COMPUTED USING A DEM WITH TREES WITH A MAXIMUM HEIGHT OF APPROXIMATELY 17 METER AGAINST THE SVF COMPUTED USING A DEM WITH TREES WITH A MAXIMUM HEIGHT OF APPROXIMATELY 20 METER. IN THE LEFT COLUMN ARE 2 EXAMPLES OF THE SVF COMPUTED AT GROUND LEVEL. IN THE RIGHT COLUMN ARE 2 EXAMPLES OF THE SVF COMPUTED 1.5 METER ABOVE GROUND LEVEL. ERRONEOUS VALUES OF WHICH THE CAUSE OF THE ERROR COULD BE EXPLAINED WERE REMOVED FROM THE ANALYSIS (22-33 AND 123-130). $R^2$ VALUE AND EQUATION BASED ON A TREND LINE FORCED THROUGH (0,0).	46
TABLE 5: $R^2$ VALUES AND TREND LINE EQUATIONS OF THE GIS BASED RST FORECASTS AGAINST THE RST FORECASTS BASED ON THE REFERENCE SVF. ERRONEOUS VALUES OF WHICH THE CAUSE OF THE ERROR COULD BE EXPLAINED WERE EXCLUDED FROM THE ANALYSIS (22-33 AND 123-130). THE TREND LINE EQUATIONS ARE BASED ON TREND LINES FORCED THROUGH (0,0).	49
TABLE 6: EXPLANATION CAPITAL LETTERS IN TOOLBOX NAMES.	78
TABLE 7: TDN CODES USED TO SELECT RELEVANT INFORMATION FROM TOP10VECTOR DATASET.	78
TABLE 8: MEANING SELECTED TDN-CODES	79
TABLE 9: EQUATIONS USED IN THE GIS COMPUTATIONS TO COMPENSATE FOR TRANSPARENCY OF THE TREES (TREE FILTERS). THE ATTRIBUTE NAME COLUMN CONTAINS THE NAME OF THE ATTRIBUTE WHICH WAS USED TO STORE THE SVF COMPUTATION RESULT IN. [VALUE] = ANNULUS NUMBER, [EXTRA_SKY_BU] = FRACTION OF SKY VISIBLE, BASED ON DEM CONTAINING NO TREES, [PERC_SKY] = FRACTION OF VISIBLE SKY BASED ON FULL DEM, [TAN_PART] = RESULT OF PART OF SVF EQUATION WHICH CAN BE COMPUTED WITHOUT THE NEED FOR INPUT DATA (SEE PARAGRAPH GENERAL DATA PRE-PROCESSING). SVF_2 TILL SVF_5 ARE EXPONENTIAL DECREASE OF TREE TRANSPARENCY FROM INNER TO OUTER ANNULUS, SVF_6 TILL SVF_13 HAVE A LINEAR DECREASE OF TREE TRANSPARENCY FROM INNER TO OUTER ANNULUS.	80
TABLE 10: SCATTERPLOTS OF THE GIS SVF WITHOUT THE APPLICATION OF A TREE FILTER AGAINST THE REFERENCE SVF. THE MIDDLE COLUMN CONTAINS THE SVF BASED ON TREES WITH A MAXIMUM HEIGHT OF APPROXIMATELY 17 METER, THE RIGHT COLUMN CONTAINS THE SVF BASED ON TREES WITH A MAXIMUM HEIGHT OF APPROXIMATELY 20 METER. THE FIRST ROW CONTAINS THE SVF COMPUTED AT GROUND LEVEL, THE SECOND ROW THE SVF COMPUTED 1.5 METER ABOVE GROUND LEVEL.	82
TABLE 11: COMPARISON OF THE COMPUTED SVF BASED ON A MAXIMUM TREE HEIGHT OF APPROXIMATELY 17 METER, WITH THE REFERENCE SVF. THE GIS SVF IS SHOWN ON THE X-AXES, THE REFERENCE SVF ON THE Y-AXIS. THE GIS SVF WAS COMPUTED AT GROUND LEVEL (LEFT COLUMN) AND 1.5 METER ABOVE GROUND LEVEL (RIGHT COLUMN). ERRONEOUS VALUES OF WHICH THE CAUSE OF THE ERROR COULD BE EXPLAINED WERE REMOVED FROM THE ANALYSIS (22-33 AND 123-130), THE TREND LINE IS FORCED THROUGH (0,0).	83
TABLE 12: COMPARISON OF THE COMPUTED SVF BASED ON A MAXIMUM TREE HEIGHT OF APPROXIMATELY 20 METER, WITH THE REFERENCE SVF. THE GIS SVF IS SHOWN ON THE X-AXES, THE REFERENCE SVF ON THE Y-AXIS. THE GIS SVF WAS COMPUTED AT GROUND LEVEL (LEFT COLUMN) AND 1.5 METER ABOVE GROUND LEVEL (RIGHT COLUMN). ERRONEOUS VALUES OF WHICH THE CAUSE OF THE ERROR COULD BE EXPLAINED WERE REMOVED FROM THE ANALYSIS (22-33 AND 123-130), THE TREND LINE IS FORCED THROUGH (0,0).	84
TABLE 13: SCATTERPLOTS OF THE GIS-BASED RST FORECAST AGAINST THE REFERENCE SV- BASED TST FORECAST FOR MARCH 14 <sup>TH</sup> , 2007 01:00 UTC. ERRONEOUS VALUES OF WHICH THE CAUSE OF THE ERROR COULD BE EXPLAINED WERE EXCLUDED FROM THE ANALYSIS (22-33 AND 123-130). THE TREND LINE EQUATIONS ARE BASED ON TREND LINES FORCED THROUGH (0,0).	87
TABLE 14: FORECASTED RST BASED ON THE GIS SVF PLOTTED AGAINST THE ACTUAL RST MEASURED BETWEEN MARCH 13 <sup>TH</sup> 23:00 UTC AND MARCH 14 <sup>TH</sup> 02:00 UTC. ERRONEOUS VALUES OF WHICH THE CAUSE OF THE ERROR COULD BE EXPLAINED WERE EXCLUDED FROM THE ANALYSIS (22-33 AND 123-130). THE TREND LINE EQUATIONS ARE BASED ON TREND LINES FORCED THROUGH (0,0).	88



TABLE 15: FORECASTED RST BASED ON THE REFERENCE SVF PLOTTED AGAINST THE ACTUAL RST MEASURED BETWEEN MARCH 13 <sup>TH</sup> 23:00 UTC AND MARCH 14 <sup>TH</sup> 02:00 UTC. ERRONEOUS VALUES OF WHICH THE CAUSE OF THE ERROR COULD BE EXPLAINED WERE EXCLUDED FROM THE ANALYSIS (22-33 AND 123-130). THE TREND LINE EQUATIONS ARE BASED ON TREND LINES FORCED THROUGH (0,0). .....	88
---	----

## Figures:

FIGURE 1: PROJECTION ( $W_s$ ) OF A WALL ( $W$ ) ONTO A HEMISPHERE. SOURCE IMAGE: JOHNSON AND WATSON, 1984 .....	3
FIGURE 2: EXAMPLE FISH-EYE IMAGE. NOTE THE BUS IN THE LOWER LEFT CORNER. THIS IS AN EXAMPLE OF A POSSIBLE ERROR. SOURCE PICTURE: WOKKE (2008) .....	3
FIGURE 3: POSITION OF 10 SATELLITES IN THE HEMISPHERICAL FIELD OF VIEW FOR (A) HIGH SVF AND (B) LOW SVF. AT A HIGH SVF, DATA CAN BE FULLY RECEIVED FROM NINE SATELLITES, WHEREAS AT LOW SVF THIS IS REDUCED TO JUST THREE. PARTIALLY OBSCURED SATELLITES WILL HAVE A LOWER SNR (SIGNAL TO NOISE RATIO) AND THEREFORE BE LESS VALUABLE IN CALCULATING THE POSITIONAL SOLUTION. SOURCE: CHAPMAN ET AL, 2004. ....	4
FIGURE 4: LEFT: DEM WITH ARROWS REPRESENTING THE DIRECTION IN WHICH A VIEWSHED IS CALCULATED. CENTRE: RASTER REPRESENTATION OF THE VIEWSHED, WITH WHITE PIXELS REPRESENTING VISIBLE SKY, GREY PIXELS REPRESENTING OBSCURED SKY. RIGHT: FISHEYE PHOTOGRAPH OF THE VIEWSHED. (SOURCE IMAGE: (ESRI 2007)).....	5
FIGURE 5: DISTRIBUTION OF THE AMBIENT OPTIC ARRAY AND INVISIBLE PARTS IN VIEWSPHERE ANALYSIS. THE CROSS-HATCHED AREA REPRESENTS THE INVISIBLE VOLUME $V$ ( $V_c + V_d$ , HATCHED AREAS), PARTS A, B AND Q REPRESENTS THE VISIBLE VOLUME ( $V_b = V_i$ ). SOURCE: (YANG 2007) .....	5
FIGURE 6: TREE WITH LEAVES (LEFT) BLOCKING THE SKY VIEW (RED ARROW) AND LEAFLESS TREE (RIGHT) WHICH IS HARDLY BLOCKING THE SKY VIEW AT ALL. ....	7
FIGURE 7: THE RESEARCH AREA OF THE RGI PROJECT IS LOCATED IN THE GELDERSE VALLEY. THE RESEARCH PROJECT WHICH IS DESCRIBED IN THIS RESEARCH FOCUSES ON SEVERAL SMALL PARTS OF THIS AREA. THE RED LINE INDICATES THE ROUTE ALONG WHICH METEO CONSULT COMPUTED THE SVF BASED ON THE PHOTOGRAPHICAL METHOD. ....	9
FIGURE 8: (A) RASTER VERSION OF THE AREA OF INTEREST WITH THE OLIVE-GREEN POLYGONS INDICATING TREE PRESENCE, THE RED POLYGONS INDICATING THE BUILT-UP AREAS AND THE BLACK VERTICAL DOTTED LINE INDICATING THE SVF MEASURING LOCATIONS, (B) RASTER DEM WITHOUT TREES, (C) GOOGLE EARTH IMAGE (2005) SHOWING THE AREA OF INTEREST AND THE SVF MEASURING POINTS (YELLOW DRAWING PINS) .....	10
FIGURE 9: GENERAL OVERVIEW TOTAL GIS WORKFLOW. NATIONAL DATASET TRAJECTORY REPRESENTED BY BLACK ARROWS, LOCAL DATASET TRAJECTORY REPRESENTED BY RED ARROWS.....	14
FIGURE 10: OVERVIEW PROCEEDINGS WITHIN SVF GIS MODEL.....	14
FIGURE 11: FRAGMENT OF THE ORIGINAL DEM (AHN) SHOWING ROADS (OUTLINE INDICATED BY BLACK LINES) AND TERRAIN HEIGHT (GREEN = LOW AND RED = RASTER RESOLUTION 5 x 5 M. ....	15
FIGURE 12: FRAGMENT OF THE ORIGINAL DEM (AHN) SHOWING BUILDINGS (BLUE LINES). (GREEN = LOW AND RED = HIGH).....	16
FIGURE 13: EXAMPLE VIEWSHED, GREEN INDICATES VISIBLE SKY, RED INDICATES INVISIBLE SKY.....	17
FIGURE 14: EXAMPLE OF EXPONENTIAL TREE TRANSPARENCY DECREASE CURVES TOWARDS OUTER TEMPLATE ANNULUS (TOP) AND LINEAR TREE TRANSPARENCY CURVE (BOTTOM).....	18
FIGURE 15: ANNULAR TEMPLATE CONTAINING 50 RINGS (LEFT) AND RASTER VERSION OF THE SAME TEMPLATE (RIGHT) WITH THE COLOUR INDICATING THE RING NUMBER (GREEN INDICATING 1 AND RED INDICATING 50) .....	20
FIGURE 16: ORIGINAL ROAD SURFACE (BETWEEN DARK LINES) (LEFT) AND SMOOTHENED ROAD SURFACE (RIGHT) .....	23
FIGURE 17: EXAMPLE OF COARSE REPRESENTATION OF BUILDING OUTLINES IN DEM (RED, YELLOW, ORANGE AND GREEN BLOCKS ARE HOUSES IN THE DEM, THE BLUE LINE IS THE CORRECT OUTLINE FROM THE BUILDING MASK (P).....	23
FIGURE 18: EXAMPLE OF POSSIBLY INCORRECT BUILT-UP CELL HEIGHT.....	23
FIGURE 19: EFFECT OF THE SVF ON THE FORECASTED RST ON DECEMBER 9 <sup>TH</sup> AND 10 <sup>TH</sup> 2007. THE SPEED AT WHICH THE ROAD SURFACE COOLS DOWN DURING THE NIGHT IS RELATED TO THE SVF. AS CAN BE OBSERVED FROM THE GRAPH, IF THE SVF IS LOWER, THE RST WILL BE HIGHER. SOURCE OF THE GRAPH: (DIJKE 2009). HOUR 1 IS 00:00 IN THE MORNING OF DECEMBER 9 <sup>TH</sup> . ....	33
FIGURE 20: SVF AS COMPUTED USING ONLY EQUATION (1) WITHOUT THE APPLICATION OF ANY KIND OF TREE LIGHT PENETRATION COMPENSATION METHOD. THE RED LINE INDICATES THE SVF COMPUTED BASED ON A MAXIMUM TREE HEIGHT OF APPROXIMATELY 20 METER (T20). THE BLUE LINE INDICATES THE GIS SVF BASED ON A MAXIMUM TREE HEIGHT OF APPROXIMATELY 17 METER (T17).....	34
FIGURE 21: AERIAL PHOTOGRAPH VIADUCT EDESEWEG / A12. (ORIENTATION EQUAL TO BACKGROUND IN FIGURE 20, NORTH TO THE RIGHT, WEST TO THE TOP). SOURCE IMAGE: GOOGLE EARTH (2005).....	35
FIGURE 22: COMPUTED AND REFERENCE SVF AT SAMPLING POINTS 124 – 130. IN THE BACKGROUND THE RASTER DEM OF THE SURROUNDINGS OF SVF ORANGE SQUARES REPRESENT TREES, GREEN BACKGROUND THE TERRAIN. THE BLUE DOTS ARE THE SVF	

SAMPLING LOCATIONS. IN THE PICTURE IT IS DIFFICULT TO SEE, BUT POINT 124 IS LOCATED JUST NEXT TO THE TREE (AS IS POINT 128) WHEREAS IS LOCATED ON TOP OF THE TREE. THE ORIENTATION OF THIS GRAPH CORRESPONDS WITH THE ORIENTATION IN FIGURE 20, NORTH TO THE RIGHT, WEST TO THE TOP. (GL MEANS GROUND LEVEL, TXX MEANS MAXIMUM TREE HEIGHT APP. XX METER) .....	36
FIGURE 23: VIEWSHEDS OF POINT 123 (LEFT TO POINT 129 (RIGHT)). THE ORIENTATION OF THE VIEWSHEDS CORRESPONDS TO THE RASTER MAP ORIENTATION IN FIGURE 22 (NORTH TO THE RIGHT AND WEST TO THE TOP). BLACK AREAS INDICATE NO-DATA, DARK-GREY AREAS INDICATE INVISIBLE SKY AND LIGHT-GREY AREAS INDICATE VISIBLE SKY. <b>NOTE THAT THE THIRD IMAGE FROM THE LEFT (POINT 125) IS ALMOST ENTIRELY LIGHT-GREY.</b> IMAGES ARE BASED ON THE MAXIMUM TREE HEIGHT OF 20 M. ....	36
FIGURE 24: DETAIL OF THE ROAD AND BUILT-UP AREA MASKS CREATED BASED ON TOP10VECTOR DATA (GREY AND RED POLYGONS) AND AN OVERLAY OF THE CORRESPONDING GBKN DATA (BLACK LINES) .....	36
FIGURE 25: OVERVIEW OF THE BUILT-UP AREAS AT POINT 1 -24 (LEFT) AND POINT 163 – 176 (RIGHT). TREES IN THE TOP10VECTOR DATASET ARE REPRESENTED BY THE BRIGHT LIGHT GREEN POLYGONS. APART FROM THE TREE AREAS IN THE TOP10VECTOR DATASET, OTHER TREES ARE CLEARLY VISIBLE IN BOTH AREAS. THE ORIENTATION IN THESE PICTURES IS EQUAL TO ORIENTATION OF THE BACKGROUND IN FIGURE 20, NORTH TO THE RIGHT, WEST TO THE TOP). SOURCE IMAGE GOOGLE EARTH (2005) .....	37
FIGURE 26: CLOSE-UP OF THE RASTER DEM OF THE SURROUNDINGS OF SVF SAMPLING POINTS 30 - 50. ORANGE SQUARES REPRESENT TREES, GREEN BACKGROUND THE TERRAIN. THE BLUE DOTS ARE THE SVF SAMPLING LOCATIONS. ORIENTATION OF THE BACKGROUND IMAGE: NORTH TO THE RIGHT AND WEST TO THE TOP. (GL MEANS GROUND LEVEL, TXX MEANS MAXIMUM TREE HEIGHT APP. XX METER) .....	37
FIGURE 27: AERIAL PHOTOGRAPH OF THE AREA SURROUNDING SVF MEASURING LOCATION 30 - 50. ORIENTATION CORRESPONDS TO RASTER MAP ORIENTATION IN FIGURE 26 (NORTH TO THE RIGHT AND WEST TO THE TOP). SOURCE IMAGE: GOOGLE EARTH (2005) .....	38
FIGURE 28: VIEWSHEDS 40 -44 (UPPER ROW, LEFT TO RIGHT) AND VIEWSHEDS 45 – 49 (LOWER ROW, LEFT TO RIGHT). BLACK AREAS INDICATE NO-DATA, DARK-GREY AREAS INDICATE INVISIBLE SKY AND LIGHT-GREY AREAS INDICATE VISIBLE SKY. ORIENTATION CORRESPONDS TO RASTER MAP ORIENTATION IN FIGURE 26 (NORTH TO THE RIGHT AND WEST TO THE TOP). IMAGES ARE BASED ON THE MAXIMUM TREE HEIGHT OF 20 M. ....	38
FIGURE 29: SVF COMPUTED AT GROUND LEVEL (GL) USING AN EXPONENTIAL TREE FILTER IN WHICH TREE TRANSPARENCY RANGES FROM 90% - 60 % IN THE INNER ANNULUS AND APPROXIMATELY 0% IN THE OUTER ANNULUS (SEE APPENDIX 4). (TXX MEANS MAXIMUM TREE HEIGHT APP. XX METER).....	39
FIGURE 30: SVF COMPUTED 1.5 M ABOVE GROUND LEVEL (GL) USING AN EXPONENTIAL TREE FILTER IN WHICH TREE TRANSPARENCY RANGES FROM 90% - 60 % IN THE INNER ANNULUS AND APPROXIMATELY 0% IN THE OUTER ANNULUS (SEE APPENDIX 4). (TXX MEANS MAXIMUM TREE HEIGHT APP. XX METER) .....	40
FIGURE 31: SCHEMATIC REPRESENTATION OF A 12 METER TREE 10 METER AWAY FROM THE SAMPLING LOCATION.....	40
FIGURE 32: SVF COMPUTED AT 1.5 METER ABOVE GROUND LEVEL (GL), USING A LINEAR TREE FILTER (WITH A LINEAR DECREASE IN TREE TRANSPARENCY FROM 95 % IN THE INNER ANNULUS TO 10 % - 50% IN THE OUTER ANNULUS). THE SVF IS BASED ON A DEM CONTAINING TREES WITH A MAXIMUM HEIGHT OF APPROXIMATELY 17 METER (t17) AND A DEM CONTAINING TREES WITH A MAXIMUM HEIGHT OF APPROXIMATELY 20 METER (t20). THE SVF FULL DEM GRAPHS SHOW THE SVF COMPUTED WITHOUT TREE FILTER.....	41
FIGURE 33: SVF COMPUTED AT 1.5 METER ABOVE GROUND LEVEL (GL), USING A LINEAR TREE FILTER (WITH A LINEAR DECREASE IN TREE TRANSPARENCY FROM 80 % IN THE INNER ANNULUS TO 10 % - 50% IN THE OUTER ANNULUS). THE SVF IS BASED ON A DEM CONTAINING TREES WITH A MAXIMUM HEIGHT OF APPROXIMATELY 17 METER (t17) AND A DEM CONTAINING TREES WITH A MAXIMUM HEIGHT OF APPROXIMATELY 20 METER (t20). THE SVF FULL DEM GRAPHS SHOW THE SVF COMPUTED WITHOUT TREE FILTER.....	41
FIGURE 34: SVF COMPUTED AT GROUND LEVEL (GL), USING A LINEAR TREE FILTER (WITH A LINEAR DECREASE IN TREE TRANSPARENCY FROM 95 % IN THE INNER ANNULUS TO 10 % - 50% IN THE OUTER ANNULUS). THE SVF IS BASED ON A DEM CONTAINING TREES WITH A MAXIMUM HEIGHT OF APPROXIMATELY 17 METER (t17) AND A DEM CONTAINING TREES WITH A MAXIMUM HEIGHT OF APPROXIMATELY 20 METER (t20). THE SVF FULL DEM GRAPHS SHOW THE SVF COMPUTED WITHOUT TREE FILTER. ....	42
FIGURE 35: SVF COMPUTED AT GROUND LEVEL (GL), USING A LINEAR TREE FILTER (WITH A LINEAR DECREASE IN TREE TRANSPARENCY FROM 80 % IN THE INNER ANNULUS TO 10 % - 50% IN THE OUTER ANNULUS). THE SVF IS BASED ON A DEM CONTAINING TREES WITH A MAXIMUM HEIGHT OF APPROXIMATELY 17 METER (t17) AND A DEM CONTAINING TREES WITH A MAXIMUM HEIGHT OF APPROXIMATELY 20 METER (t20). THE SVF FULL DEM GRAPHS SHOW THE SVF COMPUTED WITHOUT TREE FILTER. ....	42
FIGURE 36: SVF COMPUTED WITH THE SOURCE DEM (AHN 2000 5 x 5) WHICH (THEORETICALLY) DOES NOT CONTAIN TREE HEIGHTS. ....	47
FIGURE 37: FORECASTED RST BASED ON GIS SVF AND VIEWSHEDS COMPUTED WITH THE TREE FILTERS WITH 95 % TREE TRANSPARENCY IN THE INNER ANNULUS (GREY LINES) AND REFERENCE SVF (DOTTED LINE). THE RED LINE INDICATES THE	

MEASURED ACTUAL RST. ERRONEOUS VALUES OF WHICH THE CAUSE OF THE ERROR COULD BE EXPLAINED WERE REMOVED FROM THE ANALYSIS (22-33 AND 123-130).....	48
FIGURE 38: FORECASTED RST BASED ON GIS SVF AND VIEWSHEDS COMPUTED WITH THE TREE FILTERS WITH 80 % TREE TRANSPARENCY IN THE INNER ANNULUS (GREY LINES) AND REFERENCE SVF (DOTTED LINE). THE RED LINE INDICATES THE MEASURED ACTUAL RST. ERRONEOUS VALUES OF WHICH THE CAUSE OF THE ERROR COULD BE EXPLAINED WERE REMOVED FROM THE ANALYSIS (22-33 AND 123-130).....	48
FIGURE 39: EXPONENTIAL TREE FILTERS WITH PERCENTAGE OF VISIBLE SKY RANGING FROM 60 % - 90 % IN THE INNER ANNULUS AND 0 % IN THE OUTER ANNULUS. ....	81
FIGURE 40: LINEAR TREE FILTER WITH A PERCENTAGE OF 95 % OF THE SKY VISIBLE THROUGH TREES IN THE INNER ANNULUS AND RANGING FROM 10 % - 80 % IN THE OUTER ANNULUS. ....	81
FIGURE 41: LINEAR TREE FILTER WITH A PERCENTAGE OF 80 % OF THE SKY VISIBLE THROUGH TREES IN THE INNER ANNULUS AND RANGING FROM 10 % - 70 % IN THE OUTER ANNULUS. ....	81
FIGURE 42: GIS SVF COMPUTED USING THE TREE FILTERS WITH A LINEAR DECREASE IN TREE TRANSPARENCY FROM 95 % IN THE INNER ANNULUS TO 10 % - 80 % IN THE OUTER ANNULUS). ALSO, A TREE FILTER WITH A 90 % TREE TRANSPARENCY OVERALL IS INCLUDED IN THIS GRAPH. THE SVF WAS COMPUTED AT 2 LEVELS, GROUND LEVEL (GL) AND 1.5 METER ABOVE GROUND LEVEL. THE MAXIMUM TREE HEIGHT IN THE DEM USED FOR THESE COMPUTATIONS WAS APPROXIMATELY 20 METER (T20). ....	85
FIGURE 43: GIS SVF COMPUTED USING THE TREE FILTERS WITH A LINEAR DECREASE IN TREE TRANSPARENCY FROM 80 % IN THE INNER ANNULUS TO 10 % - 70 % IN THE OUTER ANNULUS). THE SVF WAS COMPUTED AT 2 LEVELS, GROUND LEVEL (GL) AND 1.5 METER ABOVE GROUND LEVEL. THE MAXIMUM TREE HEIGHT IN THE DEM USED FOR THESE COMPUTATIONS WAS APPROXIMATELY 20 METER (T20).....	85
FIGURE 44: GIS SVF COMPUTED USING THE TREE FILTERS WITH A LINEAR DECREASE IN TREE TRANSPARENCY FROM 95 % IN THE INNER ANNULUS TO 10 % - 80 % IN THE OUTER ANNULUS). ALSO, A TREE FILTER WITH A 90 % TREE TRANSPARENCY OVERALL IS INCLUDED IN THIS GRAPH. THE SVF WAS COMPUTED AT 2 LEVELS, GROUND LEVEL (GL) AND 1.5 METER ABOVE GROUND LEVEL. THE MAXIMUM TREE HEIGHT IN THE DEM USED FOR THESE COMPUTATIONS WAS APPROXIMATELY 17 METER (T17). ....	86
FIGURE 45: GIS SVF COMPUTED USING THE TREE FILTERS WITH A LINEAR DECREASE IN TREE TRANSPARENCY FROM 80 % IN THE INNER ANNULUS TO 10 % - 70 % IN THE OUTER ANNULUS). THE SVF WAS COMPUTED AT 2 LEVELS, GROUND LEVEL (GL) AND 1.5 METER ABOVE GROUND LEVEL. THE MAXIMUM TREE HEIGHT IN THE DEM USED FOR THESE COMPUTATIONS WAS APPROXIMATELY 17 METER (T17).....	86
FIGURE 46: EXAMPLES OF DEM GEOMETRY COMPLEXITY. SIMPLE GEOMETRY (A), MODERATELY COMPLEX GEOMETRY (B), COMPLEX GEOMETRY (C) AND VERY COMPLEX GEOMETRY (D). THE COLOUR GREEN INDICATES LOW TERRAIN HEIGHT AND THE COLOUR RED HIGH TERRAIN HEIGHTS. IN RASTER C AND D, THREE HEIGHT (RED DOTS) WAS EXAGGERATED FOR THE PURPOSE OF DEMONSTRATING THE LIMITATIONS OF THE SOLAR RADIATION TOOL, TREE HEIGHT HERE IS APPROXIMATELY 500 METER. THESE IMAGES WERE CREATED BASED ON THE EXACT LOCATIONS THAT WERE USED TO CREATED THE VIEWSHEDS IN FIGURE 48. ....	89
FIGURE 47: VIEWSHED 89, SHOWING A LARGE PART OF INVISIBLE SKY WITHIN THE VISIBLE SKY AREA.....	89
FIGURE 48: EXAMPLE OF VIEWSHEDS CREATED BASED ON DEM'S WITH DIFFERENT COMPLEXITY (SEE FIGURE 46) AND DIFFERENT NUMBER OF COMPUTATION DIRECTIONS. THE CIRCULAR AREA IS THE ACTUAL VIEWSHED. BLACK COLOUR INDICATES NODATA, BLUE COLOUR IS VISIBLE PART OF THE SKY AND GREEN COLOUR IS THE INVISIBLE PART OF THE SKY.....	90

# 1 Introduction

## 1.1 Background

During the spring of 2006, a new RGI (Ruimte voor Geo Informatie) project called “Preventieve Gladheidsbestrijding op basis van meteorologische, thermal-mapping en GPS data ter plekke” (Prevention of slippery roads based on local meteorological, thermal mapping and GPS data) was initiated. The aim of the project is to make the prevention of slippery roads more effective (RGI; Wokke et al. 2007).

Several organizations are involved in the project. Meteo Consult is the project leader; the NMPO (Noë Milieu Project Ontwikkeling) and NIDO (a company which provides professional road slipperiness prevention and road cleaning services) are important project partners. Nieuwland Automatisering is also involved in the project, as well as the road network managers Province of Gelderland and Rijkswaterstaat. The latter two organizations are involved in the project as potential customers.

Meteo Consult is responsible for creating a road surface temperature (RST) forecast. Based on this forecast, the NMPO computes the optimal salt distribution route. The NIDO implements the route in the actual distribution of the salt. Nieuwland Automatisering has an advising role on GIS topics and designed the website <http://rgi.meteoconsult.nl/>.

Road slipperiness is usually countered by distributing salt (or other abrasives). The decision whether or not to distribute salt is based on a road surface temperature forecast. These forecasts are created for the locations of the RWIS (Road Weather Information System) stations. In the research area (see paragraph 2.1), eight RWIS stations are present. The stations are predominantly located at the coldest sites in the road network. In order to create a forecast for the whole road network, the forecasts are extrapolated to the surrounding roads.

If a critical temperature is predicted for one of the RWIS (Road Weather Information System) stations, salt is distributed on the road network surrounding the RWIS station, regardless of possible temperature differences between different road sections.

Because RST at the same time can vary within meter, it can be possible that on one section of a road the RST is below 0 °C and on the next road section above 0 °C. The amount of salt which is distributed could be decreased if road network managers know where exactly RST will become critical and where not. Therefore, a RST prediction model with a high spatial resolution is desired.

There are several advantages to reducing the amount of salt which is distributed.

If less salt is distributed:

- road network managers can reduce the amount of salt which has to be purchased thus reducing the cost of road slipperiness prevention;
- the amount of salt which enters into the environment will be smaller (think of e.g. the soil, aquifers and water ecosystems);
- the potential corrosion damage to roads and vehicles could be decreased;
- labour cost could potentially be decreased.

In order to create the RST forecast, Meteo Consult currently uses a numerical model called “Network Model” (Wokke 2008). This model is used to create a forecast of the RST for the full road network (a so called network forecast). Using numerical models is a common method for predicting RST, several of them are in operational use across the world (e.g. (Rayer 1987; Sass 1997; Best 1998; Chapman 2001; Crevier 2001; Thornes 2005; Chapman et al. 2006; Fry et al. 2007)).

The model is based on several input parameter, among which the so called Sky View Factor (SVF). The SVF is the subject of this research.

## **1.2 Sky View Factor**

SVF is a dimensionless parameter with a value between 0 and 1. Scientific literature provides several definitions for SVF ( $\psi_s$ ), a selection of them is listed below:

- Watson and Johnson (1987) express SVF as the ratio of solar radiation received by a planar surface compared with that received from the entire hemispheric radiating environment;
- Oke (1987) defines SVF as “the ratio of the amount of the sky ‘seen’ from a given point on a surface to that potentially available (i.e. the proportion of the sky hemisphere subtended by a horizontal surface).

More recent definitions of SVF are:

- a measure of the degree to which the sky is obscured by the surroundings for a given point (Grimmond 2001);
- a geometric ratio that expresses the fraction of the visible sky at the observers location (Li, Putra et al. 2004);
- a measure of the degree of site sky visibility (Chapman et al. 2006).

Within the context of this research project, Grimmond’s definition is the most suitable to explain the term “Sky view factor” and is used as a working definition.

Several recent studies have pointed out that SVF is a main factor of influence on RST (Chapman 2001; Chapman 2001; Bradley 2002; Lindberg et al. 2003; Chapman 2004; Thornes 2005; Brown et al. 2008), but only at low wind speeds and when the sky is clear (Dijke 2008) (both factors are included in the Network model).

The SVF is used in the Network Model in order to take into account the radiation balance of the road during the night. At night, objects such as road surfaces emit long wave radiation and therefore cool down. If in the direct surroundings of the road objects (such as buildings or trees) are present which also emit long wave radiation, some of this radiation will be absorbed by the road.

This slows down the cooling process of the road surface during the night, resulting in higher RST in road segments which are surrounded by for example buildings and trees as compared to road segments in open areas. This is because open areas only receive long wave radiation from the sky, which is generally colder than radiation which is emitted by objects such as buildings and trees (Gustavsson 1995).

An important aspect of long wave radiation exchange of objects in the environment is the degree to which the sky is obscured by the surrounding objects (buildings / trees etc). This is expressed using the Sky View Factor (Johnson et al. 1984).

### 1.3 SVF computation

The SVF can be obtained in different ways. Over the past decades, several methods have been developed and some are still being developed.

The oldest method of obtaining the SVF is the analytical method. If all angles from the planar surface to the tops and sides of the surrounding objects (e.g. buildings, trees) are known (see Figure 1), SVF can be calculated directly. Depending on the geometry and the location of the objects, different equations are used to calculate the fraction of the sky which is obscured by the objects. Johnson, Watson and Oke used this method for their respective researches (Johnson and Watson 1984; Oke 1987).

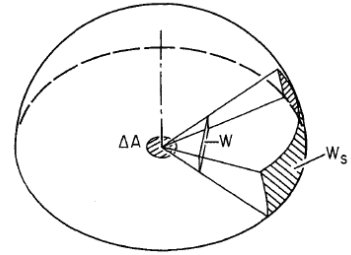


Figure 1: Projection ( $W_s$ ) of a wall ( $W$ ) onto a hemisphere. Source image: Johnson and Watson, 1984

During the eighties, a new method was developed by D.G. Steyn (Steyn et al. 1986; Blennow 1995). This method is used to calculate SVF from fisheye images (from now on, this method will be referred to as the 'photographical method').

Using a fisheye lens which is pointed at the zenith, photographs showing the full horizon (360°) are made (see Figure 2). One could say that this way, a viewshed (everything which is visible from a particular vantage point), pointing at the zenith, is created.

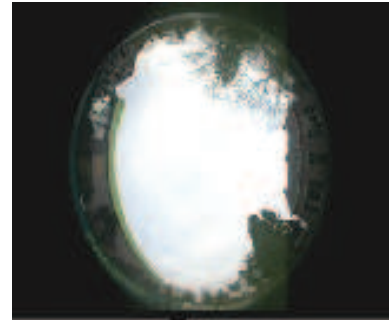


Figure 2: example fish-eye image. Note the bus in the lower left corner. This is an example of a possible error. Source picture: Wokke (2008)

Based on the histogram of each individual photograph, a threshold value is set in order to delineate sky pixels from non sky pixels. Next, an annular template is used to divide the image into a series of concentric annuli (rings), from which per annulus the percentage of sky pixels to non-sky pixels is calculated.

After this, equation (1) is applied to calculate to calculate SVF (Chapman 2004).

$$(1) \quad \psi_s = \frac{1}{4n} \sum_{i=1}^n \left[ \sin \frac{\pi(2i-1)}{2n} \right] \left( \frac{P_i}{t_i} 2\pi \right)$$

Where  $P_i$  equals the number of sky pixels found in the  $i^{\text{th}}$  template annulus (ring) and  $t_i$  is the total number of pixels in the  $i^{\text{th}}$  annulus. The total number of annuli is represented by  $n$ .

Another equation (derived from equation (1)) to compute SVF from a viewshed (this equation was derived by Wokke (2008) and used in the preliminary research (Giffen et al. 2008)):

$$(2) \quad \psi_s = 2 \sum_{i=1}^n \cos \left( \frac{\pi(i-0.5)}{2n} \right) \left[ \cos \left( \frac{\pi(i-1)}{2n} \right) - \cos \left( \frac{\pi i}{2n} \right) \right] \frac{P_i}{t_i}$$



Where  $i$  equals the number of the specific annulus,  $n$  is the total number of annuli,  $P_i$  equals the number of sky pixels found in the  $i^{\text{th}}$  template annulus and  $t_i$  is the total number of pixels in the  $i^{\text{th}}$  annulus.

Blennow (1995), Grimmond (2001) and Chapman (2004) use this method (equation 1) in their respective researches. The results of this method are widely used and accepted by the scientific community (Blennow 1995).

Another method, which is currently being developed, is the GPS method. It makes use of a handheld GPS receiver (Chapman 2002; Chapman 2004). When objects are obstructing the sky-view, fewer satellites are within the 'view' of the GPS device (see Figure 3). The signal strength (measured by the Satellite Status Index, SSI) is therefore lower.

From the empirically obtained relation between the SSI and measured sky-view, SVF can be derived. Promising results are already achieved in urban areas. The technology is less well suited for rural areas, because of the (potentially) frequent occurrence of trees. Trees are semi permeable for satellite signals (and thus could give a distorted SSI, whereas buildings are impermeable for satellite signals).

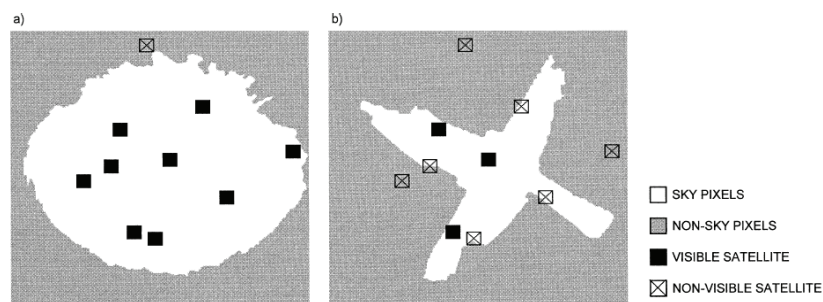


Figure 3: Position of 10 satellites in the hemispherical field of view for (a) high SVF and (b) low SVF. At a high SVF, data can be fully received from nine satellites, whereas at low SVF this is reduced to just three. Partially obscured satellites will have a lower SNR (Signal to Noise Ratio) and therefore be less valuable in calculating the positional solution. Source: Chapman et al, 2004.

Given the rapid developments in the GIS world, it was inevitable that at a given moment GIS was going to be used in the SVF computation. Souza et al. (2003) developed a 3D GIS extension for SVF assessment in urban canyons, to be used with ArcView GIS<sup>1</sup>. It computes sky view factors based on viewers location and polygons delimiting urban objects (buildings), including their height. The principals are basically the same as the photographic method, only the fisheye image is replaced with an image which is created using a GIS.

ArcGIS (ESRI 2006) provides a tool (Solar Radiation Graphics) which can be used to compute a raster representation of the fisheye image, showing the visible (white) and invisible (grey) sky pixels, see Figure 4. The computation is based on a raster digital elevation model (DEM) and the locations at which SVF needs to be computed.

The tool requires a number of directions in which the maximum angle of sky obstruction, or horizon angle has to be determined. For all unsearched directions, horizon angles are interpolated (so the more directions, the more precise the result will be), thus creating the full viewshed.

Horizon angles are then converted into a hemispherical coordinate system, thus representing a three-dimensional hemisphere of directions as a two-dimensional raster image. Each raster

<sup>1</sup> ESRI

cell of the viewshed is assigned a value that corresponds to whether the sky direction is visible or obstructed (see Figure 4, centre).

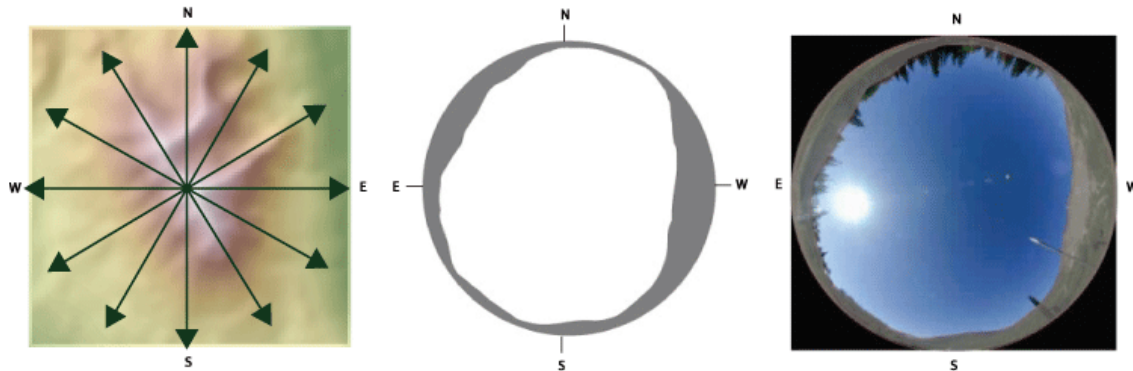


Figure 4: Left: DEM with arrows representing the direction in which a viewshed is calculated. Centre: raster representation of the viewshed, with white pixels representing visible sky, grey pixels representing obscured sky. Right: fisheye photograph of the viewshed. (Source image: (ESRI 2007))

Outputs from the Solar Radiation Graphics tool are raster representations and are not maps that correspond to the outputs from the area or point solar radiation analysis. Rather, they are representations of directions in a hemisphere of directions looking upward from a given location. In a hemispherical projection, the centre is the zenith, the edge of the circular "map" is the horizon, and the angle relative to the zenith is proportionate to the radius. (source: ESRI 2007).

Important to notice is that the top of the GIS viewshed is pointing to the north and the left side to the east, not the west (see Figure 4). This is not relevant to the SVF computation, but it is to other applications of the viewshed (the viewsheds are also used in the Network model in order to determine the so-called sun-view [the amount of direct sun light a stretch of road receives per day]).

After the computation of the viewshed, the original photographic method can be applied (application of the annular template and calculation of SVF).

Another way to compute the SVF is using a GIS to do a viewsphere visibility analysis (Yang 2007). This method is also still being developed. A viewsphere is basically the same as a viewshed, but a viewshed is a 2D image, whereas a viewsphere is a 3D sphere. The viewsphere can also be used to compute SVF. The required input data are a TIN (Triangulated Irregular Network) or raster containing elevation values and a set of observation points.

The computations involve calculating a  $V_{ij}$  value (the volume of sight, which can be defined as the 3D volumetric property of the 3D segment  $S_{ij}$ ) for each of the 360 viewing directions.

The  $V_{ij}$  value resembles the sky-view of a segment. For the equation for calculating  $V_{ij}$ , (see equation 3 and Figure 5), with  $\alpha_n$  representing the azimuthal angle between each segment,  $r_j$  the radial length of the segment  $z_j$  the vertical height of the segment and  $\beta_{ij}$  the elevation angle.

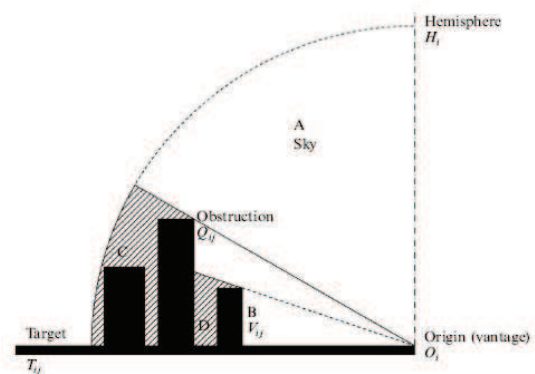


Figure 5: distribution of the ambient optic array and invisible parts in viewsphere analysis. The cross-hatched area represents the invisible volume  $V$  ( $V_C + V_D$ , hatched areas), parts A, B and Q represents the visible volume ( $V_B = V_i$ ). Source: (Yang 2007)



$$(3) \quad V_{ij} = \frac{2}{3} \times \frac{\alpha_n}{2\pi} \pi r_{ij}^2 z_j = \frac{1}{3} \alpha_n r_{ij}^3 \tan \beta_{ij}$$

Based on  $V_i$  ( $\sum V_{ij}$ ) divided by the total area of sky volume ( $H_{ij}$ ) (see equation 4)  $I$  (the viewsphere index) can be calculated (see equation 5). After this, the SVF ( $F$ ) can be computed using equation 6.

$$(4) \quad H_{ij} = \frac{2}{3} \pi r_{ij}^3$$

$$(5) \quad I = \frac{V_B}{V_A + V_B + V_C + V_D} = \frac{V_i}{\text{volume}(H_{ij})}$$

$$(6) \quad F \text{ (SVF)} = \frac{V_A}{V_A + V_B}$$

All methods described above are based on the same principles, they all are quite similar. One could say that the only difference between these methods is that they basically use different kinds of input data (geometric data, photograph, gps signal and viewshed or 3D model of the environment).

## 1.4 Problem definition

In order to obtain the SVF, Meteo Consult currently uses the photographic method. Although the results of the photographic method are adequate, the application of this method is very time consuming and accordingly expensive:

- photographs have to be made in situ, e.g. with a camera mounted on a car, driving very slowly past all points of interest (in this case one photograph every 5 or 10 m along the complete route of interest)
- all photographs have to be checked for errors manually (for an example of a common error see Figure 2);
- the photographs can only be taken under homogenous cloudy conditions (in order to counter effect overexposure / back lighting);
- ideally, the threshold for delineating sky pixels from non sky pixels has to be set manually.

Because of the drawbacks mentioned above, Meteo Consult was looking for alternative methods. Due to the developments in the field of geo-information, we currently live in a geo-data rich environment. Relevant geo-data such as landuse, Digital Elevation models (DEM) etcetera, are available at local governments (the potential clients). Also, many (open-source) GIS software products are being developed nowadays.

Inspired by these facts, Meteo Consult started exploring the possibilities of replacing the fisheye image with a viewshed which is created using a GIS and geo-data. The project started when a preliminary research project was executed by a group of students at Wageningen University.

The results of this project pointed out that although the quality of the results needs improvement, it is possible to obtain a SVF using just geo-data and a GIS (Giffen et al.

2008). The method which was used, used a 3D representation (raster DEM) of the environment in order to create a viewshed. Based on the viewshed, the SVF was computed.

The 3D representation of the environment is where most improvements had to be made. During the preliminary research, the AHN2000 was used as a base DEM. Trees were modelled as square, impermeable cubic objects with a minimum cell size of 5 x 5 meter (DEM resolution). This is not a realistic representation of a geometrically complex object such as a tree. Two aspects are important with regard to this issue, the temporal aspects (yearly cycle of foliage and size of the tree) and the general geometry of the trees.

The condition (leaves / no leaves) of the trees has a big influence on the SVF. When looking through a foliated tree, one usually can barely see the sky. When looking through a bare tree, the fraction of visible sky is usually larger than 0 (see Figure 6).

Also the distinction between deciduous and coniferous trees has to be made because during the winter (when road slipperiness usually occurs), coniferous trees still carry needles while deciduous trees generally do not carry leaves anymore.

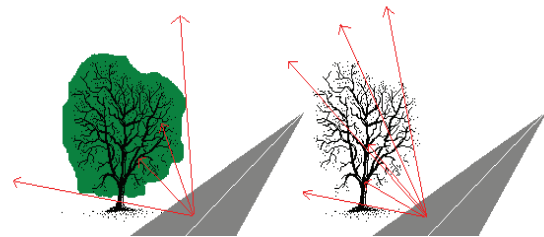


Figure 6: Tree with leaves (left) blocking the sky view (red arrow) and leafless tree (right) which is hardly blocking the sky view at all.

Furthermore, the shape and size of the crown will influence SVF. Long thin shaped crowns will have a different impact on SVF than big round crowns. This factor also had to be taken into account.

During the preliminary research, the locations of trees were extracted from the TOP10vector dataset. In this dataset, the areas where trees are located are indicated by polygons of groups of trees and lines for rows of trees (e.g. alongside a road).

Although the distinction between coniferous forest, deciduous forest or mixed forest is made, no specific information on the exact location of individual trees, species and size / shape of the tree is included in this dataset. The facts mentioned above make it difficult to create a correct digital 3D representation of the environment.

Summarizing the above, one could say that -apart from minor improvements of the actual model and obtaining accurate source data- the major problems lie in the correct modelling of trees in the 3D model of the environment and the compensation of the fraction of sky which is visible through trees.

## 1.5 Research objectives

This thesis research has focused on improving the accuracy of the SVF which was computed using a GIS and geo-data. The method which was used during the preliminary research project was used as a starting point. The aim of this project was to achieve a SVF quality equal to that which is achieved using the photographic method. The goal was to do so by improving the method itself as well as by trying to find better suited input datasets.

In order to define the content of this thesis research, the following research question was defined:

**Is it possible to accurately compute SVF using a GIS and geo-data, of a quality equal to that of the SVF computed using the photographic method?**

In order to be able to answer the research question, a number of sub-questions have been defined:

Regarding the use of a GIS:

1. What is the quality of the SVF based on a viewshed which is created using a GIS, as compared to the SVF which is measured using fisheye photographs (photographical method)?

Regarding model improvements:

2. What GIS model input parameter are required in order to be able to compute a SVF of acceptable quality to be used in the Meteo Consult Network Model?
3. How can the modelling of the trees in the GIS SVF model be improved?

Regarding the dataset improvements:

4. In which datasets can the required data be found?

## **1.6 Report Outline**

Chapter 1 contains the introduction to this research. As this thesis research was a spinoff of a larger research project., in the first paragraph a concise description of this larger project is given.

The next paragraph (1.2) contains more information on the so called Sky View Factor, the subject of this research project. The third paragraph (1.3) gives an overview of the methods which currently exist for computing the Sky View Factor. This paragraph is followed by the problem description (1.4) and the research objectives (1.5).

Chapter 2 (the methodology) starts with a description of the research area (2.1). Also the datasets and software which were used (2.2.1 and 2.2.2) are described. The last part of this chapter contains the methodological framework (2.3).

In the third chapter, the results of this research are discussed. The discussion of the results is also included in this chapter. Chapter 4 contains the conclusion and recommendations for further research.

## 2 Methodology

### 2.1 Research area

The research area of the RGI project “Preventieve Gladheidsbestrijding op basis van meteorologische, thermal-mapping en GPS data ter plekke” is the area called the Gelderse Vallei, which is located in the east of the Netherlands (see Figure 7).

This area is located close to the office of Meteo Consult and features many combinations of different road and landscape types which is essential for the research project. The red line in the map indicates the route along which Meteo Consult has measured the SVF using the photographic method.

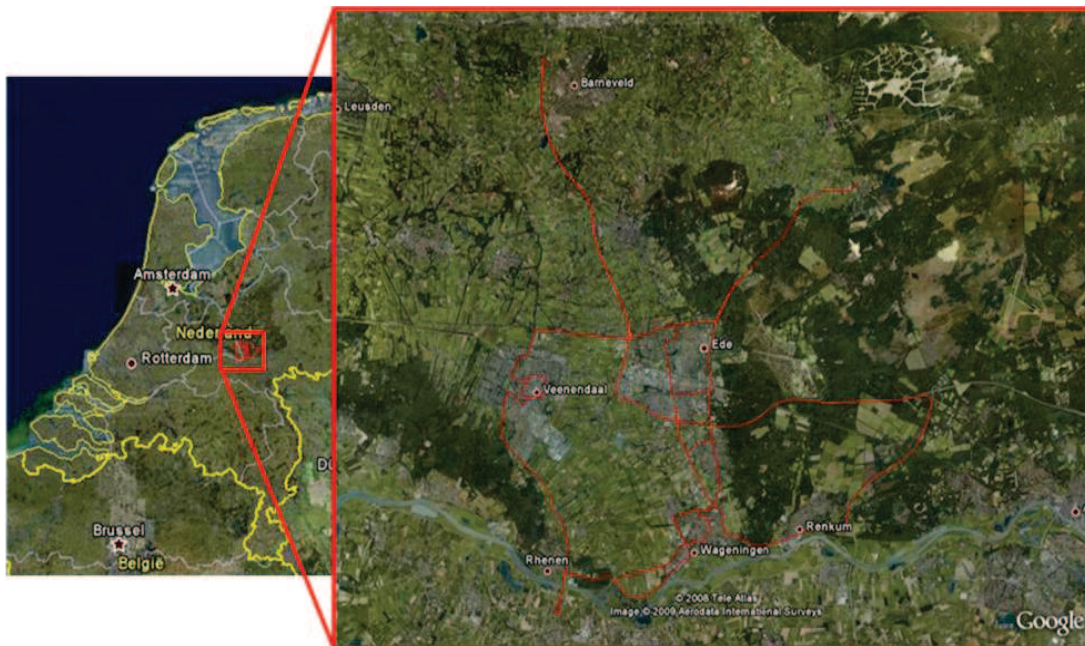


Figure 7: The research area of the RGI project is located in the Gelderse Valley. The research project which is described in this research focuses on several small parts of this area. The red line indicates the route along which Meteo Consult computed the SVF based on the photographic method.

In order to reduce computing time, a small subset of the research area was tested during this research. The maximum number of points in the model was limited to approximately 200. Because one of the goals of this research is to find a method to compensate for the fraction of sky which is visible through trees, it was essential that the research area contains different types of forested areas. Also important are built up areas.

The municipality of Ede was selected to be the area of interest for this research project. Apart from the occurrence of different road side landscape types, another reason to select this area was important. The municipality of Ede is considered to be very progressive in the GIS field, they have a lot of suitable GIS data available and are potential customers for the final product (the RST forecast). They made the so called “Local datasets” (see paragraph 2.2.1) available for this research project.

For all the reasons mentioned above, and the fact that the author is very familiar with this road, (part of) the “Edeseweg” was chosen to be the subject of this research. This road connects Bennekom to Ede and runs from the south to the north.



The selected stretch of road is surrounded by many different types of ‘forested’ areas. There are tree lines (single row of trees) with pastures behind it, there are areas with several trees behind each other in the viewing direction and there are completely forested areas (see Figure 8).

The SVF in open areas was also tested. Due to the fact that the source DEM does not contain tree height information, forest areas on the original source DEM are flat thus representing open areas (see image b in Figure 8). During the SVF computations, these areas were used to mimic open areas.

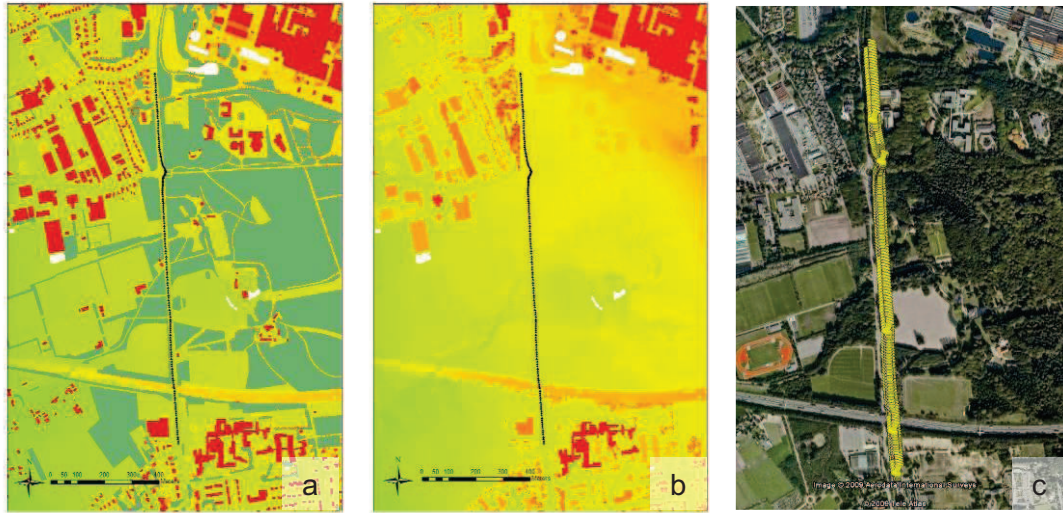


Figure 8: (a) raster version of the area of interest with the olive-green polygons indicating tree presence, the red polygons indicating the built-up areas and the black vertical dotted line indicating the SVF measuring locations, (b) raster DEM without trees, (c) Google Earth image (2005) showing the area of interest and the SVF measuring points (yellow drawing pins)

## 2.2 Materials

### 2.2.1 Datasets

Datasets originating from two different sources were used during this project. In order to be able to compare test results with the preliminary research, both datasets used during the preliminary research (TOP10VECTOR and AHN 5x5) were used again as input for a general model which computes SVF which was based on the approach during the preliminary research. These datasets will be referred to as the 'national datasets'.

Also part of this research was the question in which datasets can the data required for the SVF computation be found. Within the framework of this question, it was tested whether potentially suitable datasets which were made available by the municipality of Ede, (a potential customer of the final product (RST prediction)), were actually suitable for the SVF computation. These datasets will from now on be referred to as 'local datasets'.

National datasets:

- TOP10VECTOR
  - The TOP10vector dataset is produced by Kadaster (the Dutch land registry office). It is a vector dataset covering the Netherlands containing detailed topographical information on landuse. The scale is 1: 10,000 and the revision frequency is 4 years<sup>2</sup>.  
Every type of landuse has a so called "TDN-code" assigned to it. Examples of landuse types are: building / house, high-rise building, highway with separated lanes, deciduous forest, arable land etc. In total, 77 different categories are being distinguished. Based on expert advice, the decision was made not to include the TOP10 point dataset.
- AHN 2000 5x5 (Actueel Hoogtebestand Nederland)
  - This is a raster digital elevation model of the Netherlands with a resolution of 5 x 5 m. This raster is based on a point file containing height measurements which are obtained by means of laser altimetry. Measuring points are distributed unevenly over the area, depending on the data gathering technique used by the contractor (many different contractors were used).  
The 5x5 dataset is the most detailed version of this dataset which is currently available (apart from the raw source point dataset). The terrain heights are calculated using the 'inverse squared distance weighting' technique. When no laser altimetry measurements are available in the search area surrounding the raster cell of which the height has to be computed, a no-data value is assigned to the cell. Tree heights were filtered from the dataset.  
The cell values in the current version of the AHN are based on at least 1 measuring point per 16 m<sup>2</sup> in rural areas and at least 1 point per 36 m<sup>2</sup> in forest rich areas. The revision frequency of this dataset is once every 5 to 10 years<sup>3</sup>.

---

<sup>2</sup> Source: [www.kadaster.nl](http://www.kadaster.nl)

<sup>3</sup> Source: [www.ahn.nl](http://www.ahn.nl)

Local datasets:

- GBKN (Grootschalige BasisKaart Nederland – Large scale base map Netherlands)
  - This dataset also is a digital topographical base map of the Netherlands. The usable scale range is about 1 : 500 to 1 : 5,000. This dataset contains the geometry of all buildings, but also roads and other infrastructural features in the Netherlands. Also, semantic information is included (street names and sometimes house numbers). The GBKN is constantly being updated, there is no fixed update frequency<sup>4</sup>.
- AHN 2000 5 x 5 (see above)
- GBI (Geïntegreerd Beheers Informatiessysteem – Integral management information system) for location and characteristics of individual trees.
  - The GBI is not actually a dataset, it is a management system. The municipality Ede uses this system to manage the trees which fall under their supervision. The dataset which was made available is a point feature dataset containing information on all trees which are managed by the municipality of Ede. In this file, tree height (categorized), trunk diameter (categorized), tree species and location can be found. The data within this dataset is constantly being monitored.

Apart from these datasets, the SVF as measured by Meteo Consult was used as reference SVF data for this project. This dataset was created by driving past the locations of which the SVF was required. Approximately every 5 to 10 meter, a photograph was taken in the direction of the zenith, using a fisheye lens.

The photographs were checked for errors (see Figure 2). After this, the SVF was computed from the fraction of visible sky in the photographs. This dataset is the result of a single sampling session. Although maximum care was used while collecting and processing the images, some errors might still occur. For the sake of this research however, the assumption was made that the reference SVF was 100% accurate.

## 2.2.2 Software

Several manufacturers / organizations offer GIS software nowadays. At Wageningen University, ArcGIS 9.2 (ESRI, 2006) was available at the time of the project, therefore this GIS was used during the research project. An ArcInfo license was available, as well as the Spatial Analyst extension which is essential for the SVF computation.

Due to the rapid developments in the GIS field of work, also several organizations and companies have made their open source GIS available to the public. New programs are developed as we speak. This led to the decision to also explore the possibilities of using an open-source GIS for the SVF computation. The combination of GRASS and QuantumGIS was selected, predominantly for reasons of continuity.

GRASS is a very well-known open source GIS packages. It was developed by the United States Army Construction and Engineering Research Laboratories. GRASS is available under the gnu open source license, and is used in academic and commercial settings as well as by several governmental agencies.

Previously, GRASS was an OSGeo (Open Source Geospatial Foundation) project but very recently, GRASS was adopted by the Joint Research Centre of the European Union. This means that in the future, GRASS will be used by many governmental agencies, which in turn will guarantee the continuity of the program.

---

<sup>4</sup> Source: [www.gbkn.nl](http://www.gbkn.nl)

## 2.3 Methodology

### 2.3.1 Reading directions methodology

Before continuing to the actual description of the methodology, it is recommended to read the following reading directions.

#### **Dataset / GIS model names and hierarchy**

Datasets and model nomenclature follows a specific system. All toolset names start with "SVF" followed by "\_", a capital letter (see Table 6 in appendix 2) and a short description. For example "SVF\_A\_data\_preprocessing\_general". The letter (5<sup>th</sup> character) is used to identify which toolset it is and can be found back in all models within that toolset, as well as in the output of those models.

All model names also start with "SVF" followed by "\_" and a letter. The letter is the indicator of the toolset which contains the concerning model. The letter is followed by "\_", a number (starting with 00 or 01) and a short description. This number can also be found in the name of the output of the concerning model.

The combination of letter and number is used to easily identify the model which was used to create a certain output file. Sometimes the number is followed by a prefix (a, b, c, etc) to indicate that the concerning model is part of a larger model (sequence).

#### **Some points which can be of use when reading the following chapter.**

- in case the term 'model' is used, this means Arc-GIS model builder model, unless otherwise explained;
- ('xxxxxxx') including the brackets refers the tool which is used;
- words enclosed by square brackets [ ], like for instance [OBJECTID] refer to attribute names;
- words in italic font (e.g. *SVF\_A\_00\_create\_project\_cilpbox*) are table, feature class or model, toolset or toolbox names;
- In case the term 'measured SVF' is used, the SVF as computed by Meteo Consult (using the photographic method) is meant;
- In case the term 'mask' is used, either a raster file or polygon feature is meant. (r) is used to indicate a raster mask, (p) is used to indicate a polygon mask;
- The term 'tree transparency' will be used from now on to indicate the fraction of sky which is visible through a bare tree;
- The term 'tree filter' is used to indicate the algorithms which are used to compensate for tree transparency in the SVF computations;
- A graphic representation of all models used in the computations is presented in appendix 1.



As mentioned before, the use of two different sets of datasets was tested during this research. Although these datasets differ, large parts of the methodology theoretically applies to both datasets. The overall GIS workflow during this project is visualized in Figure 9. In Figure 10, an overview of the proceedings within the GIS SVF computation model (blue box in Figure 9) is shown.

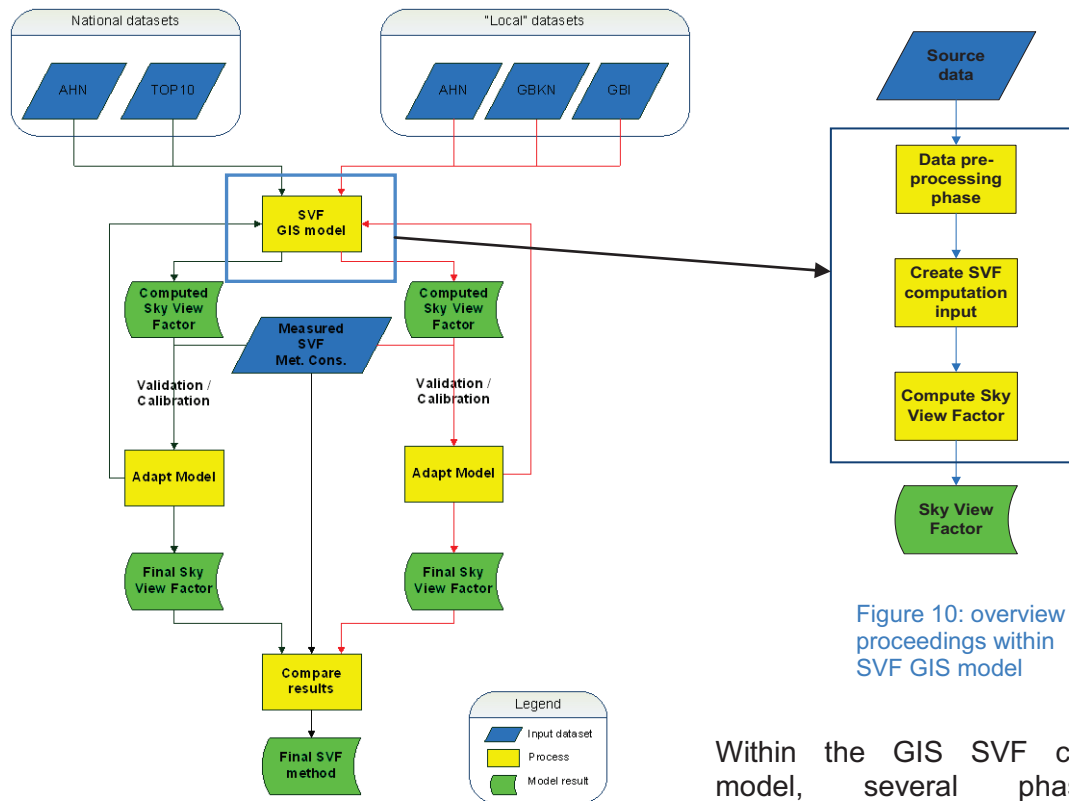


Figure 9: General overview total GIS workflow. National dataset trajectory represented by black arrows, Local dataset trajectory represented by red arrows.

Figure 10: overview proceedings within SVF GIS model

Within the GIS SVF computation model, several phases are distinguishable. To start with, the general data pre-processing (see paragraph 2.3.3). This phase entailed the non dataset specific pre-

processing activities such as e.g. the creation of the project clipbox delimiting the area of interest and the creation of the annular template.

The next phase was the dataset specific pre-processing (see paragraph 2.3.4). During this phase, relevant information was extracted from datasets, and data was manipulated in order for it to be used in the SVF computation.

The third phase was the last pre-processing phase (see paragraph 2.3.5). During this phase, the trees were modelled. This was followed by the actual SVF computation (paragraph 2.3.6).

During this phase, the viewsheds were created and based on the sky which was visible in those viewsheds, the SVF was computed. The models which were used during this part are based on the models which were used during the preliminary research (Giffen et al. 2008) .

The final step (see paragraph 2.3.7) was to validate the results and determine the quality of the GIS SVF. In order to do so, the computed SVF was compared with the SVF measured by Meteo Consult. In addition, the computed SVF was used in the Network Model in order to determine whether the use of the GIS SVF would affect the outcome of the Network model (RST forecast).

## 2.3.2 Methodological approach

### General data pre-processing

The part of the data pre-processing which could be done without any requirement for other datasets is included in the general data pre-processing phase. Before the source data could be processed, several products had to be created and a number of requirements had to be met:

1. A clipbox delimiting the area of interest had to be created;
2. SVF measuring points had to be uniformly and consecutively numbered;
3. The projection of the SVF measuring point locations had to be correct (points must be located within the borders of the roads);
4. An annular template containing the rings, based on which the SVF would be calculated (see paragraph 1.3) had to be created;
5. A table containing all results of calculations which could be done without the need for extra input data was created in order to save time during the actual SVF computation.

The toolset used in this phase is called *SVF\_A\_data\_preprocessing\_general*

The methods and models used during this phase are described in paragraph 2.3.3.

### Dataset specific pre-processing national datasets

During this phase, the datasets (TOP10vector, AHN 2000 and SVF measurements by Meteo Consult) were processed in order to be used in the SVF computation. Several actions were required in order to be able to start computing the SVF:

6. All source datasets had to be clipped to match the area of interest, in order to reduce the amount of data during the computations;
7. Relevant information had to be selected from the TOP10vector dataset (the location of roads, buildings and trees), thus creating polygon object masks of those landuse types;
8. A table containing measuring locations for the SVF computation had to be created;
9. Raster versions of the previously mentioned object masks had to be created in order to be able to use specific parts of the raster DEM;
10. Overlaps between different masks had to be eliminated. Due to the facts that the information from TOP10VECTOR came in vector format (smooth poly lines with the exact shape of the feature) and the information in the AHN is contained in 5 x 5 m square cells, sometimes an overlap in different filters can come into being when transforming the vector masks to a raster mask.
11. Because the road surface in the DEM was still rough due to outliers (see Figure 11), the road surface had to be smoothened to remove outliers, in order to prevent SVF measurements from being taken on top of a tree;
12. The modelling of the buildings in the DEM had to be improved, as can be seen in Figure 12 (next page), the modelling of buildings in the original DEM is very coarse. Theoretically, computation accuracy can be improved by modelling the correct building outline and height;

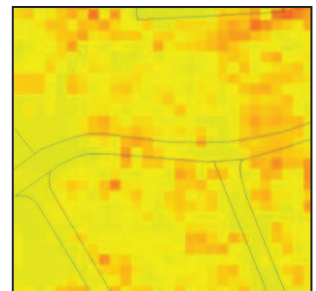


Figure 11: fragment of the original DEM (AHN) showing roads (outline indicated by black lines) and terrain height (green = low and red = Raster resolution 5 x 5 m).

The toolset used in this phase is called *SVF\_B1\_data\_preprocessing\_national\_datasets*

The methods and models used during this phase are described in paragraph 2.3.4.

## Dataset specific pre-processing local datasets

Experiments with the local datasets which were available at the time of the research, (AHN, GBKN and GBI) have proven the unsuitability of the GBKN for use within the SVF application. This is due to the fact that this dataset consists of line features rather than closed polygons. Due to the complexity of converting a line feature dataset into a polygon feature dataset, it was (within the time span of this project) impossible to create polygon feature masks based on the information in the GBKN.

For this reason, no methodology concerning the local datasets is included in this report. However, the possibilities of using locally available datasets must not be discarded, because other (suitable) datasets are potentially available (Westerbroek, 2008)). See paragraph 3.2 for a more elaborate report with regard to this topic.

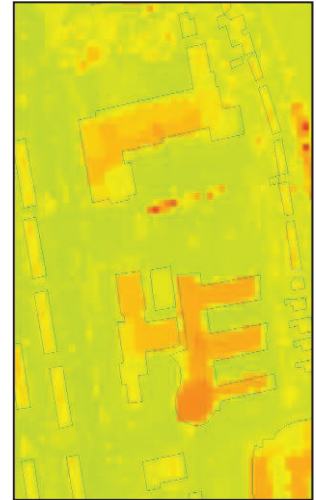


Figure 12: fragment of the original DEM (AHN) showing buildings (blue lines). (green = low and red = high).

## Improving the modelling of trees

One of the research objectives was: *'How can the modelling of the trees in the GIS SVF model be improved'* (see paragraph 1.5). In general, this problem can be split up into two parts, a source data part and a methodological part. The methodological part is where the improvements are made.

The methodological improvements can be split up into two parts, namely the method for putting the trees in the DEM and the creation of a method to compensate for the amount of sky which is visible through a tree. The latter part is discussed in the next paragraph (SVF computation), but the first part is discussed here. Also part of this phase was the creation of a DEM containing no trees. This was required in order to facilitate the new SVF computation approach (see paragraph 2.3.6).

13. The SVF computation method which was designed during this research requires two viewsheds, one based on a DEM containing all 3D structures in the environment (buildings, trees etc) and on based on a DEM from which the trees are removed (see paragraph 2.3.6 for more details). Therefore also a DEM with updated roads and buildings but without trees had to be prepared;
14. The AHN 5 x 5 does not contain tree heights (these are filtered out by the supplier of the data). In order to be able to accurately compute the SVF, the trees have to be integrated in the DEM.

The toolset used in this phase is called *SVF\_B3\_prepare\_tree\_mask*. Step 13 and 14 are discussed in paragraph 2.3.5.

## The SVF computation

This phase is where the second part of the improvement of the modelling of the trees (the adaptation of the computation of the SVF) takes place. Using the photographic SVF method, the following steps have to be taken to compute the SVF:

- A viewshed had to be created;
- Using an annular template, the viewshed had to be divided into a number of annuli;
- Finally, using equation (1), the SVF could be computed,

In the GIS method the photographic viewshed is replaced with a viewshed which is created using a GIS, based on a raster DEM representing the environment. The rest of the method is basically the same, apart from the fact that in a photographic version of the viewshed, one can simply count the visible sky pixels (also the pixels which are visible through trees). In a viewshed which is created using a GIS, this is not the case, because trees are modelled as non-transparent (square) objects.

No relevant literature was available at the time of this research, so a new approach was developed. Two approaches to modelling the transparency of the trees were considered. One strategy was adapting the DEM in a way that trees are represented as they are, a 3D structures containing open spaces. The other strategy was to adapt the computation which is used to compute the SVF in order to incorporate the fraction of sky which is visible through bare trees in the computed SVF.

Because the 'Solar Radiation Graphics' tool input raster DEM can only consist one layer of information (terrain height in this case), trees can only be modelled as square cubic objects existing of 5 x 5 m square cells. No open spaces within trees can be modelled. Neither is it possible to apply any kind of 'transparency factor' to the tree height value in the raster DEM, as this would reduce the height of the modelled trees, thus altering the angle from which the sky is visible or not.

The second approach seemed more suitable and was therefore implemented in the computations. In order to be able to calculate the fraction of sky which is visible through the trees based on a GIS viewshed (see Figure 13), the fraction of sky which is obscured purely and only by the trees had to be calculated.



Figure 13: example viewshed, green indicates visible sky, red indicates invisible sky.

The required result could be achieved by creating not one, but two viewsheds. One viewshed based on the full DEM (including buildings, trees etcetera) and the second based on a DEM including all objects, except the trees.

By subtracting the number of sky pixels visible in the viewshed based on the full DEM from the number of sky pixels visible in the viewshed based on the DEM without trees, the number of sky pixels obscured by trees could be determined for every annulus.

This made it possible to reduce the fraction of the sky pixels which were obscured by trees according to the transparency of the trees. This was done by adding a fraction of the obscured pixels to the total number of visible sky pixels in the viewshed based on the full DEM, thus increasing the SVF. This approach also made it possible to use a different transparency level for each individual annulus (see Figure 14, next page). During the brief period of research on the topic of tree structure and the amount of sky which is visible through a tree, no literature was found from which to extract a suitable tree transparency level.

Using this method, the number of visible sky pixels can never exceed the number of visible sky pixels in the viewshed based on the DEM without the trees. Therefore, the computed SVF can never exceed 1 (the theoretical limit of the SVF).

Observations in the field showed a large fraction (estimations ranged between 70 and 95 %) of visible sky when looking upward through a tree to the zenith. Barely any sky was visible looking through a tree standing at the far end of the horizon. Standing in a forest, starting while looking upwards to the zenith and moving the direction of the view to the horizon, the tree transparency seemed to decrease with an increase in viewing angle relative to the zenith. Based on these observations and estimations, the decision was made to range the percentages from 80 % to 95 % percent in the inner annulus and (close to) 0 % in the outer annulus.

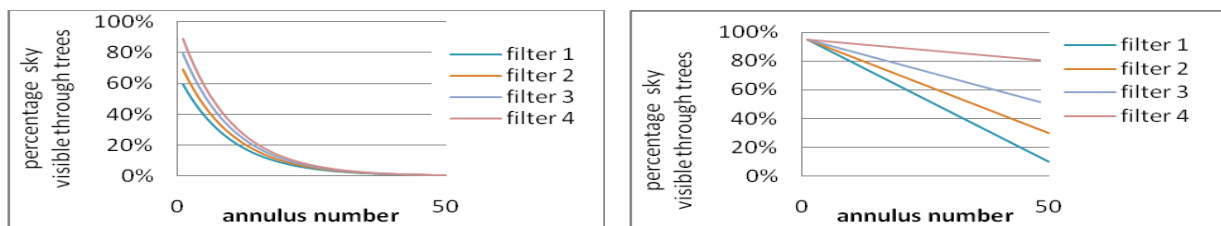


Figure 14: example of exponential tree transparency decrease curves towards outer template annulus (top) and linear tree transparency curve (bottom).

Two forms of tree transparency decrease were tested, a linear decrease and an exponential decrease (see Figure 14). It is clear that the parameterisation of the tree transparency needs more research. Using this tree filter it is not yet possible to automatically make the distinction between a single row of trees blocking the sky view or a forest blocking the sky view. When looking horizontally through a forest, the blocking effect will be much larger as compared to a single tree. The blocking effect is also depending on tree species, no method to include this parameter in the GIS model was found yet either.

In the current method, no distinction between coniferous and deciduous trees was made. This does not however influence the results of the current research, as there are no coniferous trees present (according to the TOP10vector dataset) in the research area.

The problem could be solved by modelling the coniferous trees in what is currently the DEM without trees (model it as a 'hard object'). This way, the fraction of sky obscured purely by deciduous trees can be computed.

All of the above resulted in the following sequence of required activities:

15. A separate database containing only relevant / required data for the SVF computation had to be created in order to put all relevant data within one database;
16. Two viewsheds had to be created. The first viewshed was based on the DEM without trees, the second on the DEM with trees;
17. Using an annular template, the viewshed had to be divided in 50 annuli and the fraction of visible sky per annulus had to be calculated;
18. Based on the fraction of visible sky in each annulus, the SVF had to be computed using equation (1) (see paragraph 1.3) and a tree transparency compensation algorithm.

## Validation of the results

After the SVF was computed, the results were validated using the reference SVF and the Network model. This process is described in paragraph 2.3.7



### 2.3.3 General data pre-processing

- 1 To begin with, a project clipbox was created (in order to be able to clip the relevant data from each dataset. The extent of the clip area is (coordinates RD\_NEW):

X-min: 172000	Y-max: 449500	X-max: 175000
	Y-min: 446500	

The clipbox was created by first creating a constant raster ('create constant raster') with the previously mentioned extent. This raster was then converted to a polygon ('raster to polygon').

(SVF\_A\_00\_create\_project\_clipbox in appendix 1.1)

- 2 The second step was to import the table containing the reference SVF. The table contained the location of each measurement point and the SVF computed by Meteo Consult at that point. In order to be able to do computations with this file, every location was assigned an id, called SVF\_id. This was done by assigning the [OBJECTID] value to the SVF\_ID field, thus numbering the locations starting from 1.

(SVF\_A\_01\_import\_gps\_locations\_reference\_SVF and SVF\_A\_02\_add\_location\_ids\_to\_SVF\_tables in appendix 1.2)

- 3 Although Meteo Consult measured the SVF on the road, several locations of the SVF measurement points did not coincide with the roads extracted from the TOP10VECTOR (and GBKN) dataset, most likely due to differences in projection methods.

The points have to be located on the road, where the DEM surface is flat. If measurement points are located next to the road, they could be situated on top of e.g. a tree, resulting in an incorrect SVF. This problem was solved by manually increasing or decreasing the [X] and [Y] values in the attribute table of the feature containing the measured SVF. The result of this operation was checked visually.

(SVF\_A\_03\_reproject\_SVF\_sample\_locations in appendix 1.3)

- 4 In order to be able to compute the SVF based on a viewshed, an annular template containing 50<sup>5</sup> concentric rings with equal width had to be created. During the analysis, a viewshed resolution of 200 x 200 pixels and cell size of 1 x 1 (no unit) was used, these are the default values of the Solar Radiation Graphics tool (ESRI 2007).

In order to create the annular template, first a viewshed with a resolution of 200 \* 200 pixels at a random location was created ('solar radiation graphics'). After this, the centre point of the viewshed was buffered 50 times, with the distance increasing 2 pixels at a time, creating a polygon feature containing 50 concentric rings with each a width of 2 pixels (see Figure 15).

(SVF\_A\_04\_create\_annular\_templates in appendix 1.4)

---

<sup>5</sup> Previous research by Meteo Consult pointed out that 50 is the optimal number of rings (Wokke, 2008)

5 In order to increase computing speed, a raster version of the annular template was created (see Figure 15). This was done using the ('feature to raster') tool.

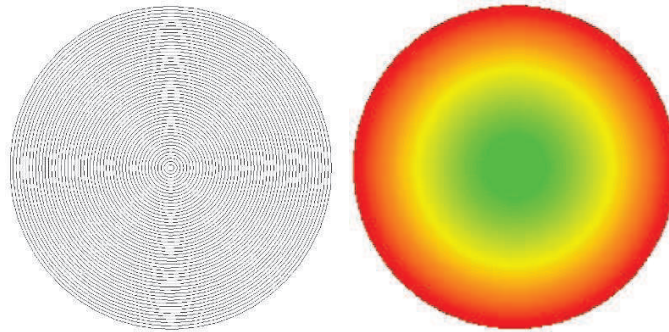


Figure 15: annular template containing 50 rings (left) and raster version of the same template (right) with the colour indicating the ring number (green indicating 1 and red indicating 50)

The computation speed was further increased by executing as much of the calculations as possible beforehand. A table containing the total surface area of each annulus was created. This was done by copying the attribute table of the annular template. Several fields were added to the table in order to be utilized later on: [SVF\_select], [perc\_sky], [extra\_sky\_1], [extra\_sky\_2], [TANH\_part] and [SVF\_1] to [SVF\_15]. The use of these fields is explained further at the appropriate GIS model steps.

Furthermore, the major part of equation (1) as shown below (see paragraph 1.3 for the complete equation) does not require any input and can therefore be computed beforehand.

$$\frac{1}{4n} \sum_{i=1} \left[ \sin \frac{\pi(2i-1)}{2n} \right] (2\pi)$$

The result of this part of the equation was stored in the [TANH\_part] field using MS Excel (Microsoft 2007). All other fields which were added previously were set to 0 in order to prevent computation errors due to empty fields.

(SVF\_A\_05\_create\_raster\_annular\_template in appendix 1.5)

### 2.3.4 Dataset specific pre-processing national datasets<sup>6</sup>

**6** The first step of this phase was to clip all source datasets to match the area of interest. This was done by clipping the source datasets using the ('clip') tool. The clipbox which was created earlier (see paragraph 2.3.3) was used as clip feature. The results were stored as feature datasets.

(SVF\_B1\_01a\_clip\_source\_data\_to\_aoi in appendix 1.6)

**7** Next, the relevant data was selected from the TOP10vector dataset. This was done by making a selection based on [TDN\_CODE] using the tool ('select'). For the exact selected TDN codes, see Table 7 in appendix 3. As the TOP10vector dataset contains tree line features, these were stored as a line feature, the rest were saved as polygon features. This way, the polygon version of the masks was created. For the tree masks, both line and polygon data were used, point data was left out of the analysis.

Although the TOP10vector dataset also contains the locations of bridges and viaducts, these objects are not yet used in the SVF computation. Due to the input requirements of the 'Solar Radiation Graphics' tool it is not possible to model these objects in the DEM in a way that compensates for the specific characteristics of such objects. The SVF at the locations of these objects has to be corrected by means of an overlay operation after the SVF computation.

(SVF\_B1\_01b\_select\_relevant\_data\_from\_top10\_data in appendix 1.7)

**8** In order to prevent the original source data from being altered in any way, a new feature containing the sample locations had to be created. This was done by creating an XY layer ('Make XY Event') based on the clipped original sample locations. This layer was copied ('Copy Feature') and saved as a feature dataset.

(SVF\_B1\_02\_Create\_model\_sampling\_points in appendix 1.8)

**9** After this, based on the data which was selected previously (at step 7), the required raster object masks were created. Initially, 4 masks (p) were created: a road mask, a built-area mask, a tree line mask and a tree polygon mask. All masks were created in the same way. The feature dataset containing the required features was used as a mask to extract the corresponding pixels from the DEM (AHN 2000) ('Extract by Mask').

In order to make sure that all pixels containing road surface were selected from the DEM, the road feature was extended with a 5 meter buffer at both sides of the road. The tree line feature was also buffered, 2,5 m to each side in order to create polygons which could be used as a mask to extract the relevant pixels from the DEM. The clipbox created during the first step of the general pre-processing phase was used as an extent for the extraction. Pixels within the mask were given the value 1, pixels with nodata were given the value -99999 ('Reclassify').

---

<sup>6</sup> Note: An observant reader might notice that in this paragraph, the model names do not contain a consecutive numbering. This is due to the fact that during the research some models were developed which later proved to be superfluous.



(SVF\_B1\_05a\_create\_object\_masks\_for\_DEM in appendix 1.9)

**10** Some of the masks (r) had an overlap with the road mask. These overlaps are caused by the transformation from polygon mask to raster mask, due to the raster resolution (5 x 5 m). This problem was solved by assigning the priority to road cells. In other words, if a cell had an overlap between road and for example buildings, the cell was assigned the value for roads.

Overlaps between buildings and trees were solved later on by first integrating the trees into the DEM, followed by the buildings (this way, overlaps between buildings and trees were overwritten with the building pixel values).

This order was chosen because for the SVF computation it is essential that the road surface does not contain any other objects such as trees or buildings. Therefore it was given first priority. The buildings were given second level priority because they are 'hard objects' of which one can be certain that they are present at the specified location, whereas the location of the trees is most uncertain of all.

The overlaps between the road masks and other masks were eliminated by executing a conditional statement ('Single Output Map Algebra'). If a pixel had the value 1 in e.g. both the road and the tree mask, the pixel was assigned to the road mask by assigning the nodata value of -99999 to that same pixel in the tree mask.

(SVF\_B1\_05b\_remove\_road\_pixels\_from\_masks in appendix 1.10)

**11** The next step was to erase the incidentally occurring peaks / anomalies from the roads (as shown in Figure 11). The smoothing method was based on the assumption that the maximum slope of roads in the Netherlands equals 20 %<sup>7</sup>.

Based on this assumption, the maximum range in road surface height over a distance of 50 meter is be 10 meter. This criterion was used to eliminate outliers from the road. If the range in road surface height in a circular neighbourhood with a radius of 5 cells (total diameter = 50 meter) exceeded 10 meter, the road surface height value was replaced with the minimum value in that same area (the nodata-value was ignored in the calculations).

To start with, using the road mask (r) , the road pixels were extracted from the DEM resulting in a raster containing pixels with the actual road surface height (nodata for pixels outside the road). Next, using the ('Block Statistics') tool, the range of the road surface height was determined for circular neighbourhoods with a radius of 5 cells (total diameter 10 cells x 5 m = 50 m). Next, the minimum road surface height was determined using the same tool and the same neighbourhood. Using a conditional statement ('Single Output Map Algebra') the minimum value of the neighbourhood was assigned to pixels with a range exceeding 10 meter.

The final step was to replace the road pixel values in the original DEM with the new road surface height values. This was done by again evaluating a conditional statement (if a pixel in the new road surface height raster contains a value other than the nodata value, this pixel value was copied into the a copy of the original DEM, the rest of the pixels in the copy of the original DEM keep the old cell values).

---

<sup>7</sup> This assumption was made during the preliminary research. During this research, the use of this assumption was continued.

Initially, the evaluation of the previously mentioned conditional statements did not yield satisfactory results. Visual assessment of the results showed that parts of the road surface still contained unexpected peaks.

Further research showed that the problem lied within the size of the neighbourhood which was used to determine the minimum road surface height, because on several occasions sudden unexpected increases in road surface height occurred over distances of in some cases 50 to 80 meter. Increasing the neighbourhood size to 20 cells (total diameter 100 m) led to satisfactory results (see Figure 16).

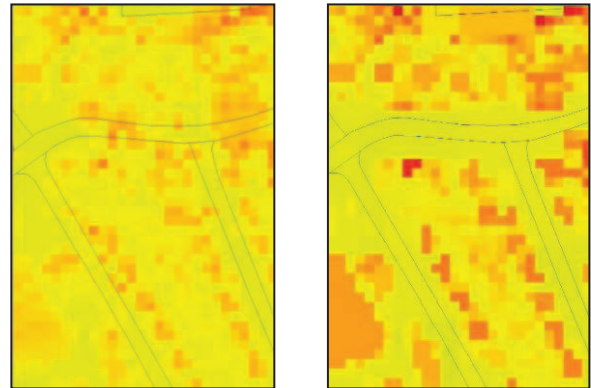


Figure 16: original road surface (between dark lines) (left) and smoothened road surface (right)

(SVF\_B1\_06a\_filter\_trees\_from\_roads\_in\_DEM and SVF\_B1\_06b\_filter\_trees\_from\_roads\_in\_DEM in appendix 1.11)

**12** The last step of this phase was aiming to increasing the accuracy of the representation of buildings in the DEM. Two problems had to be solved:

1. due to the raster resolution, the outlines of the buildings could not be modelled correctly (see Figure 17);
2. due to the method of cell height assignment (see paragraph 2.2.1) it was possible for a built-up area cell to contain the terrain height value of the neighbouring terrain instead of the roof height (see Figure 18).

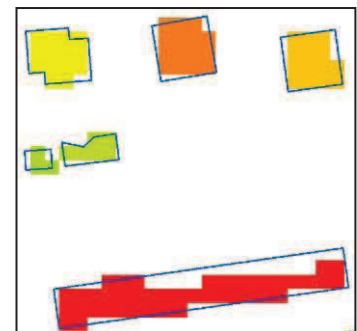


Figure 17: example of coarse representation of building outlines in DEM (red, yellow, orange and green blocks are houses in the DEM, the blue line is the correct outline from the building mask (p).

Improving the modelling of the building outlines in the raster DEM could only be done by increasing the raster resolution. In order not to affect the cell values of the original DEM, the resolution had to be improved 500 % to 1m x 1m (when using other resolutions for example 2m x 2m, the cell outline will not coincide with the 5m x 5m cell outline, thus changing the terrain heights for the non-overlapping cells).

Unfortunately, using the available computers it was impossible to process rasters with a 1m x 1m resolution of the required extent.

The roof height of each individual building was updated using the building mask (p) and a conditional statement. First the pixels containing built-up area were extracted from the mask ('Single Output Map Algebra').

Next, the height of the individual buildings was determined by computing a geometric intersection ('Identity') between the building mask (p) and the DEM. In order for this to be possible, the DEM had to be converted to a polygon ('Raster to Polygon') where the terrain height value was assigned to the polygons in the output dataset.

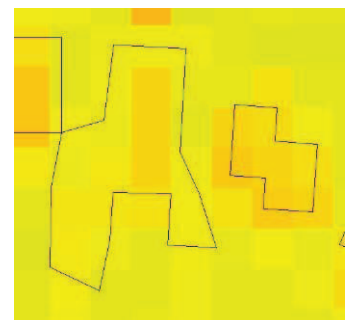


Figure 18: example of possibly incorrect built-up cell height.

Furthermore, the individual buildings in the building mask (p), had to be given an id code in order to be able to make computations with individual polygons. This was done by adding a field called [Poly\_ID] (and a field called [building\_height]) to the attribute table of the building mask. After this, the individual polygons were numbered by copying the value of the [ID] field into the [Poly\_ID] field.

After the geometric intersection, using the ('Summary Statistics') tool, the maximum height within each individual building polygon was determined. The resulting statistics table was joined ('Add Join') to the attribute table of the building mask (p) based on the common attribute [Poly\_ID]. The individual building heights were added to the building mask by copying the values from the summary statistics table to attribute table of the building mask.

In order to be able to replace the building height values in the DEM, the building mask (p) containing the building heights had to be converted to a raster ('Feature to Raster'), assigning the building height values to the built-up areas and assigning a no-data value to the rest of the pixels. The project clipbox was used as the extent for this operation. Finally, using a conditional statement ('Single Output Map Algebra'), the original building height values in the DEM were replaced with the newly computed values, resulting in a DEM containing smooth roads and updated building heights.

(SVF\_B1\_07a\_model\_buildings\_in\_DEM and SVF\_B1\_07b\_model\_buildings\_in\_DEM in appendix 1.12)

### 2.3.5 Improving the tree modelling

**13** In order to create the DEM containing only the buildings and roads, first a copy of the clipped source DEM (AHN 2000) was created. Using a conditional statement ('Single Output Map Algebra'), the updated buildings were incorporated in the DEM, replacing the old built-up cell values with the updated values.

This was done using the building height raster which was created earlier during the pre-processing of the national datasets (see step 12, see paragraph 2.3.4). After this, the smoothened road surface height pixels (created during step 11, see paragraph 2.3.4) were also incorporated in the DEM.

Finally, the smoothened road pixel height values were integrated in this DEM using the same method. This resulted in a DEM where (theoretically) the only objects obstructing the Sky View are the buildings.

(SVF\_B3\_04\_create\_built\_up\_DEM in appendix 1.13)

**14** In order to put the trees in the DEM, initially the same approach as used during the preliminary research was followed. This method was based on the assumption that although the DEM was filtered, still pixels containing the tree values were present in the DEM (Causing this assumption is the fact that certain otherwise unexplainable terrain height values occur, for example as showed earlier in Figure 16 in paragraph 0).

Based on the tree mask (p) which contained the different polygons of tree zones of specific kinds (defined by their TDN code), the maximum and minimum terrain height was determined per individual zone. Assuming that the maximum height was measured on top of a tree and the minimum height at ground level, a tree height could be determined per zone.

Next, the previously computed tree height value was assigned to all pixels of the corresponding zone within the raster version of the tree mask. After this, the raster tree mask was transformed to a point feature, where the GRIDCODE attribute (containing the tree heights) was used to assign values to the created points. This resulted in a grid like feature with 2 m in between points (trees).

In order to mimic a symmetrical distribution of trees throughout the tree zones, a selection of the created points was transformed to a raster. The selection was made by executing the selection expression  $(\text{mod}(\text{OBJECTID}, 6) = 0)$  thus selecting all points of which the OBJECTID could be divided by 6. This resulted in a tree density of 1 tree (ground surface 5x5 m) per 1.5 cells (37.5 m<sup>2</sup>).

The final step was to incorporate the trees in the DEM which was created in the previous step. This was done by adding the tree height value to the terrain height value in the DEM in case a tree was present at the corresponding pixel, using a conditional statement ('Single Output Map Algebra').

Unfortunately, the tree height which was computed using this method was too low. The maximum computed tree height was close to 6 meter, whereas the GBI (if information was available) indicated a tree height over 15 meter in a lot of these cases.

Estimation of the tree height in situ also indicated much higher trees. Therefore, based on the estimations in the field, 11 resp. 14 meter was added to the tree height which was computed (2 datasets were created). This resulted of a maximum tree height of about 17 resp. 20 meter. Obviously, further research into the actual tree height is required, see chapter 4 for elaborate comments of potential improvements to this method. The GBI dataset was not used in this research (apart from comparison of tree locations) for several reasons which are mentioned in paragraph 3.2.

To finalize this phase, the terrain height values in the DEM were transformed from centimetres to meter ('Single Output Map Algebra) and from integer to floating ('Float') values.

(SVF\_B3\_05\_insert\_trees\_in\_DEM and SVF\_B3\_06\_create\_float\_DEM in appendix 1.14)

### 2.3.6 SVF computation

**15** To start with, two file-geodatabases were created. One for storing the viewsheds and one for storing the data required for the SVF computation as well as the SVF results. The databases were named *viewsheds\_xx* and *SVF\_xx* where xx was replaced with the capital letter indicating the corresponding toolset (see Table 6 on page 78).

The next step was to copy the required raster DEM's (the results of step 13 and 14 in paragraph 2.3.5) into the *SVF\_xx* database ('Copy Raster'). Finally, a selection of the model sampling locations feature was made and stored in the SVF database.

15 new attributes called [SVF\_1] to [SVF\_15] and an attribute called [SVF\_select] were added to the attribute table. The [OBJECTID] was copied into the [SVF\_select] in order to make model computations per SVF sampling location (and model iterations based on sample location number) possible. The attributes [SVF\_1] to [SVF\_15] were added to facilitate the SVF computation using 15 different tree filters at the same time later on in the computations.

(*SVF\_J\_01\_prepare\_input\_viewshed\_computation* in appendix 1.15)

**16** The viewsheds were created using the 'Solar Radiation Graphics' tool. Three parameters had to be set within this tool, the sky size for the viewshed, the height offset and the number of calculation directions. The default sky size (200 x 200 pixels) was used.

Although the help function of the ('Solar Radiation Graphics') tool stated that the default value of 32 directions should be adequate for complex topography, increasing the number of calculation directions improved the result drastically. Therefore, the maximum number of directions (360) was used. Two different height offsets were used, the viewsheds were computed at ground level height and at 1.5 m above ground level (mimicking the same height at which Meteo Consult measured the SVF).

The 'Solar Radiation Graphics' tool requires 2 inputs, a raster DEM and a point feature specifying the location for the viewshed computation. The point feature was created by selecting a point from the points feature. The raster DEM's which were copied in to the *SVF\_xx* database were used as input DEM's.

Because the viewshed of the full DEM is also used in the Network model, a copy of each viewshed was stored in the *viewsheds\_xx* geodatabases. While working with the 'Solar Radiation Graphics' tool, a potential bug was discovered. For a description see appendix 9

(*SVF\_J\_03a\_SVF\_computation\_create\_viewsheds* in appendix 1.16)

**17** The next step is to compute the fraction of visible sky per annulus for both viewsheds. First, the viewshed is divided into 50 annuli. This is done by executing a conditional statement ('Single Output Map Algebra') using the raster annular template which was created in step 5 (paragraph 2.3.3).

In the viewshed, the visible sky was assigned the value 1. Using the conditional statement, every pixel with value 1 in the viewshed was assigned the value of the corresponding pixel in the annular template (the annulus number). Other pixels received the nodata value. This



resulted in a viewshed containing only the visible sky pixels, but with the value of the number of the corresponding annulus (1 – 50).

The fraction of visible sky was computed by joining the attribute table to the attribute table of the viewshed containing only the visible sky pixels. The number ([count] attribute) of visible sky cells was divided by the total number of cells ([count] attribute) per annulus. The result was stored in a new field called [PERC\_SKY]. This procedure was followed for both viewsheds.

(SVF\_J\_03b\_SVF\_computation\_compute\_sky\_area and SVF\_J\_03c\_SVF\_computation\_compute\_extra\_sky\_area\_building\_method in appendix 1.17)

**18** Finally, the SVF could be computed. Several steps were required to get to the actual SVF. The first step was to compensate for the fraction of sky which is visible through the trees. In order to do so, the fractions of visible sky from both viewsheds had to be stored within one table. The table which was created for this purpose during step 5 (paragraph 2.3.3) already contains the results of the parts of the SVF equation which could be calculated without the fraction of visible sky.

2 Attributes of this table were edited: first, the number of the sample location was stored in the field [SVF\_select]. This was done to be able to create relationships with other tables, based on the sampling location. Second, the fraction of visible sky based on the viewshed including the trees was stored in the field [PERC\_SKY] using a join between the attribute table of the viewshed and the table created during step 5.

The fraction of visible sky in the viewshed based on the DEM with only the buildings was stored in the same table, in the field called [extra\_sky\_bu]. The same method was applied to do so.

(SVF\_J\_03e\_SVF\_computation\_compute\_SVF and SVF\_J\_03f\_SVF\_computation\_compute\_SVF in appendix 1.18)

**19** Now that both fractions of visible sky per annulus were known, compensation for the tree transparency could be applied. 15 Different equations (or tree filters, see Table 9 in appendix 3 for the exact equations) were used to compute the fractions of visible sky per annulus, compensated for tree transparency. The results of this computation were stored in the fields [SVF\_1] – [SVF\_15].

In general what happened was that the fraction of visible sky in the full viewshed (including the trees) was subtracted from the fraction of visible sky in the viewshed based on the DEM without trees. The result is the fraction of sky which is purely obscured by trees.

Using the tree filters, a percentage of the fraction of sky obscured purely by trees was added to the fraction of visible sky in the full viewshed. Note that all these computations still are applied per individual annulus. Based on the updated fractions of visible sky, the SVF per annulus was calculated by multiplying this fraction with the result of the part of the SVF equation which was calculated beforehand (stored in the [TAN\_part] attribute).

The only thing left in order to compute the SVF was to summarize the results of all annuli. This was done using the 'Summary Statistics' tool. The result of this action was a table containing 15 different SVF's for 1 sampling location.

(SVF\_J\_03h\_SVF\_computation\_compute\_all\_SVF in appendix 1.19)

To finalize the SVF computation, the SVF's were stored in the SVF feature containing all sampling locations within the area of interest. This was done by joining the summary statistics table containing the 15 different SVF's to the attribute table of the SVF feature and copying the SVF's into the corresponding fields ('calculate field'). The join was based on the [SVF\_select] field, containing the number of the sampling location.

*(SVF\_J\_03j\_SVF\_computation\_add\_SVF\_to\_SVF\_feature in appendix 1.19)*

The whole process described in this paragraph was automated by merging all models into a single model. By using the variable '%n% + 1' (the model iteration count + 1)<sup>8</sup> as a selection criterion for the sample location, the model could be iterated based on the number of sampling locations.

By using the same variable to store the sample location number in the [SVF\_select] field during step 18, the whole process could be fully automated. Apart from the location of the correct databases for the model output, only the number of model iterations, the input DEM's and the SVF feature containing the sampling locations had to be specified.

*(SVF\_J\_03\_SVF\_computation\_full in appendix 1.19)*

---

<sup>8</sup> The model iteration count + 1 was used because by default the counting starts at 0. In order to start with 1, 1 had to be added to the iteration count.

### 2.3.7 Validation of the results

The only way to conclude whether the quality of the GIS SVF satisfies the requirements of Meteo Consult, was to determine whether the use of the GIS SVF would affect the outcome of the Network model.

After all, the quality of the GIS SVF is acceptable for Meteo Consult, when the advice as to whether or not road slipperiness prevention is required, remains unaffected as compared to the advice based on the use of the reference SVF.

Therefore, based on expert knowledge at Meteo Consult, the decision was made to run the Network model using fixed parameters. The only variables were the computed GIS SVF and the computed GIS viewsheds<sup>9</sup>. The results were compared with results that were based on the reference SVF and viewsheds.

This way, the effects of 2 variables (computed SVF and computed viewshed) were tested at the same time, where normally the effects of only 1 variable is tested. However, in this case, the effects of the two variables were interweaved so much, that the experts at Meteo Consult decided to test the effects of the 2 variables at the same time.

Apart from running the GIS SVF in the network model, another way of validating / calibrating the GIS method which was considered, was to select a test area of which all objects in the environment could be modelled exactly replicating reality. As the AHN 2000 contains information on building height, one could assume that in areas without trees, theoretically the GIS SVF computation should yield exactly the same SVF as the photographic method.

This method was not used for 2 reasons:

1. So far, Meteo Consult has not been able to quantify a quality criterion which defines the maximum deviation of the GIS SVF from the reference SVF. Although the results can be compared visually in a graph, there is not yet a criterion based on which one can say that the GIS SVF equals the reference SVF (or not).
2. Using a raster DEM to model the environment resulted in some limitations. The raster resolution of 5 x 5 m made it impossible to model buildings to the exact correct outline. Also, although building heights are included in the AHN, these heights are the results of interpolation operations and might not be the exact real height. So compared to the photographic method, the input data is just not accurate enough to be an exact replication of the environment.

---

<sup>9</sup> The viewsheds are also required to determine the Sun View (amount of time per day that a location receives direct sun light), which is a parameter in the network model.



### 2.3.8 Methodological differences between preliminary research and this research.

Although the methodology which was used during this research project was based on the methodology used during the preliminary research, several differences occur. The major differences are mentioned below:

- During the preliminary research, only a small subset of the DEM was used for the creation of the viewshed. The measuring point was buffered 50 meter, the buffer was used to clip the corresponding area from the DEM resulting in a circular DEM with a radius of 50 meter. So the distance from horizon to horizon was 100 meter.

Using the photographic method, the full extent of the area which is visible around the measuring points is used. Objects further away than 50 meter can still influence SVF. Imagine for example a large 30 storey flat that is 51 meter away from the measuring point. For this reason, the full DEM (or to a distance of at least 1000 meter away from the measuring point) was used during this research project;

- The filter which was used to remove trees from the roads (smoothing the road surface) during the preliminary research used a threshold standard deviation value which was based on the surface height of two neighbouring cells. The assumption that the maximum road surfaces slope in the Netherlands is 20 % was used to define the threshold value.

The filter in this research is based on the same assumption, but uses a different threshold value, namely the range in road surface height over a distance of 50 meter. If for a certain pixel this value exceeds 10 meter, the minimum road surface height of that area was assigned to the corresponding pixel.

This might seem like a coarse filtering technique, but visual inspection of the DEM showed road segments of up to 40 meter with very high road surface height values, compared to the neighbouring pixels, whereas in situ, the road surface was perfectly horizontal;

- The modelling of the trees during this project was based on the same methodology which was used during the preliminary research. But due to the fact that modelled trees seemed too low, and too sparsely modelled compared to the real situation, the amount of modelled tree cells was increased, as well as the tree height.
- The sampling locations which were used during the preliminary research did not coincide with the points at which the SVF was measured by Meteo Consult. In order to make comparison between the GIS SVF and the reference SVF possible, the exact same locations were used during this research.
- During the preliminary research, no process to correct for the amount of sky which is visible through bare trees was used. During this research, such an algorithm was developed and tested. The results are presented in paragraph 3.3.2;
- During the preliminary research, terrain height values lower than the value of the measuring point were removed from the DEM. The reasons for this exclusion are unclear, therefore during the current research, no pixels were removed from the DEM.

### 3 Results and discussion

As the title explains, in this chapter the results of this research project are discussed. The most obvious result is the computed SVF. Apart from that, this research project also generated some less obvious results. An example is a conclusion with regard to the suitability of the open-source GIS GRASS. The less obvious results will be discussed first (in paragraph ), the next paragraph contains the results of the SVF computations.

#### 3.1 Use of GRASS

Given the current developments in open-source GIS, the decision was made to test the suitability of such a GIS for the computation of the SVF. GRASS was selected as this SVF was the most promising for several reasons (see paragraph 2.2.2).

In order to be able to compute a SVF, several tools are required. The most important is a tool which can compute a viewshed representing sky pixels which are visible from the observers location and sky pixels which are not.

Although GRASS contains a tool which computes a viewshed (*r.los*<sup>10</sup>), this viewshed cannot be used in the SVF computation without adaptations because the computed viewshed represents the cells of the input DEM that are visible from the observers location. They are marked with integer values that represent the vertical angle (in degrees) required to see those cells (Khawaja 2002).

Due to time limitations and the complex mathematics involved in reprogramming the tool, the decision was made to concentrate on the use of ArcGIS (ESRI 2006) for SVF computation, because this software already offers a tool which creates the desired viewshed.

The creation of the correct tools in GRASS could be well worth the effort, considering the potential reduction in computation time (as well as costs). ArcGIS (ESRI 2006) has to load all modules, data and tools into memory before any computations can be executed. GRASS just loads the required modules and data, which could save a considerable amount of computing time.

#### 3.2 Local availability of suitable datasets

It could be beneficial for both Meteo Consult and the 'consumer' of the product (the RST forecast), if relevant GIS data is available at the customer, as this could potentially mean a reduction in cost price of the product. In order to determine whether such information was available, the municipality of Ede was contacted. This municipality was selected because of their reputation of being very progressive in their use of GIS and geo-data.

Three datasets were made available for research purposes: AHN2000 5 x 5 (same as available in the so called 'national dataset', the GBKN and the GBI (for a description of these datasets, see paragraph 2.2.1). Research pointed out that the GBKN (landuse dataset) could not be used to create the required masks without very complicated processing. The reason for this is that this dataset does not contain closed polygons of the required landuse types, but line features instead.

---

<sup>10</sup> [http://grass.itc.it/grass53/manuals/html53\\_user/html/r.los.html](http://grass.itc.it/grass53/manuals/html53_user/html/r.los.html)

The GBI could be very interesting for the use in this application. By law, local governments are required to monitor the status of trees under their supervision. Several engineering companies offer software to manage the administration of all relevant information. The municipality of Ede uses such a system called GBI (Geïntegreerd Beheer Informatiesysteem which translates as “integrated Management Information System), made by Oranjewoud.

The GBI has proven to potentially be very useful. As mentioned before, this dataset contains information on all individual trees which are managed by the municipality. Information on location, species, trunk diameter and height are all included in this dataset. Two problems occurred while evaluating the use of this dataset:

1. Only the trees managed by the municipality occur in the dataset, so trees next to the road but on private land are not included. In order to be able to correctly model the trees, data on all trees is required.
2. The data on the tree height (which is very important in the SVF computation) is very coarse. Instead of the exact height of the tree, 4 categories are used. These categories are: 0 – 6 meter, 6 – 9 meter, 9 – 15 meter and >15 meter. Accurately modelling the trees based on these numbers is not possible, more details such as for instance actual height and crown size are also required.

These problems are currently limiting the use of this dataset. As mentioned before, the viewshed which is created using ArcGIS is in fact a representation of the angles at which the sky is visible from the viewing point (sampling location). The centre of the viewshed is the zenith, the edge of the circular "map" is the horizon, and the angle relative to the zenith is proportionate to the radius (ESRI 2007).

Altering each of the previously mentioned characteristics (tree shape, tree height and tree location) results in a different SVF. Consider for example a 10 meter high tree at 10 meter from the sampling point. The angle (to the zenith) at which the sky is visible in the direction of the tree is 45 degrees. If the same tree is 15 meter high, the angle decreases to 34 degrees.

This way, the variation within the GBI height class of 9 to 15 meter results in angle between 48 and 34 degrees. Assuming the sampling location is completely surrounded by trees, the computed SVF based on a tree height of 9 meter would be 0.64. Based on a tree height of 15 meter the computed SVF would be 0.44, resulting in a difference of 0.2.

Based on Figure 19 (next page), in the worst case, a deviation in SVF of 0.2 could cause a difference of almost 2 °C in the forecasted road surface temperature. That could be the difference between a road surface slipperiness risk or not.

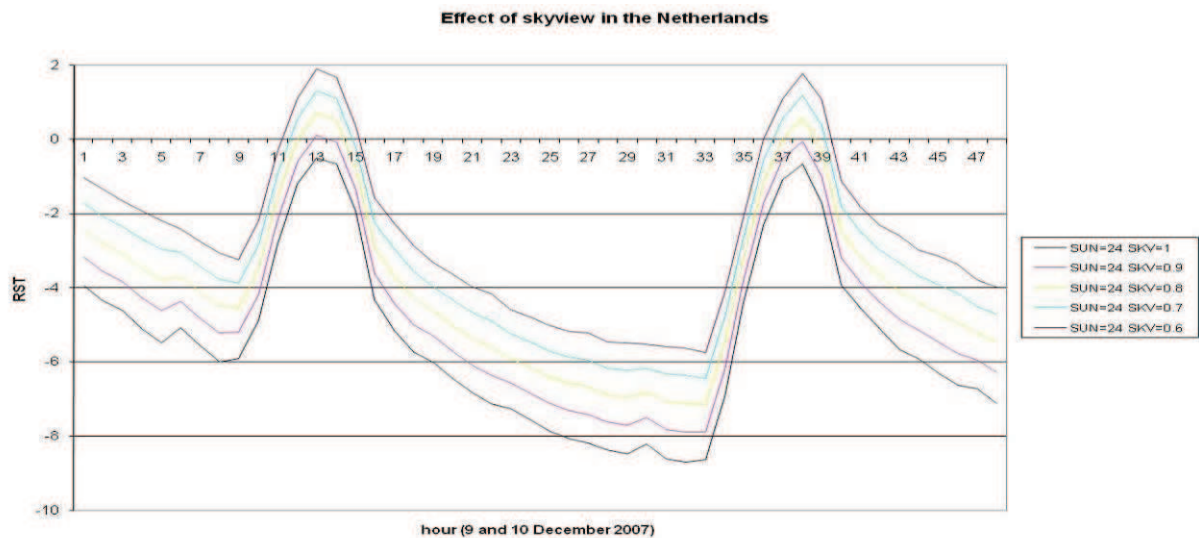


Figure 19: Effect of the SVF on the forecasted RST on December 9<sup>th</sup> and 10<sup>th</sup> 2007. The speed at which the road surface cools down during the night is related to the SVF. As can be observed from the graph, if the SVF is lower, the RST will be higher. Source of the graph: (Dijke 2009). Hour 1 is 00:00 in the morning of December 9<sup>th</sup>.

Despite the problems mentioned before, this is the most accurate and complete description of trees known to the author so far. The only other approach to gaining accurate tree height data could be using the unfiltered version of the AHN.

In this dataset, height measurements of all tree areas are present, although the sampling resolution (at least 1 point per 16 m<sup>2</sup> and 1 point per 36 m<sup>2</sup> in forest rich areas ) could be improved. Fortunately, this will be the case when AHN II will be published (scheduled in 2012, this DEM has an accuracy better than 5 centimetre and a minimum of 7 to 10 measuring points per m<sup>2</sup> (www.ahn.nl).

Although this research has proven that the GBKN is not suitable as input dataset for the SVF computation, the possibilities of using locally available datasets must not be discarded. Further communications with the municipality of Ede revealed that also available is the BRT (Basis Registratie Topografie / Basic Registration Topography) also known as TOP10NL.

This dataset contains similar information as the TOP10vector dataset, but it has an object oriented structure. So possibly using the combination of AHN 2000 and TOP10NL as source data could generate the same results as using AHN 2000 and TOP10vector. An interesting detail about the TOP10NL dataset is that it is renewed every 2 years. The AHN is renewed every 5 to 10 years (www.ahn.nl).

### 3.3 Computed SVF

First, the results of the SVF computation without any compensation for the amount of sky visible through the trees are shown. These results are obtained using just equation (3). After this, the results of SVF computation which was compensated for the fraction of sky which was visible through the trees is discussed.

Important to keep in mind is the fact that the network model (RST prediction model) only accepts a SVF between 0.6 and 1 (Wokke 2008). All SVF's below 0.6 are changed to 0.6 before computations are made.

#### 3.3.1 SVF without tree filter

The graph below shows the SVF computed using a GIS, without any kind of compensation for the fraction of sky which is visible through bare trees.

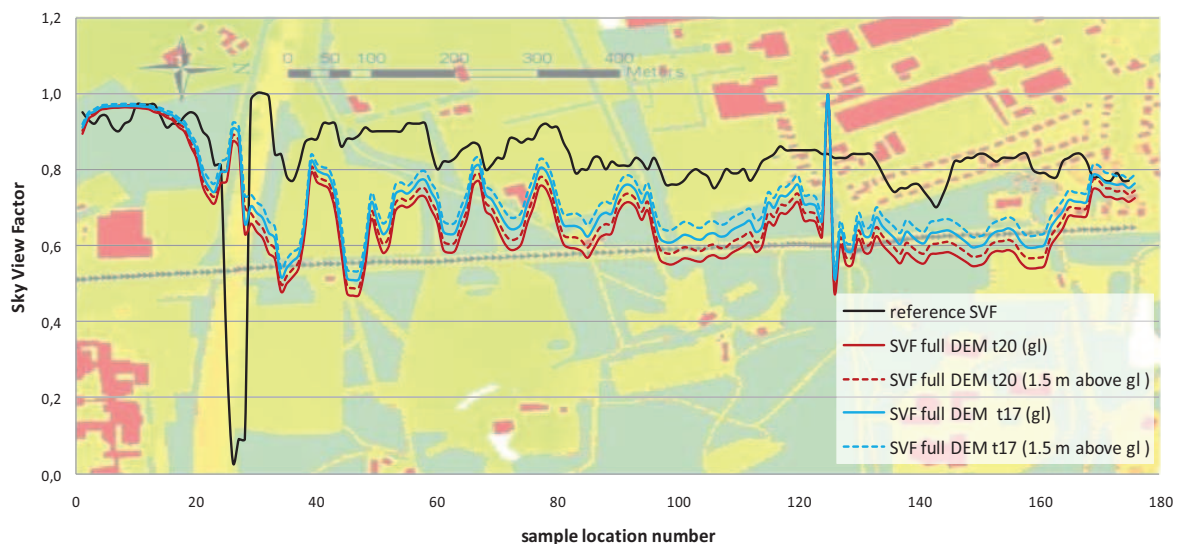


Figure 20: SVF as computed using only equation (1) without the application of any kind of tree light penetration compensation method. The red line indicates the SVF computed based on a maximum tree height of approximately 20 meter (t20). The blue line indicates the GIS SVF based on a maximum tree height of approximately 17 meter (t17)

Looking at Figure 20 several striking features can be observed:

1. In general, the SVF computed using the GIS method is underestimating the measured SVF although the magnitude of the underestimation differs. Two features in the graph stand out (see point 2 and 3);
2. Around point 21 – 24, the computed SVF overestimating the SVF, the computed SVF is close to 1 whereas the reference SVF approaches 0;
3. At sample location 124 – 130, some unexpected large fluctuations in computed SVF are shown;
4. In built-up areas where according to the TOP10vector dataset no trees are present (point 1 – 17) the GIS SVF is a fluent almost horizontal line, whereas the reference SVF shows much more variation;
5. In some locations (33 – 37 and 44 – 48), large negative peaks in the underestimation of the SVF occur.



### AD 1:

It is immediately clear that in general the computed SVF is underestimating the true SVF (see the trend line equations in Table 10 in appendix 5). This was expected, because the area of interest contains tree-rich areas and the computed SVF shown in Figure 20 is not compensated in any way for the amount of sky which is visible through trees. The magnitude of the underestimation can be explained by the difference in height, size and location of the modelled trees as compared to the real trees. This will be explained further in the following paragraphs.

### AD 2:

This overestimation was expected. Point 21 – 24 is the location at which the Edeseweg is crossed by the A12 (highway), at this location a viaduct is present (yellow/orange feature running from the left end of the scale bar in the background image to label “20” at the X-axis) in Figure 20.

Due to the fact that it is impossible to mimic a viaduct in a single-layer raster DEM, it is not possible to compute a SVF underneath such an object. The SVF in this case is computed from the road surface of the elevated highway instead of under the viaduct. In the graph of the reference SVF, this feature is clearly visible as a steep decline in SVF at points 25 -28.



Figure 21: aerial photograph viaduct Edeseweg / A12. (orientation equal to background in Figure 20, north to the right, west to the top). Source image: Google Earth (2005)

The steep incline to a reference SVF of almost 1 right after the viaduct is also unexpected. As can be seen in Figure 21, the stretch of road to the right of the viaduct is surrounded by trees.

One would not expect a SVF of (close to) 1 in such an area. This error could be explained by assuming the viewshed photograph was overexposed due to the sudden change of light intensity after leaving the ‘tunnel’ underneath the A12.

### AD 3:

The strong fluctuations at point 124 – 130 are caused by the combination of the location of the modelled trees and the location of the SVF measuring points. The peak at point 125 (computed SVF = 1) is caused by the fact that the sample location coincides with the location of a modelled tree (see Figure 22, next page). In the GIS model, this results in the creation of a viewshed with a base height on top of a tree. No objects in the surrounding area are higher, so no obstruction of the Sky View occurs, resulting in a SVF of 1.

This error is caused due to inaccuracy of the data on which the masks for manipulating different essential landscape types in the DEM (roads, built-up areas, forested areas etcetera) are based, the TOP10vector dataset. This is visible in Figure 24 (next page) where the road information extracted from the TOP10 dataset is shown in an overlay with the information provided by the municipality of Ede (GBKN). A number of blue hexagons (representing SVF measuring points) fall outside the TOP10vector road polygon (grey polygon), but within the road surface delineated by the GBKN map (black lines).



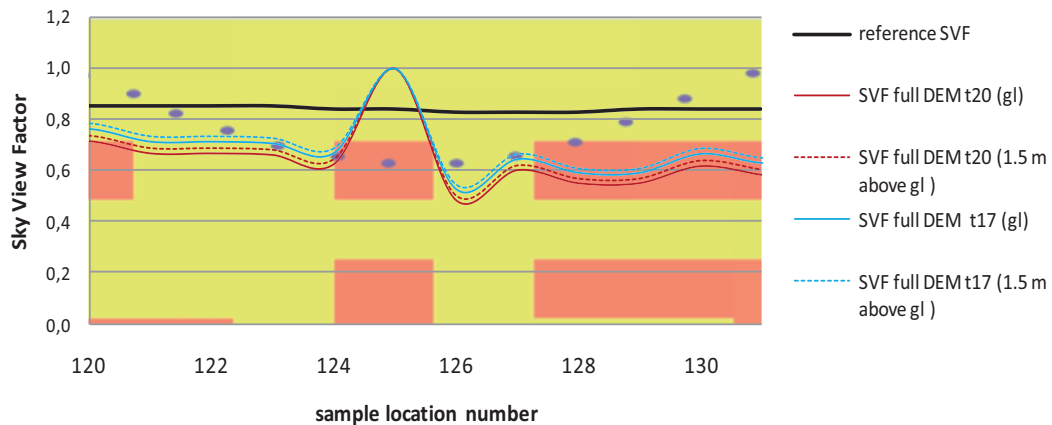


Figure 22: Computed and reference SVF at sampling points 124 – 130. In the background the raster DEM of the surroundings of SVF Orange squares represent trees, green background the terrain. The blue dots are the SVF sampling locations. In the picture it is difficult to see, but point 124 is located just next to the tree (as is point 128) whereas is located on top of the tree. The orientation of this graph corresponds with the orientation in Figure 20, north to the right, west to the top. (gl means ground level, txx means maximum tree height app. xx meter)



Figure 23: viewsheds of point 123 (left to point 129 (right)). The orientation of the viewsheds corresponds to the raster map orientation in Figure 22 (north to the right and west to the top). Black areas indicate no-data, dark-grey areas indicate invisible sky and light-grey areas indicate visible sky. **Note that the third image from the left (point 125) is almost entirely light-grey.** Images are based on the maximum tree height of 20 m.

The other fluctuations in this area (124 – 130) are caused by the fact that the distance between some of the measuring points and the modelled trees varies. Points 126 and 27 are located in between 2 trees (see Figure 22), resulting in a low SVF (0.56). The neighbouring points are located further away from the trees, resulting in a higher SVF. The corresponding viewsheds are shown in Figure 23.

As can be seen in Figure 23, almost the entire firmament is visible in viewshed 125. The effect of putting a sample location in between 2 trees can be observed in viewshed 126 (fourth viewshed from the left). Two semi-triangular areas of invisible sky to the left and the right from the centre of the viewshed are clearly visible. These areas cause the low SVF (0.58) at that location.

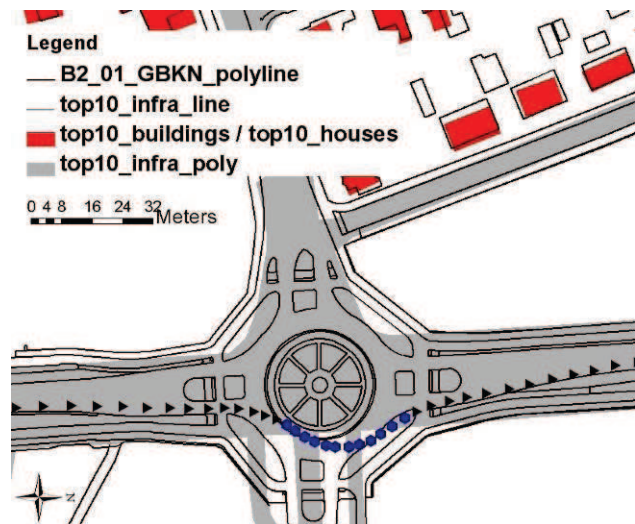


Figure 24: Detail of the road and built-up area masks created based on TOP10vector data (grey and red polygons) and an overlay of the corresponding GBKN data (black lines).

The black triangles and blue hexagons indicate the SVF sampling locations. The Blue hexagons are the sampling locations as shown in Figure 22. The orientation of this image corresponds with the orientation of the background of Figure 22.

#### AD 4:

A closer examination of the source data led to an explanation of the over- / underestimation of the SVF at point 1 - 24 (and also at point 163 – 176). In the raster DEM, it seems that the Sky View is only obstructed by buildings. In reality trees are also present in these areas. In the TOP10vector dataset (which is used to extract the location of trees from) these trees are not present (see Figure 25). Not taking the trees into account leads to an underestimation of the obscured fraction of the sky, resulting in an overestimated SVF.

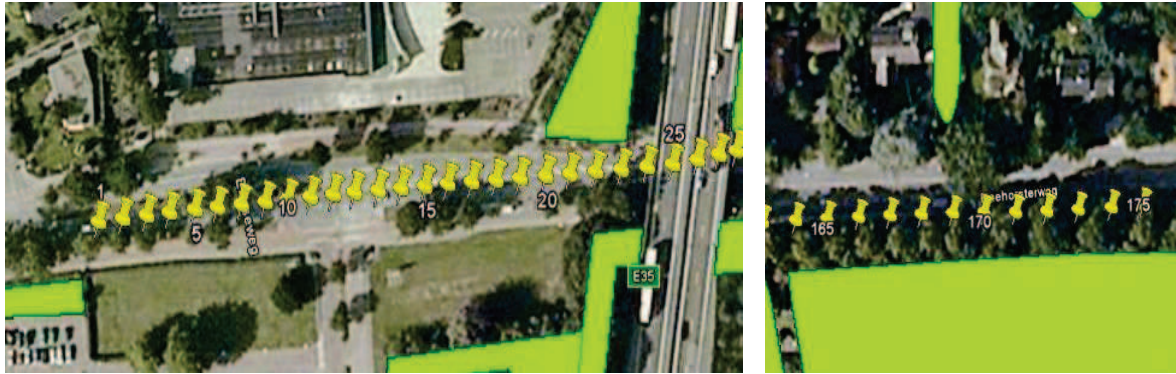


Figure 25: Overview of the built-up areas at point 1 -24 (left) and point 163 – 176 (right). Trees in the TOP10vector dataset are represented by the bright light green polygons. Apart from the tree areas in the TOP10vector dataset, other trees are clearly visible in both areas. The orientation in these pictures is equal to orientation of the background in Figure 20, north to the right, west to the top). Source image Google Earth (2005)

#### AD 5:

The same principle as described above applies to the underestimation of the SVF at point 33 – 37 and point 44 – 47. At these points the trees are modelled closer to the sampling points than in the actual real environment (see Figure 26 for the raster DEM and Figure 27 for the aerial photograph).

This results in a lower SVF because the parts of the viewsheds which correspond to the areas west of the sampling locations, show predominantly obscured sky (see Figure 28 for example viewsheds of points 40 - 49).

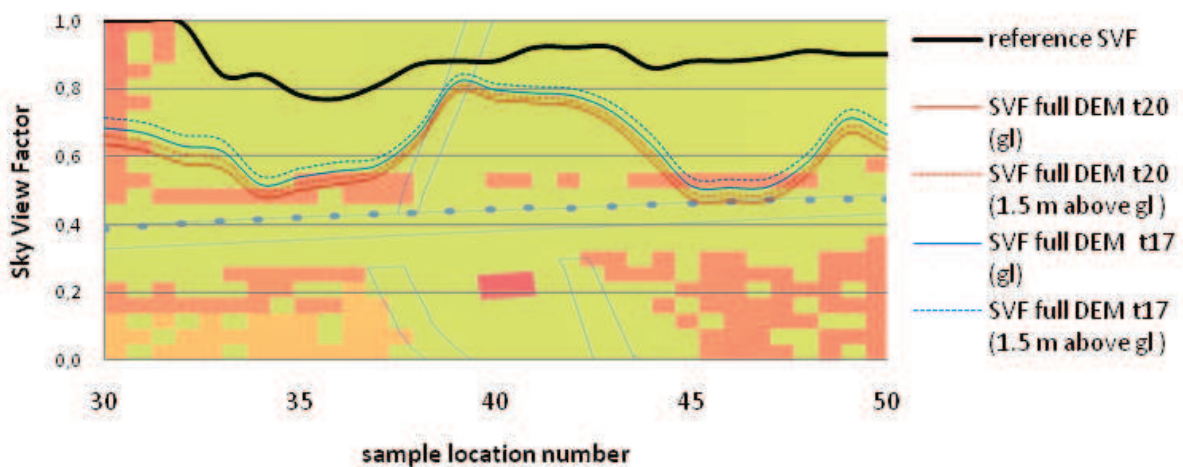


Figure 26: close-up of the raster DEM of the surroundings of SVF sampling points 30 - 50. Orange squares represent trees, green background the terrain. The blue dots are the SVF sampling locations. Orientation of the background image: north to the right and west to the top. (gl means ground level, tx means maximum tree height app. xx meter)



Figure 27: aerial photograph of the area surrounding SVF measuring location 30 - 50. Orientation corresponds to raster map orientation in Figure 26 (north to the right and west to the top). Source image: Google Earth (2005)

In Figure 28 the blocking effect of a row of trees is illustrated. Viewshed 44 – 47 are located close to a row of trees (west of the sampling locations), whereas the rest of the points are further away from the trees. Especially in viewshed 45 – 47 one can see that the upper half of the viewshed consist predominantly of obscured sky.

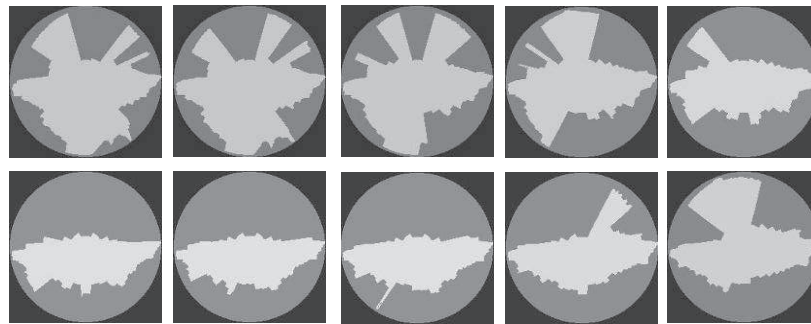


Figure 28: viewsheds 40 -44 (upper row, left to right) and viewsheds 45 – 49 (lower row, left to right). Black areas indicate no-data, dark-grey areas indicate invisible sky and light-grey areas indicate visible sky. Orientation corresponds to raster map orientation in Figure 26 (north to the right and west to the top). Images are based on the maximum tree height of 20 m.

Apart from the issue mentioned above, compared to the true situation the modelling of the trees in the raster DEM is not correct. The trees at the bottom of the graph in Figure 26 are located further away from the sampling points than they are in reality (see Figure 27). In addition to this, the modelled row of trees west of points 44 – 47 in the raster DEM in reality consists of a number of small and bushes, as can be seen in Figure 27.

### 3.3.2 SVF with tree filter

Two different algorithms (called “exponential tree filter” and “linear tree filter”) were used to compensate for the fraction of sky which is visible through bare trees. Two different types of tree transparency curves (see paragraph 2.3.5 and appendix 3 and 4) were used. An exponential decrease of tree transparency towards the outer annulus and a linear decrease towards the outer ring.

#### Results exponential tree filter

The results of the exponential tree filter are shown in Figure 29 (SVF computed at ground level) and Figure 30 (SVF computed 1.5 m above ground level). As can be observed, the effect of the exponential tree filter is minimal (especially compared to the linear tree filters, see Figure 32, Figure 33, Figure 34 and Figure 35).

In Figure 29 and Figure 30 (below and next page) no separate graphs are distinguishable. The graphs were created this way on purpose in order to demonstrate that the differences between the exponential filters are very small.

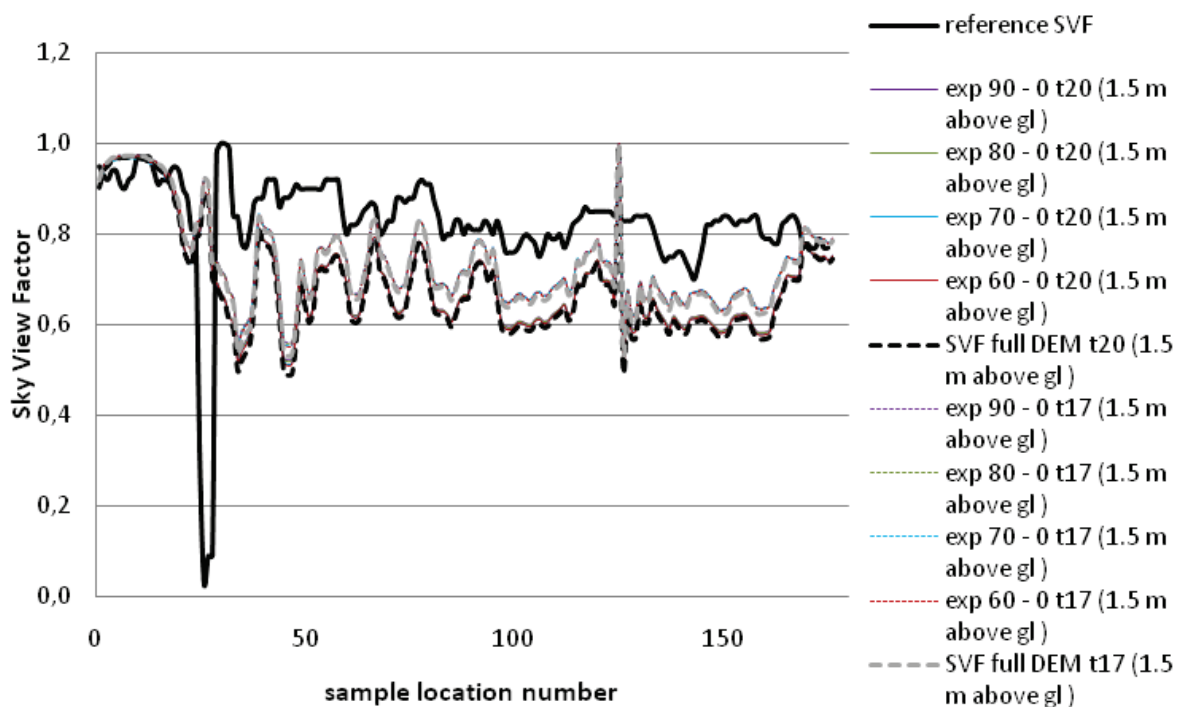


Figure 29: SVF computed at ground level (gl) using an exponential tree filter in which tree transparency ranges from 90% - 60 % in the inner annulus and approximately 0% in the outer annulus (see appendix 4). (txx means maximum tree height app. xx meter)



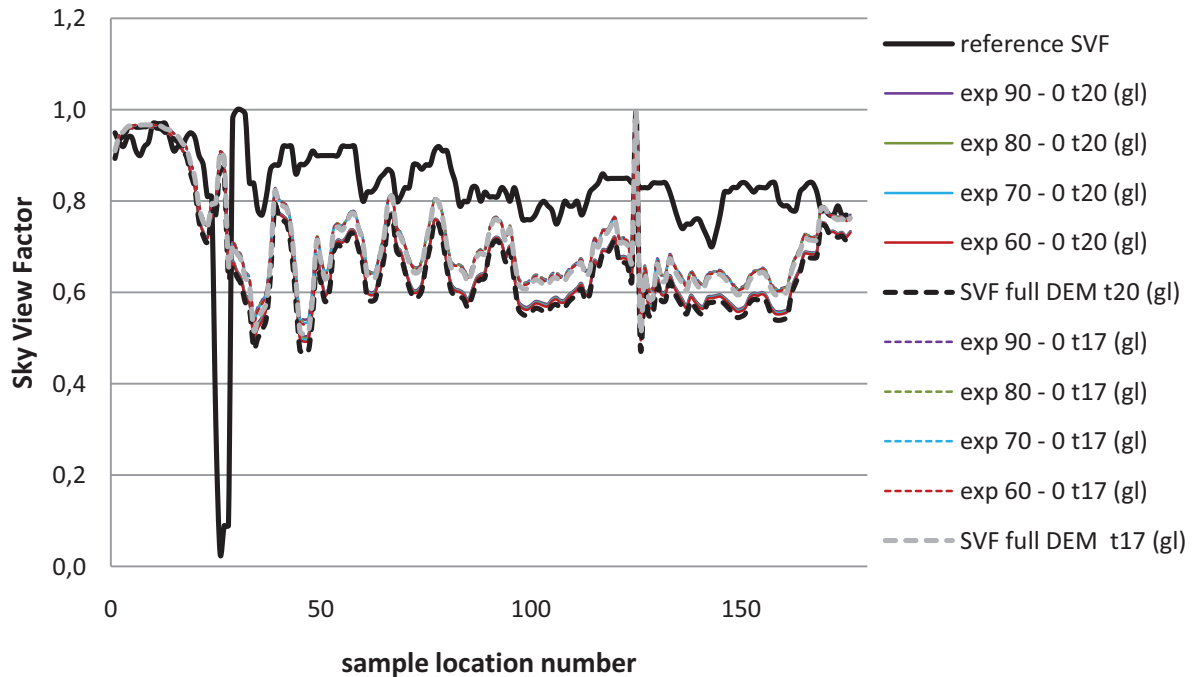


Figure 30: SVF computed 1.5 m above ground level (gl) using an exponential tree filter in which tree transparency ranges from 90% - 60 % in the inner annulus and approximately 0% in the outer annulus (see appendix 4). (txx means maximum tree height app. xx meter)

The cause of the minimal effect is the steep decline of tree transparency towards the outer viewshed annulus (see Figure 39) which is used in the algorithm to compute the fraction of sky which is visible through the trees. The largest effect of this algorithm is visible in the first 20 annuli, after that, the tree transparency drops below 10 %. That means that the angle (relative to the zenith) at which the sky is visible must be below approximately 40 degrees in order to reduce the sky area which is obscured by trees with 10 %.

To give an example, a 12 meter high tree 10 meter away from the sampling location (see Figure 31) would obscure the sky to an angle of approximately 50 degrees, the angle with the zenith would therefore be 40 degrees. The resulting fraction of sky which is obscured by this tree would be compensated for the fraction of sky which is visible through the tree with only 10 percent. In reality, this percentage might be larger.

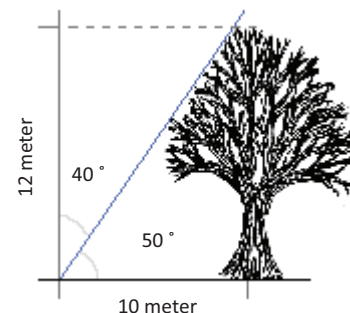


Figure 31: schematic representation of a 12 meter tree 10 meter away from the sampling location

## Results linear tree filter

Two linear filters were tested. The difference lies within the percentage of visible sky in the inner annulus, either 95 % tree transparency or 80 % tree transparency (for all tree transparency curves, see appendix 4. The effect of an overall tree transparency of 90 % was also tested.

In appendix 6, graphs containing all results of the SVF computation using linear tree filters are included (Figure 42 to Figure 45). Two different DEM's were used to create these results, one with a maximum tree height of approximately 17 meter and one approximately 20 meter. The results are split up over 4 graphs (Figure 32 to Figure 35), showing the GIS SVF per filter (either 95 % or 80 % tree transparency in the inner annulus) and computation height (at ground level or 1.5 m above ground level).

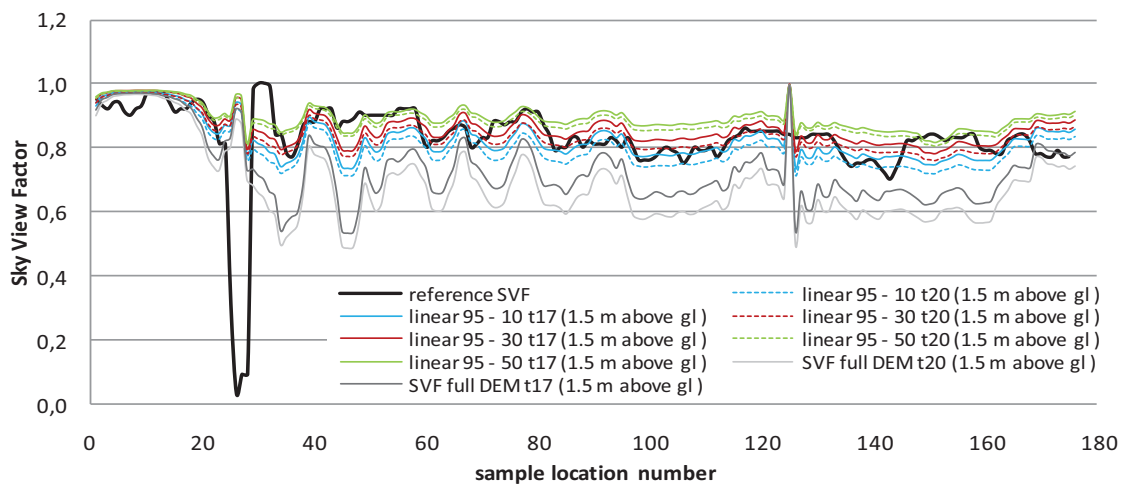


Figure 32: SVF computed at 1.5 meter above ground level (gl), using a linear tree filter (with a linear decrease in tree transparency from 95 % in the inner annulus to 10 % - 50% in the outer annulus). The SVF is based on a DEM containing trees with a maximum height of approximately 17 meter (t17) and a DEM containing trees with a maximum height of approximately 20 meter (t20). The SVF full DEM graphs show the SVF computed without tree filter.

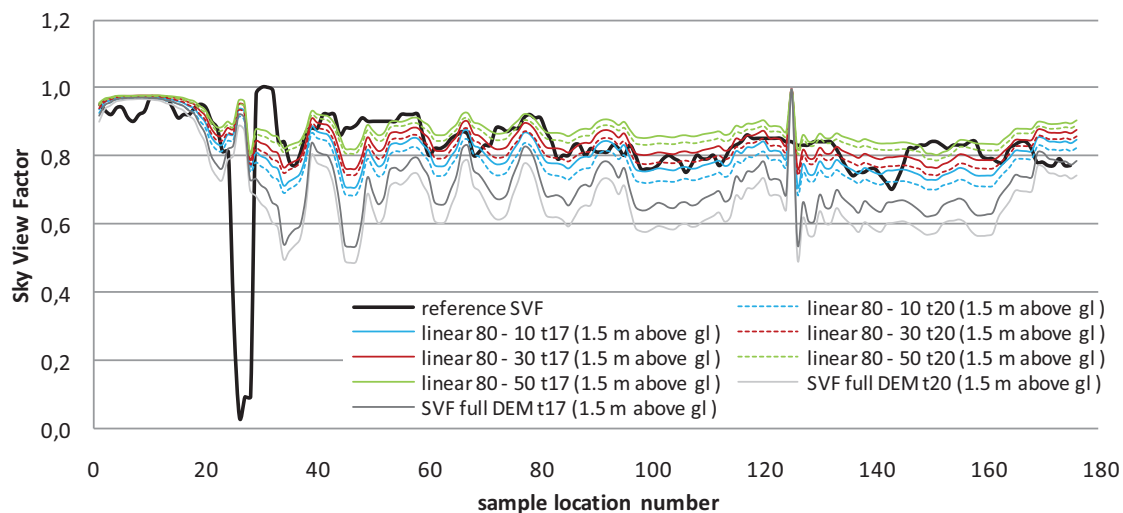


Figure 33: SVF computed at 1.5 meter above ground level (gl), using a linear tree filter (with a linear decrease in tree transparency from 80 % in the inner annulus to 10 % - 50% in the outer annulus). The SVF is based on a DEM containing trees with a maximum height of approximately 17 meter (t17) and a DEM containing trees with a maximum height of approximately 20 meter (t20). The SVF full DEM graphs show the SVF computed without tree filter.



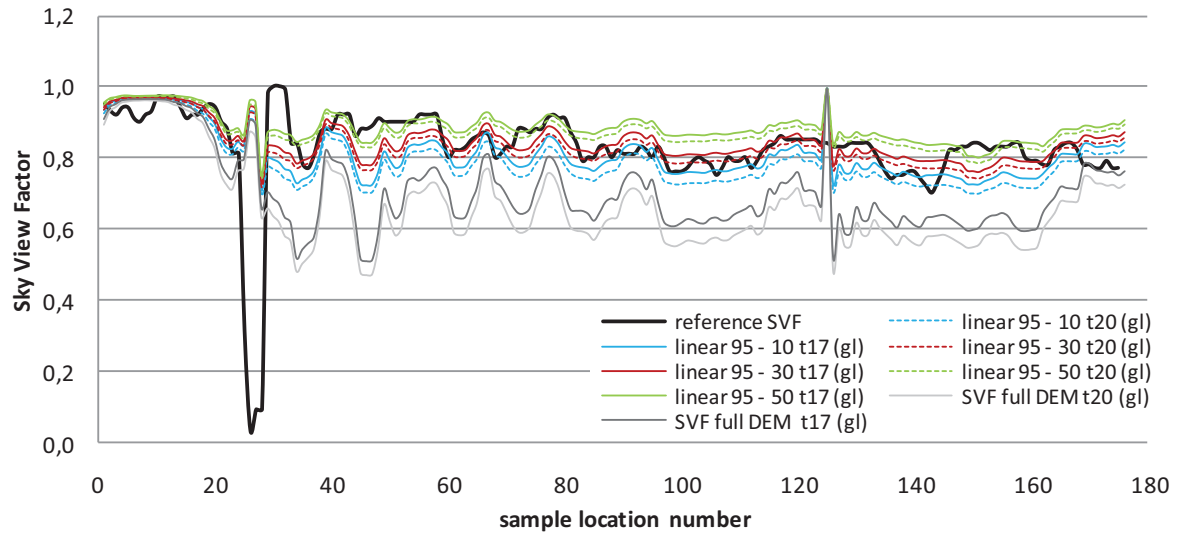


Figure 34: SVF computed at ground level (gl), using a linear tree filter (with a linear decrease in tree transparency from 95 % in the inner annulus to 10 % - 50% in the outer annulus). The SVF is based on a DEM containing trees with a maximum height of approximately 17 meter (t17) and a DEM containing trees with a maximum height of approximately 20 meter (t20). The SVF full DEM graphs show the SVF computed without tree filter.

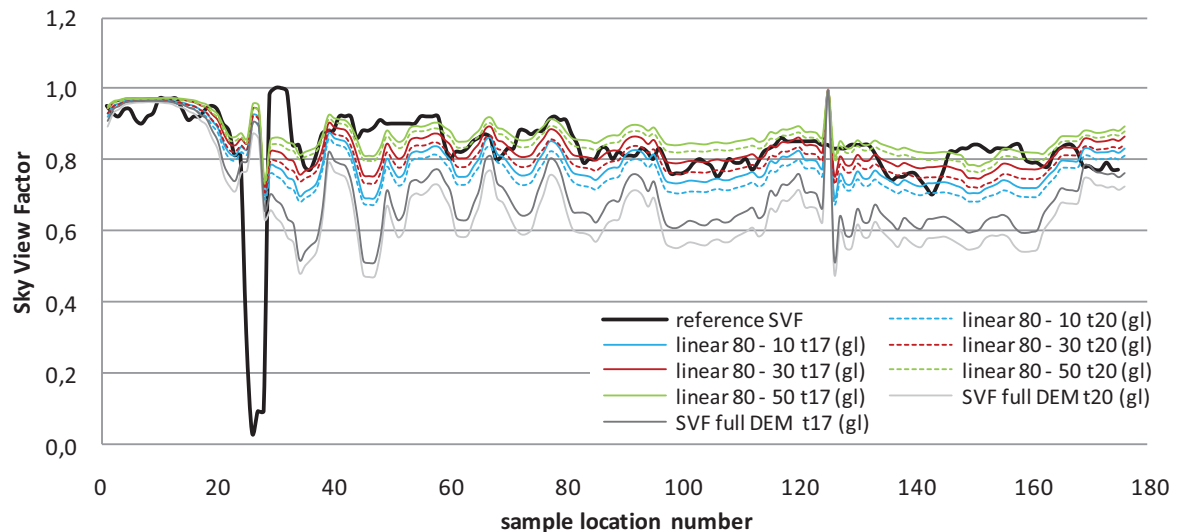


Figure 35: SVF computed at ground level (gl), using a linear tree filter (with a linear decrease in tree transparency from 80 % in the inner annulus to 10 % - 50% in the outer annulus). The SVF is based on a DEM containing trees with a maximum height of approximately 17 meter (t17) and a DEM containing trees with a maximum height of approximately 20 meter (t20). The SVF full DEM graphs show the SVF computed without tree filter.

Several observations can be made:

1. The application of the linear tree filters brings the computed SVF much closer to the reference SVF compared to the SVF computed without compensation for tree transparency. The graphs of the 95 % to 30% filter and the 80 % - 30 % filter seem to be the closest to the graph of the reference SVF, the other filters are over- or underestimating the SVF to a greater extent.
2. The steep peaks (positive and negative) and variations in trend of the graphs which are visible in the SVF computed without a tree filter are weakened by the application of the tree filters. The higher the tree transparency in the outer annulus of the tree filter, the larger the damping effect;

3. In certain areas the magnitude of the effect of the tree filter differs from other areas. Compare for example the difference in the computed SVF with and without tree filter at point 5 – 10 with the SVF at for example points 100 – 120. At point 5 – 10 the effect is barely noticeable whereas the effect is clearly visible (an increase in SVF) at points 100 – 120;
4. On first sight, no large differences between the SVF computed at ground level and the SVF computed at 1.5 m above ground level can be observed. The use of the different maximum tree heights does make a difference. The difference seems to be larger with the filters with a low tree transparency in the outer annulus, compared to the filters with a high tree transparency in the outer annulus;
5. The effect of the tree filter seems increase if the SVF computed without a tree filter decreases.

#### AD 1:

The improvement of the GIS SVF caused by the application of the tree filters is confirmed by the scatterplots,  $R^2$  values and trend line equations of the GIS SVF with and without tree filter against the reference SVF (see Table 10, Table 11 and Table 12). In Table 1 the best results per DEM per SVF measurement height are shown.

Table 1: Maximum improvements of the GIS SVF results caused by the application of the tree filters. The results are based on the scatterplots of the GIS SVF against the reference SVF as shown in Table 10, Table 11 and Table 12.

SVF computation method	Max increase $R^2$	Trend line equation ( $y = \dots$ ) improvement (no tree filter applied) $\rightarrow$ (tree filter applied)
Trees max 17 m, at ground level	0.0003	(0.8436 X) $\rightarrow$ (1.0064 X)
Trees max 17 m, 1.5 m above ground level	0.0445	(0.8719 X) $\rightarrow$ (1.0067 X)
Trees max 20 m, at ground level	0.1288	(0.7929 X) $\rightarrow$ (0.9858 X)
Trees max 20 m, 1.5 m above ground level	0.1009	(0.8182 X) $\rightarrow$ (0.998 X)

Looking at the graphs (Figure 32 to Figure 35) one can observe that a tree filter which approaches the reference SVF closely at one location might be further away from the reference SVF in other locations. This phenomena can be explained by 2 factors: the accuracy of the data and the accuracy of the model.

Inaccuracy of the data is causing the two main features (errors) in the graphs (at points 22 – 33 and points 123 – 130 (see paragraph 3.3.1 for an explanation of these errors). The phenomena described above is most likely caused by a combination of the inaccuracy of the data and errors in the GIS model (the parameterization of the tree filter and the modelling of the trees in the DEM to be more specific). Further comprehensive analysis of the results is required to determine to what extent the deviations can be put down to data inaccuracies, model inaccuracies or a combination of both.

In order to determine which of the GIS SVF results on average approached the reference SVF the best, scatterplots of the GIS SVF against the reference SVF were created. In Table 2 the  $R^2$  values and the trend line equations of the GIS SVF against the reference SVF from Figure 32 to Figure 35 are shown. The corresponding scatterplots are included in Table 11 and Table 12 in Appendix 5.

Based on the hypothesis that the GIS SVF is exactly the same as the reference SVF one would expect an  $R^2$  value of 1 and a trend line equation of  $Y = X$  (through (0,0)). In Table 2 (next page) one can see that such a result was not obtained.

Table 2:  $R^2$  values and trend line equations of the SVF computed at ground level (left) and  $R^2$  values and trend line equations of the SVF computed at 1.5 m above ground level (right). The SVF computations are based on 2 different maximum tree heights (17 and 20 meter [t17 and t20]) and 2 different tree filters (95 % and 80 % tree transparency in the inner annulus).

Erroneous values of which the cause of the error could be explained were removed from the analysis (22-33 and 123-130). In both sides of the table the 3 highest  $R^2$  values are marked (bold and italic), as well as the three trend line equations approaching  $Y = X$  the closest. In the trend line equation  $Y$  is the GIS SVF,  $X$  is the reference SVF. The trend line was forced through (0,0).

Tree filter	$R^2$	Trend line equation ( $y = \dots$ )	Tree filter	$R^2$	Trend line equation ( $y = \dots$ )
t17 95 - 10	0.3205	<b><i>1.0064 X</i></b>	t17 95 - 10	0.42	0.979 X
t17 95 - 30	-0.207	1.0502 X	t17 95 - 30	0.2189	1.202 X
t17 95 - 50	-3.622	1.1155 X	t17 95 - 50	-0.455	1.0616 X
t20 95 - 10	<b><i>0.4969</i></b>	0.9365 X	t20 95 - 10	<b><i>0.4767</i></b>	0.9507 X
t20 95 - 30	0.4156	<b><i>0.9858 X</i></b>	t20 95 - 30	0.3614	<b><i>0.998 X</i></b>
t20 95 - 50	0.0215	1.0352 X	t20 95 - 50	-0.125	1.0453 X
t17 80 - 10	0.3911	<b><i>0.9911 X</i></b>	t17 80 - 10	<b><i>0.4368</i></b>	0.9653 X
t17 80 - 30	0.0686	1.0349 X	t17 80 - 30	0.3107	<b><i>1.0067 X</i></b>
t17 80 - 50	-0.979	1.0786 X	t17 80 - 50	-0.117	1.0479 X
t20 80 - 10	<b><i>0.4917</i></b>	0.9177 X	t20 80 - 10	<b><i>0.478</i></b>	0.9335 X
t20 80 - 30	<b><i>0.4624</i></b>	0.9671 X	t20 80 - 30	0.422	<b><i>0.9809 X</i></b>
t20 80 - 50	0.2499	1.0164 X	t20 80 - 50	0.145	1.0281 X

Looking at the (marked) values in Table 2, one can see that in all cases, the filters with the lowest tree transparency (10 %) in the outer annulus have the highest correlation with the GIS SVF. The trend line resembling the reference SVF the closest however, is in most cases the filter with 30 % tree transparency in the outer annulus.

This fact is most likely caused by the increasing dampening effect of the filters as the tree transparency in the outer annulus increases. Although the application of the tree filters brings the GIS SVF results closer to the reference SVF, at the same time it dampens the trends in the computed SVF. This results in a trend line equation closer to  $Y = X$ , but a lower correlation between GIS SVF and reference SVF.

## AD 2 and 3:

The dampening effect is most likely caused by the coarse modelling of reality using a raster DEM with 5 x 5 m resolution. This method does not allow for very detailed modelling, whereas the photographic method uses the most accurate representation of reality, namely reality itself. This way, much more details are included in the analysis, resulting in a much more detailed SVF computation.

The difference in magnitude of the effect of the tree filters was expected, due to the nature of the computation of the amount of sky which is visible in through trees (see paragraph 2.3.5 and 2.3.6). The tree filter is used to add a fraction of the sky which is obscured by trees to the fraction of visible sky in the viewshed. If there are no trees present, no extra visible fraction of sky will be added, but if the number of trees present (or the size) increases, the fraction of sky which is added to the fraction of visible sky will increase with it.

Depending on the amount, location and size of the trees which are present in the area surrounding the sampling location, the magnitude of the effect changes.

This also shows in the graphs: in the area surrounding point 1 – 20, in the GIS model no trees are present. Therefore, the application of the tree filter has no effect. But in the area surrounding for example point 30 – 50, tree rows occur on both sides of the sampling locations. In these areas, an increase of almost 0.2 in computed SVF can be observed (compared to the GIS SVF without tree filter).

#### AD 4:

From the graphs, hardly any difference between the SVF computation at ground level and the SVF computation at 1.5 m above ground level is visible. This is confirmed by the computation of the  $R^2$  value and the calculation of the equation of the trend line which was forced through (0,0).

As can be seen in Table 3 none of the  $R^2$  values are below 0.99, indicating a strong correlation between the SVF measured at ground level and 1.5 m above ground level. From the equations, one can observe that on average the SVF at ground level is systematically slightly lower than at 1.5 m above ground level (largest average deviation in Table 3 is 1.9%).

Table 3: 4 Randomly selected examples of scatterplots of the SVF computed at ground level against the SVF computed at 1.5 m above ground level. The left column contains results SVF results based on a DEM containing trees of maximum 20 meter high, the left column 17 meter. ). Erroneous values of which the cause of the error could be explained were removed from the analysis (22-33 and 123-130).  $R^2$  value and equation based on a trend line forced through (0,0).

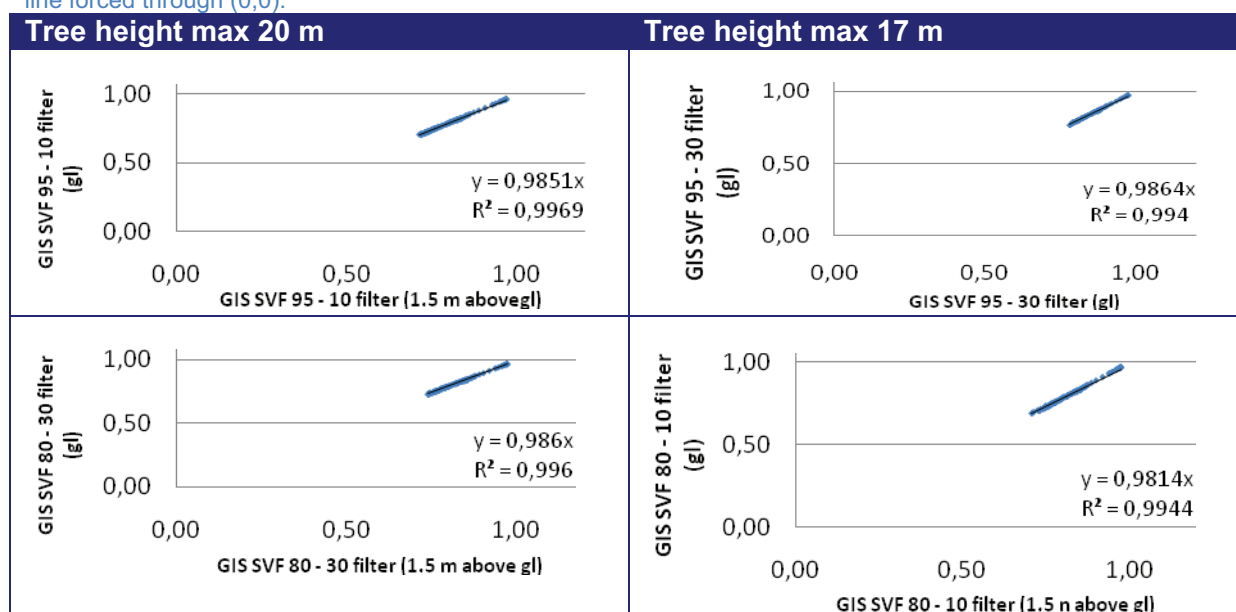
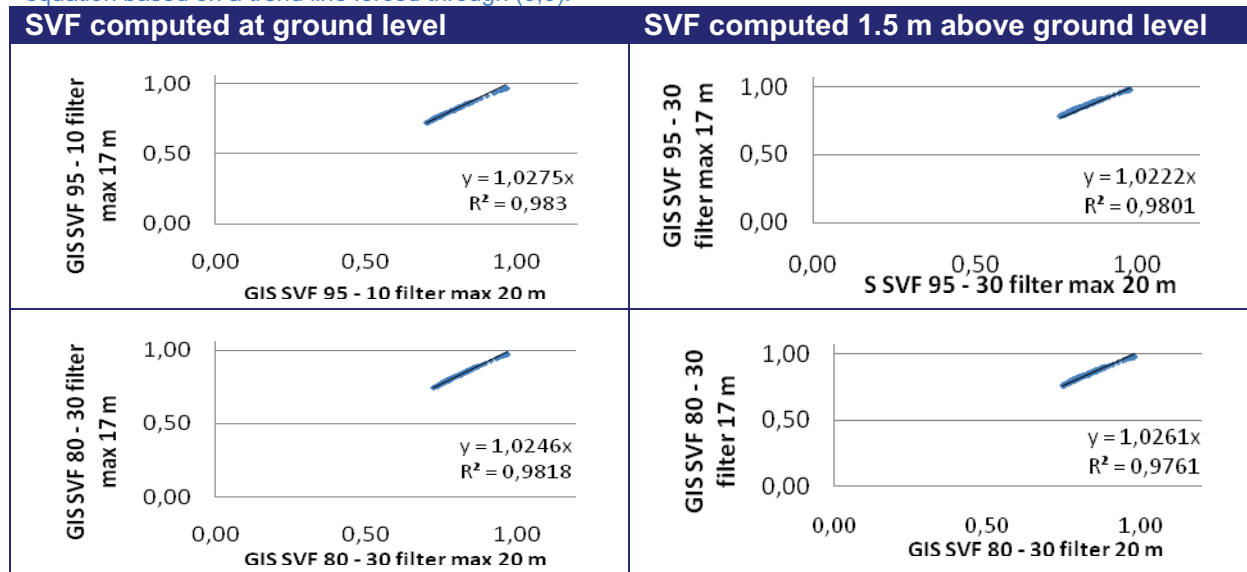


Table 4: 4 Randomly selected examples of scatterplots showing the SVF computed using a DEM with trees with a maximum height of approximately 17 meter against the SVF computed using a DEM with trees with a maximum height of approximately 20 meter. In the left column are 2 examples of the SVF computed at ground level. In the right column are 2 examples of the SVF computed 1.5 meter above ground level. Erroneous values of which the cause of the error could be explained were removed from the analysis (22-33 and 123-130).  $R^2$  value and equation based on a trend line forced through (0,0).



From Table 4 one can observe that there is a strong correlation (for these examples  $> 0.976$ ) between the SVF based on a maximum tree height of 17 and 20 meter. From the trend line equations one can observe that the difference between the SVF based on a maximum tree height of 17 meter on average is systematically higher than the SVF based on a maximum tree height of 20 meter. This was to be expected since the obstruction of the sky view increases with an increase in tree height.

**AD 5:** This phenomena predominantly occurs in tree rich, building poor areas. It is caused by the mathematical nature of the tree filter. Areas with trees are abundant in the area of interest, whereas buildings occur only incidentally. Computation of the SVF in these areas results in low SVF's if the trees are taken into account. If trees are left out of the computation, the SVF approaches 1 in large parts of the area (see Figure 36).

The tree filter adds a percentage of the difference between the SVF computed with and without trees to the final SVF result, in order to compensate for the fraction of sky which is visible through trees.

The SVF in an areas with a high tree density will be lower than the SVF in areas with a low tree density (leaving buildings out consideration for now). If the SVF without trees approaches 1, in tree rich areas the difference between SVF with trees and without trees will be larger compared to areas with fewer trees.

A larger fraction of sky obscured purely by trees will thus result in a larger fraction of sky added to the already visible fraction of sky compared with areas with only a small fraction of the sky obscured purely by trees.

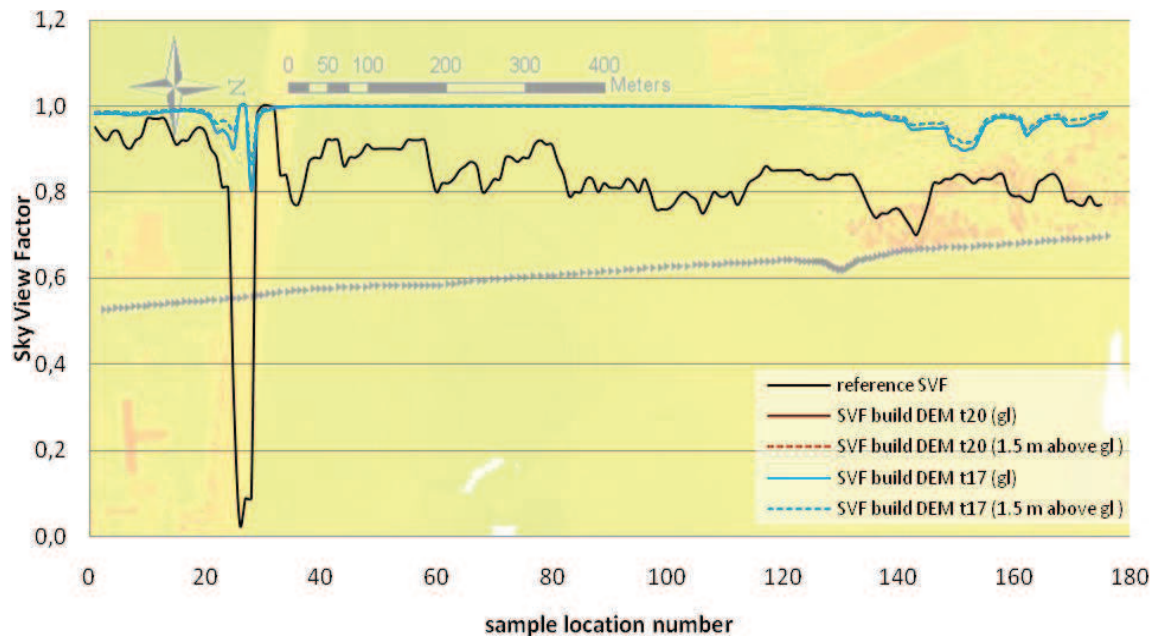


Figure 36: SVF computed with the source DEM (AHN 2000 5 x 5) which (theoretically) does not contain tree heights.



## 3.4 Validation of the results

### 3.4.1 Validation using the Network model

The validation of the results of this research was executed by M. Wokke at the Meteo Consult office. Due to time limitations only the GIS SVF and viewsheds based on a DEM containing trees with a maximum height of approximately 17 meter (measured 1.5 meter above ground level) were tested. The forecasted RST was compared with the forecasted RST based on the reference SVF and the actually measured RST.

The RST was computed (forecasted) for March 14<sup>th</sup> 2007, 01:00 UTC. The actual RST was measured using an infrared measuring device mounted behind a car, between March 13<sup>th</sup> 23:00 UTC and March 14<sup>th</sup> 02:00 UTC. Note that the temperature sampling locations do not exactly coincide with the location at which the SVF is computed and the RST forecasted. A difference of 0 – 6 meter is possible (Wokke 2008).

Below, the results of the RST forecast using the network model and the GIS / reference SVF and viewsheds is shown. The measured RST at the time of the forecast is also included in the graphs.

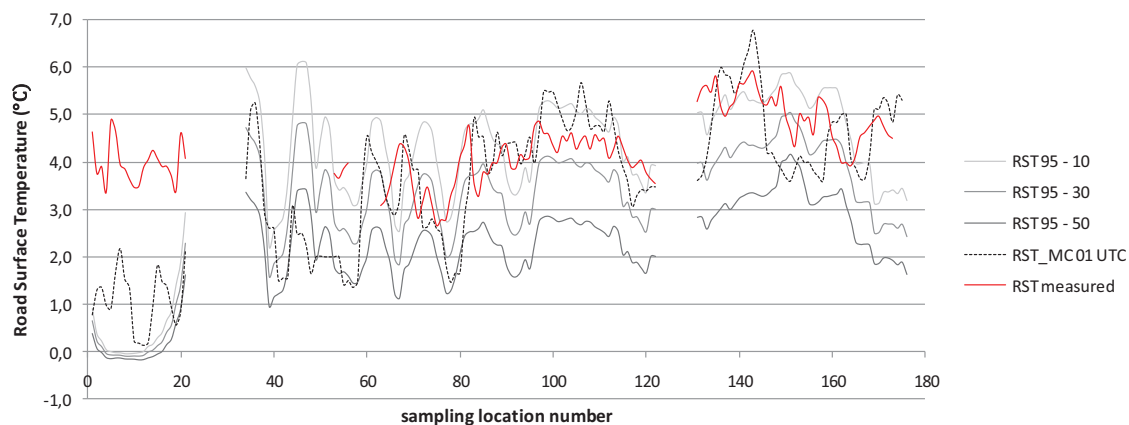


Figure 37: Forecasted RST based on GIS SVF and viewsheds computed with the tree filters with 95 % tree transparency in the inner annulus (grey lines) and reference SVF (dotted line). The red line indicates the measured actual RST. Erroneous values of which the cause of the error could be explained were removed from the analysis (22-33 and 123-130).

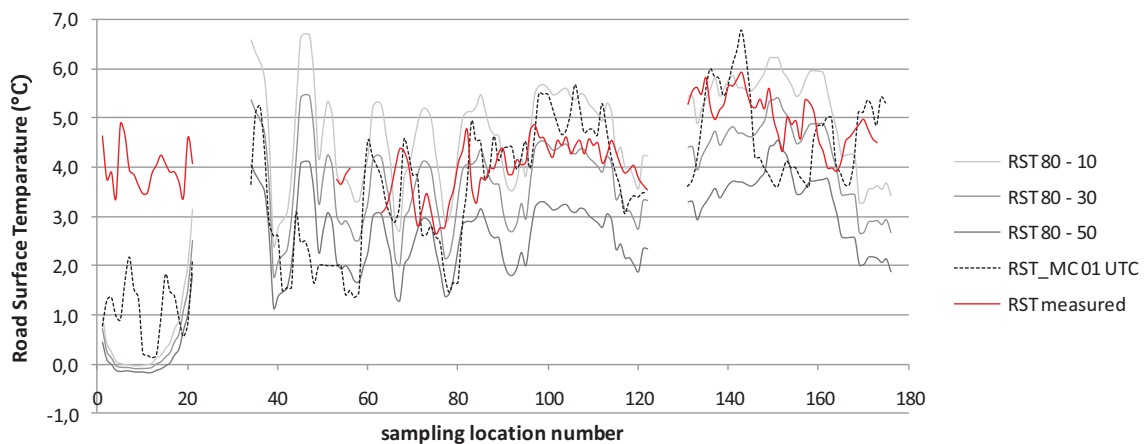


Figure 38: Forecasted RST based on GIS SVF and viewsheds computed with the tree filters with 80 % tree transparency in the inner annulus (grey lines) and reference SVF (dotted line). The red line indicates the measured actual RST. Erroneous values of which the cause of the error could be explained were removed from the analysis (22-33 and 123-130).

The main features to focus on in Figure 37 and Figure 38 is the comparison between the forecasted RST based on GIS data and the forecasted RST based on the reference SVF. In the graphs, at certain locations the GIS-based RST matches the reference SVF-based RST, in other locations differences over 3 °C occur. The magnitude of this difference can be traced back to the differences in SVF as shown in Figure 32 to Figure 35. If the GIS SVF is overestimating the reference SVF, the GIS-based forecasted RST will be lower than the reference SVF-based RST and vice versa. The magnitude of the difference depends on the magnitude of the difference between the GIS SVF and the reference SVF.

At sample location 142 for example, the difference between the RST 80 - 50 and the reference SVF-based RST is 3.4 °C. The difference in SVF at this point is approximately 1.2. Compare this to a location with the GIS SVF matching the reference SVF (point 78 for example) and the forecasted RST based on the GIS SVF lies within 0.1 °C from the reference SVF-based RST.

This way, all differences can all be traced back to the phenomena described in paragraph 3.3.1 and 3.3.2. Further analysis of the results is required to determine precisely what is causing the differences, data errors, model errors or a combination of both.

In order for the GIS application to be able to replace the photographic method, the results of the GIS-based RST forecast should match the results of the reference SVF-based RST forecast. Because Meteo Consult does not use a specific threshold temperature for road slipperiness risk, but a combination of amongst others air moisture level and temperature (Wokke 2009), for this research the threshold value of 0 °C (the temperature at which water freezes) was used. In this particular case, based on the reference RST no risk of water freezing occurs. Based on the GIS RST this is not the case, with freezing risk at sample locations 4 to 16.

A striking feature in Figure 37 and Figure 38 is that the GIS based RST forecast clearly shows less variation than the reference SVF-based RST forecast. This phenomena is caused by the same phenomena which dampens the trends in computed SVF as described in paragraph 3.3.2 (page 39).

From the graphs it is difficult to say which tree filter on average approached the reference SVF-based RST the closest. In order to determine the best result, scatterplots were created of the GIS based RST forecast against the RST forecast based on the reference SVF. The scatterplots are included in Table 13 in appendix 7.

Table 5:  $R^2$  values and trend line equations of the GIS based RST forecasts against the RST forecasts based on the reference SVF. Erroneous values of which the cause of the error could be explained were excluded from the analysis (22-33 and 123-130). The trend line equations are based on trend lines forced through (0,0).

Filter	$R^2$ value	Trend line equation (Y = ...)
RST 95 - 10	0,3891	1,0602 X
RST 95 - 30	0,4294	0,8319 X
RST 95 - 50	0,4678	0,5892 X
RST 80 - 10	0,3744	1,1334 X
RST 80 - 30	0,3821	0,9016 X
RST 80 - 50	0,4234	0,6661 X

From Table 5 one can see that although the application of tree filters 95 – 30 and 95 – 50 show the highest  $R^2$  values, the 95 – 10 and 80 – 30 tree filter based RST forecasts are on average closer to the reference SVF-based RST, with trend line equations approaching Y = X.

In Figure 37 and Figure 38 the actual measured RST at the time of the RST forecast is also shown. From the graphs it is obvious that none of the forecasts (neither GIS-based nor reference SVF-based) closely approach the actual RST (see also Table 14 and Table 15 in appendix 8 for scatterplots of the forecasted RST plotted against the measured RST, measured temperature can deviate +/-0.5 degrees (Wokke 2009)).

The major cause of these differences is the fact that the RST forecast itself is (amongst others) based on forecasted weather conditions. This causes a level of uncertainty in the RST forecast. Apart from that, not all parameters influencing the RST are included in the Network model, simply because that is not feasible. Heavy traffic for instance, can increase RST. Local variations in asphalt / soil properties can also influence RST.

### **Comparison with other scientific researches**

Unfortunately, scientific literature does not provide any reference to comparable GIS SVF results. However, several methods of computing SVF using a GIS are being described.

Souza et al. (2003) developed a GIS 3D Sky View extension for computing SVF. This extension computes SVF based on vector data (specifying building polygons and their height) and a point feature specifying the viewers location (coordinates, elevation and height). Their method was only applied to urban areas without trees. No actual results or quality of the results were included in their report.

Li et al. (2004) also used a GIS for computing the SVF. They applied their method in urban areas, leaving trees out of consideration. Also, instead of ArcMap / ArcCatalog and a raster DEM, ArcScene and a TIN (Triangulated Irregular Network) were used. A custom tool capable of computing SVF based on a TIN and a point shapefile containing viewing locations was developed for this purpose.

In this study, SVF was computed for 11 locations on the Singapore Management University campus. The quality of the SVF results or the accuracy of their method were not quantified. Li et al. (2004) conclude that SVF can be computed in ArcGIS effectively and efficiently for urban environment (including existing built area and proposals) although technical limitations exist. These findings are confirmed by this research project.

Gál et al (2008) also used a GIS to compute SVF. Again, a custom tool for SVF calculation was developed. Both a vector DEM and a raster DEM (resolution 2 x 2 m) were used to compute SVF. The SVF was only computed in urban areas (without trees).

Although the relation between the annual mean heat island and the SVF calculated by different methods is quantified (using  $R^2$  values and regression equations), the actual quality of the SVF results is not.

The conclusion was drawn that the use of vector and raster DEM's yielded very similar results for urban geometry, although in the vector approach, more (geometrical) details could be included. An advantage of the raster based method is that it was significantly faster than the vector based method.

## 4 Conclusion and recommendations

### 4.1 Conclusion

As the results of the validation process of this research pointed out, the forecasted RST based on the GIS SVF differed from the RST forecast based on the reference data. For certain locations the GIS based RST forecast showed temperatures below 0 °C whereas the reference SVF-based RST forecast did not. Therefore the conclusion was drawn that the quality of the GIS SVF method is not yet equal to the photographic method.

There are two main factors which are causing deviations between the GIS SVF and the reference SVF: inaccuracy of the source datasets and current limitations of the method which compensates for the fraction of sky which is visible through bare trees (methodological inaccuracies). The largest errors in the results could be traced back to errors in the datasets, but further research is required to determine in detail to what extent other errors or anomalies are caused by data inaccuracies, model inaccuracies or a combination of both.

With regard to the improvement of the modelling of the trees the conclusion was drawn that trees were successfully integrated in the GIS SVF computation. The integration of trees in the model and the application of the so-called tree filter resulted in increased correlation coefficients between GIS SVF and reference SVF. Also, after the application of the tree filter, on average the GIS SVF approached the reference SVF closer than before (trend line equations of scatterplots of GIS SVF against reference SVF closer to  $Y = 1 X$  (GIS SVF equals reference SVF))

As mentioned before, the modelling of the trees in the DEM is based on assumptions and estimations in the field. The GIS model requires accurate and comprehensive data on the location and geometry of all 3D static objects in the environment (for example trees and buildings).

This research has shown that the datasets which were used during this project (TOP10vector and AHN 2000 5x5) contain inaccuracies which affect the outcome of this research. Most important is the lack of information with regard to the location, species and geometry of the trees in the research area. But also inaccuracies in the outline of for instance roads in the TOP10vector dataset caused errors in the SVF computation.

Obtaining accurate and comprehensive data on location and geometry of all 3D static objects in the research area would not only increase the SVF model accuracy, it would also make it possible to eliminate the possibility of data inaccuracies while tracing back the cause of errors in the SVF computation.

During this research, several datasets were screened for suitability for the GIS SVF computation. The most accurate dataset containing information with regard to trees known to the author is the GBI (see paragraph 3.2) which was provided by the municipality of Ede. A drawback of this dataset is that only trees managed by the municipality are included in this dataset. Further information on trees on private land as well as more accurate height measurements are essential in order to be able to accurately compute SVF.

Other datasets containing relevant information are the TOP10NL dataset, the point data of the TOP10vector dataset and the GBKN (see paragraph 3.2), also available at the municipality of Ede. One dataset in particular might solve the problem of missing tree height data: the in 2012 to be released AHN-2 (see paragraph 3.2). This is the new version of the DEM of the Netherlands. The raw version of this dataset should contain accurate, high resolution (at least 1x1 meter) height measurements in areas containing trees.

## **4.2 Recommendations**

### **4.2.1 Improvement of the GIS SVF computation**

Potential improvements of the GIS SVF computation can be split up into two categories:

- obtaining (or developing) datasets which are more accurate and comprehensive than the TOP10vector and AHN 2000 datasets;
- improving the GIS SVF computation method.

#### **Dataset improvements**

As mentioned before, new datasets like the AHN II can potentially increase the quality of the GIS SVF. Apart from the datasets mentioned in the conclusion, Meteo Consult will have to monitor the development of new datasets in order to be able to react when a suitable dataset becomes available.

Relevant information is most likely available at municipalities, given the legal requirements with regard to for instance management of trees under the supervision of the municipality (GBI or comparable databases) or detailed information with regard to buildings and roads etcetera (GBKN). The only problem is that in many cases this data is not (yet) available as suitable geodata.

Due to developments in the geo-data field of work, new datasets are being created constantly. An excellent example are the cyclorama's created by Cyclomedia<sup>11</sup>. They are spherical panoramic photographs put together to mimic a 3D environment. These photographs contain information on buildings and trees etcetera. It is not yet possible to extract this information in a way that it is usable in a SVF computation, but the rapid developments in GIS technology might bring these possibilities in the future.

Part of the GIS SVF method is the validation of the results. Specifying and quantifying certain SVF quality criteria (especially the allowed level of deviation from the reference SVF) by means of statistical parameters would make the validation process much more efficient. Due to the fact that the reference dataset so far is based on only 1 observation, this was not yet possible. More research on the validation process and expanding the reference datasets is therefore recommended, as well as creating a dataset with measured RST temperatures (also for validation purposes).

#### **Methodological improvements**

With regard to the current status of the tree filters, it is important to realize that the tree transparency fractions in the tree filters are based on a combination of estimations in the field and trial and error of different parameterizations. More research is required into this as the fraction of visible sky through a bare tree is depending on several factors, for example viewing angle, viewing distance, tree species and age.

Also, currently, the tree filter cannot make the distinction between a single tree and a row of trees (in the viewing direction) obstructing the sky view. This is the difference between looking through a single row of trees next to the road, or a forest next to the road. A different fraction of sky is visible through a single tree as compared to a forest. This also depends on the species of trees and the crown density of the tree or the forest. Implementing these components in the tree filter would benefit the accuracy of the GIS SVF method.

---

<sup>11</sup> <http://www.cyclomedia.nl/>

### 4.2.2 Temporal aspects

Apart from improving the SVF computation method, it is also essential to take temporal aspects into account. So far, these effects have been left out of the research. These effects however, are a relevant component of the SVF computation and require some attention.

The objects influencing the SVF are subject to constant change. Trees grow, die, are trimmed, cut down and or replaced. Buildings are demolished, new buildings are built. Therefore, the SVF is a dynamic factor, it can and will change over time to a certain extent.

The important question is whether these changes will influence the SVF in a way that the forecasted road surface temperature is significantly affected. The answer to this question is essential in determining the rate at which the SVF measurements / computations have to be 'refreshed'. This question occurs regardless from which type of SVF determination method (photographic, using a GIS or otherwise) is used.

In case of the GIS approach, this is predominantly a source data problem. As mentioned before, the AHN is updated every 5 to 10 years. If this dataset is used to extract the tree height / size information and building height from, this information could potentially be 10 years old. The same applies for e.g. building outline information. The TOP10vector dataset which is used in this research has a revision interval of 4 years. In such a time span, major changes can occur.

### 4.2.3 Scientific relevance

Apart from the application in the RST forecasting model described in this report, the development of the GIS SVF application might also benefit other fields of application:

Personal communications with researchers at PBL (Plan Bureau voor de Leefomgeving (Breedijk, M. 2008)) pointed out that researchers were using a similar half product (combined digital elevation model and TOP10vector data) for modelling particle removal by trees and other objects alongside roads. Using an adapted version the SVF computation model, it might be possible to automate the computation the effective filtering surface area of trees alongside roads.

Currently the SVF also is important in other disciplines (for instance urban planning and urban climatology). There is for instance a strong correlation between SVF and the occurrence of so-called 'urban heat islands' (Grimmond et al. 2001, Li et al. 2004, Gál et al. 2008). Having an automated model which can compute SVF might benefit the research on this phenomena.

Another example is the GIS based visibility analysis for urban design evaluation (Yang et al. 2007) or the analysis of sunlight penetration in urban areas. The results of an automated SVF computation method could be used in assessing such parameters.



## Cited References

- Best, M. J. (1998). "A model to predict surface temperatures." Boundary-Layer Meteorology **88**(2): 279-306.
- Blennow, K. (1995). "Sky View Factors from High-Resolution Scanned Fish-eye Lens Photographic Negatives." Journal of Atmospheric and Oceanic Technology **12**(6): 1357.
- Bradley, A. V. (2002). "Modelling spatial and temporal road thermal climatology in rural and urban areas using a GIS." Climate research **22**(1): 41-55.
- Brown, A., S. Jackson, et al. (2008). New techniques for route-based forecasting. Sirwec 2008, Prague.
- Chapman, L. (2001). "Modelling of road surface temperature from a geographical parameter database. Part 2: Numerical." Meteorological applications **8**(4): 421-436.
- Chapman, L. (2001). "Modelling of road surface temperature from a geographical parameter database. Part I: Statistical." Meteorological applications **8**(4): 409-419.
- Chapman, L. (2002). "Sky-view factor approximation using GPS receivers." International journal of climatology **22**(5): 615-621.
- Chapman, L. (2004). "Real-time sky-view factor calculation and approximation." Journal of Atmospheric and Oceanic Technology **21**(5): 730-741.
- Chapman, L. and J. E. Thornes (2006). "A geomatics-based road surface temperature prediction model." Science of The Total Environment **360**(1-3): 68-80.
- Crevier, L. (2001). "METRo: A new model for road-condition forecasting in Canada." Journal of applied meteorology **40**(11): 2026-2037.
- Fry, R., L. Slade, et al. (2007). A GIS based approach to predicting road surface temperatures. Lecture Notes in Computer Science (including subseries Lecture Notes in Artificial Intelligence and Lecture Notes in Bioinformatics). Cardiff. **4857 LNCS**: 16-29.
- Gál, T., F. Lindberg, et al. (2008) "Computing continuous sky view factors using 3D urban raster and vector databases: comparison and application to urban climate." Theoretical and applied climatology **Volume**, DOI: 10.1007/s00704-007-0362-9
- Giffen, H. v., L. Huis, et al. (2008). Assessment of sky-view and other environmental properties based on digital maps. Wageningen, Wageningen UR.
- Grimmond, C. S. B. (2001). "Rapid methods to estimate sky-view factors applied to urban areas." International journal of climatology **21**(7): 903-913.
- Gustavsson, T. (1995). "A study of air and road-surface temperature variations during clear windy nights." International Journal of Climatology **15**(8): 919-932.
- Johnson, G. T. and I. D. Watson (1984). "The determination of view-factors in urban canyons." Journal of Climate & Applied Meteorology **23**(2): 329-335.
- Li, W., S. Y. Putra, et al. (2004). GIS Analysis for the climatic evaluation of 3D urban geometry - The development of GIS analytical tools for sky view factor. GISDECO 2004, Universiti Teknologi Malaysia, Skudai, Johor, Malaysia

- Lindberg, F., I. Eliasson, et al. (2003). Urban geometry and temperature variations. 5th International Conference on Urban Climate, Lodz, Poland.
- Oke, T. R. (1987). Boundary Layer Climates.
- Rayer, P. J. (1987). "The Meteorological Office forecast road surface temperature model." Meteorological Magazine **116**(1379): 180-191.
- Sass, B. (1997). "A numerical forecasting system for the prediction of slippery roads." Journal of applied meteorology **36**(6): 801-817.
- Souza, L. C. L., D. S. Rodrigues, et al. (2003). "A 3D-GIS extension for sky view factors assessment in Urban environment." Proceedings of the 8th International Conference on Computers in Urban Planning and Urban Management.
- Steyn, D. G., J. D. Hay, et al. (1986). "The determination of sky-view factors in urban environments using video imagery." J Atmos Oceanic Technol **3**: 759-764.
- Thornes, J. E. (2005). "XRWIS: The use of geomatics to predict winter road surface temperatures in Poland." Meteorological applications **12**(1): 83-90.
- Watson, I. D. and G. T. Johnson (1987). "Graphical estimation of sky view-factors in urban environments." Journal of climatology **7**(2): 193-197.
- Wokke, M. J. J. and J. S. P. Wisse (2007). Meteorologen onderzoeken invloeden op wegdektemperatuur. Land + Water. **12**: 28-29.
- Yang, P. P. (2007). "Viewsphere: a GIS-based 3D visibility analysis for urban design evaluation." Environment & planning. B **34**(6): 971.

#### **Personal communications:**

- Breedijk, M. (2008). Navteq data PBL / Wageningen University meeting. Utrecht
- Dijke, D. v. (2008). Thesis subject meeting. J. J. M. Steenbergen. Wageningen.
- Dijke, D. v. (2009). Effect of Sky View in the Netherlands. J. J. M. Steenbergen. Wageningen.
- Wokke, M. J. J. (2008). RST model description. J. J. M. Steenbergen. Wageningen.
- Wokke, M. J. J. (2009). Validation GIS SVF. J. J. M. Steenbergen. Wageningen.

#### **Online resources:**

- ESRI. (2007, March 15, 2007). "ArcGIS 9.2 desktop help." Retrieved 2008-09-27, 2008, from <http://webhelp.esri.com/arcGISdesktop/9.2/>.
- ESRI. (2007, 2007-03-27). "ArcGIS Desktop Help 9.2." Retrieved 2008-09-27, 2008, from <http://webhelp.esri.com/arcGISdesktop/9.2/>.
- Khawaja, K. Q. (2002). "r.los - Line-of-sight raster analysis program." Retrieved 2008-10-03, 2008, from [http://grass.itc.it/grass53/manuals/html53\\_user/html/r.los.html](http://grass.itc.it/grass53/manuals/html53_user/html/r.los.html).
- RGI. "<http://www.rgi.nl/>." Retrieved 2008/07/18, 2008.

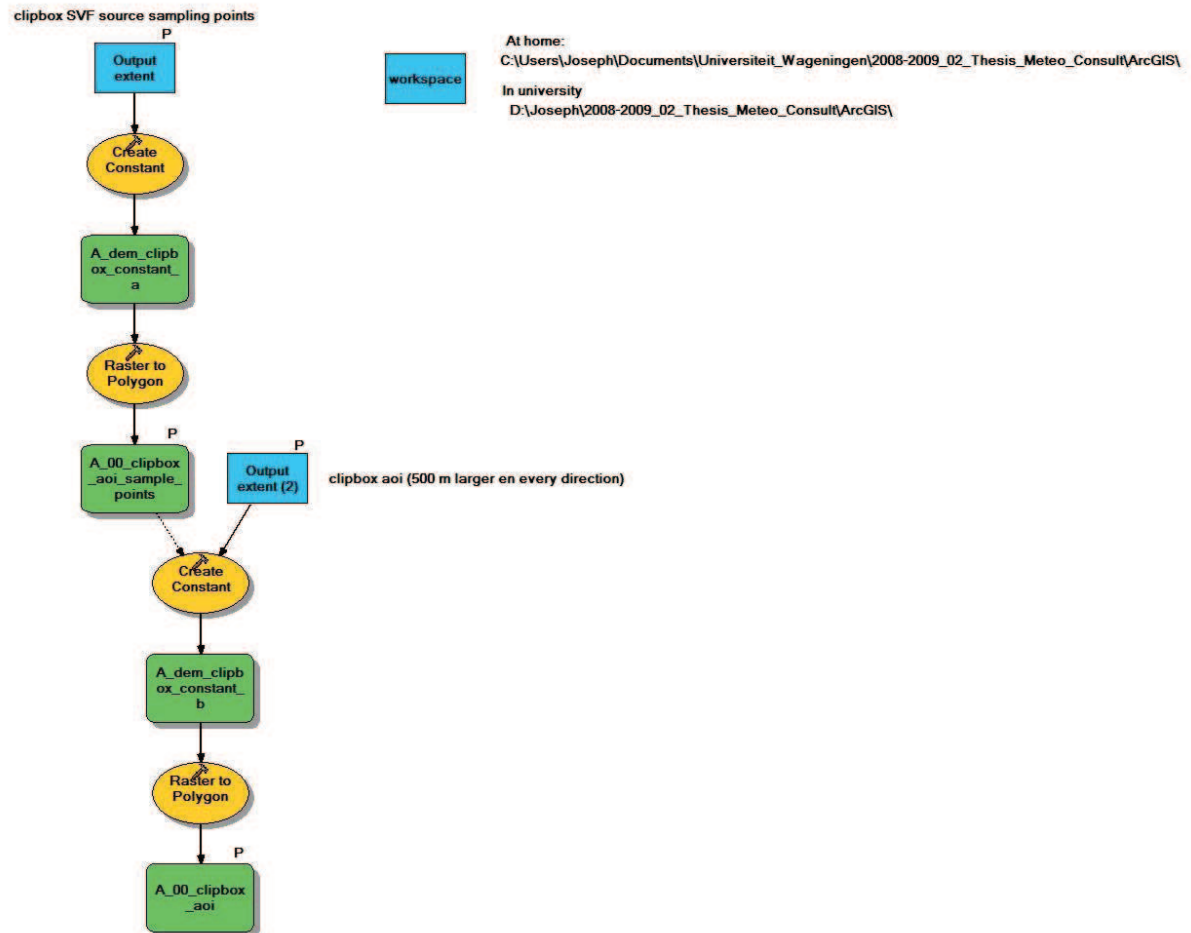
#### **Software:**

- ESRI (2006). Arc-GIS. Redlands.

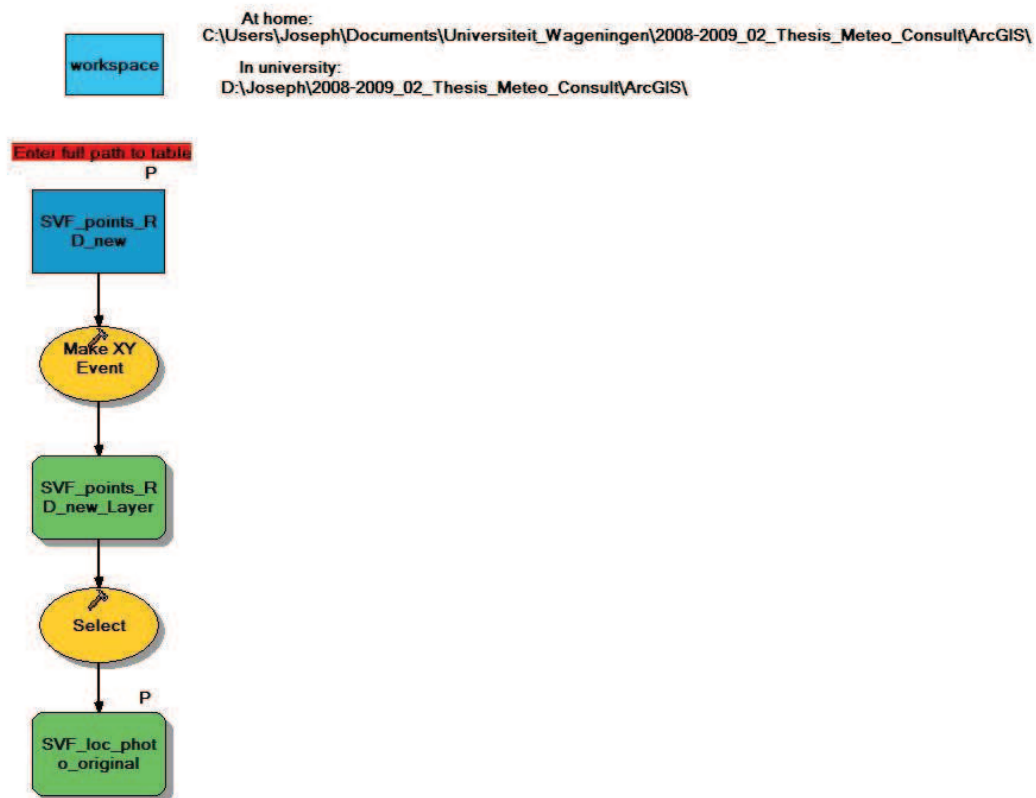
# Appendices

## Appendix 1: Model graphics.

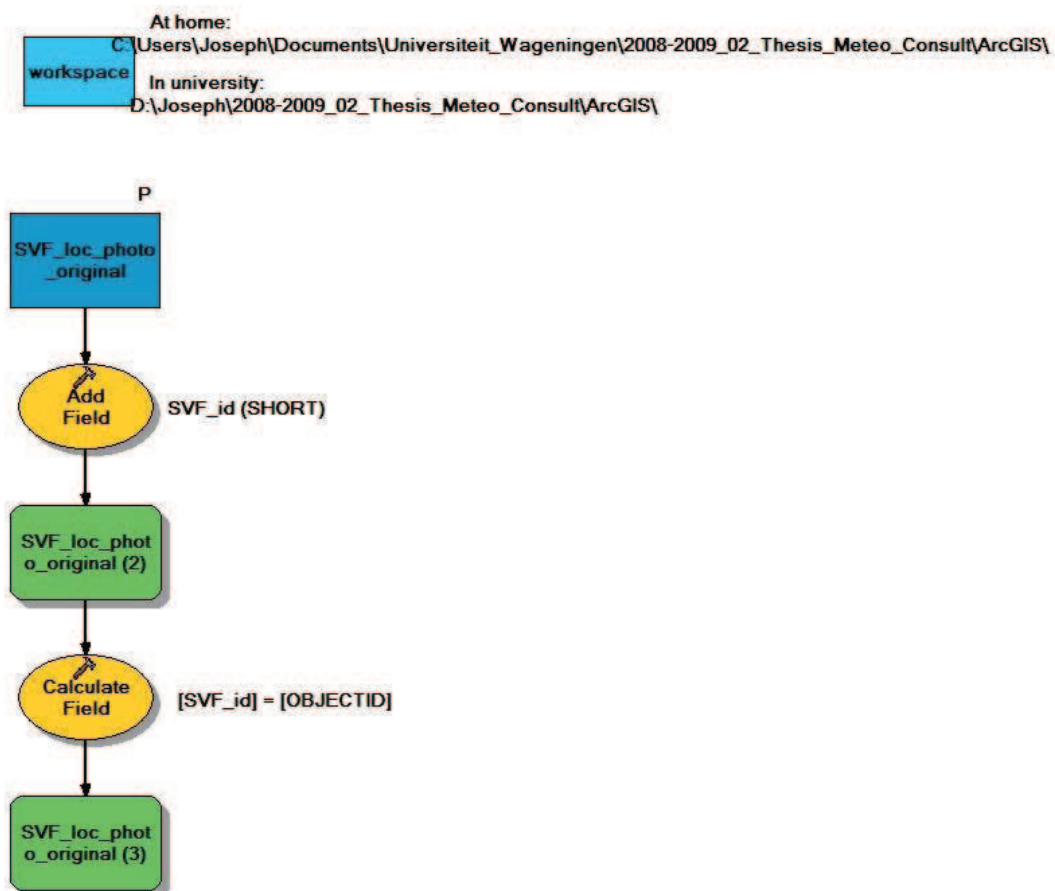
### 1.1: SVF\_A\_00\_create\_project\_clipbox



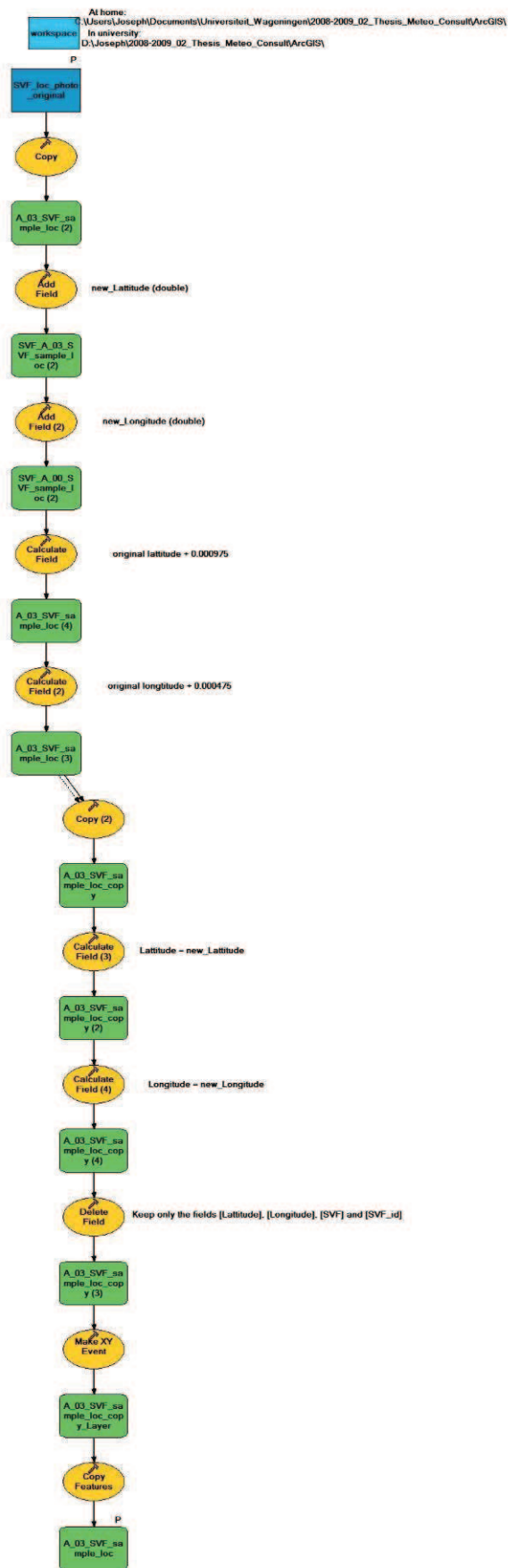
## 1.2: SVF\_A\_01\_import\_gps\_locations\_reference\_SVF



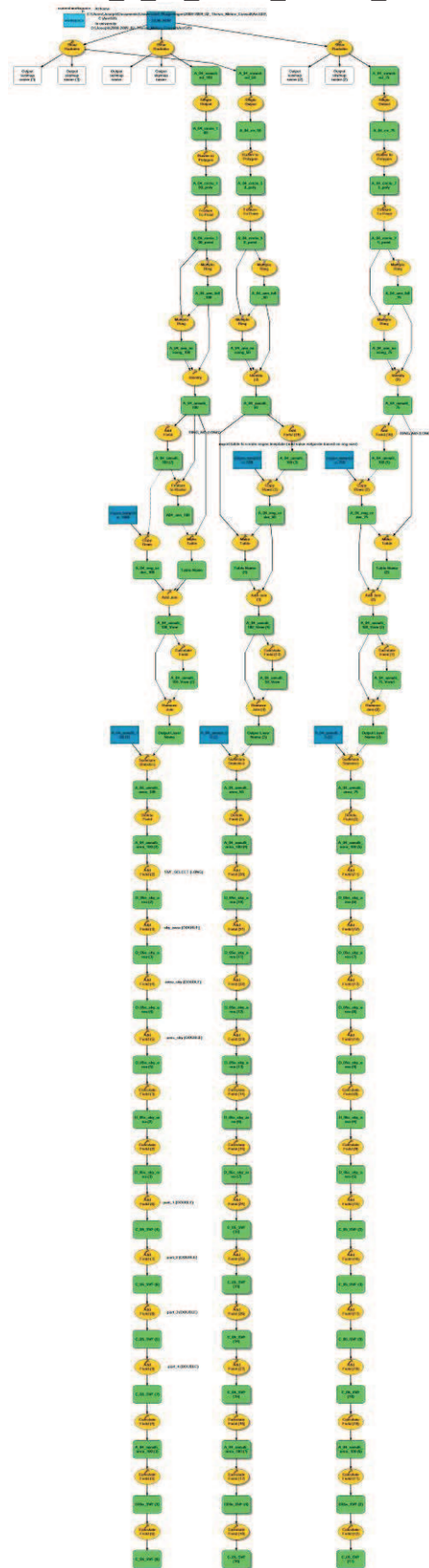
## SVF\_A\_02\_add\_location\_ids\_to\_SVF\_tables



### 1.3: (SVF\_A\_03\_reproject\_SVF\_sample\_locations)



#### 1.4: SVF\_A\_04\_create\_annular\_templates

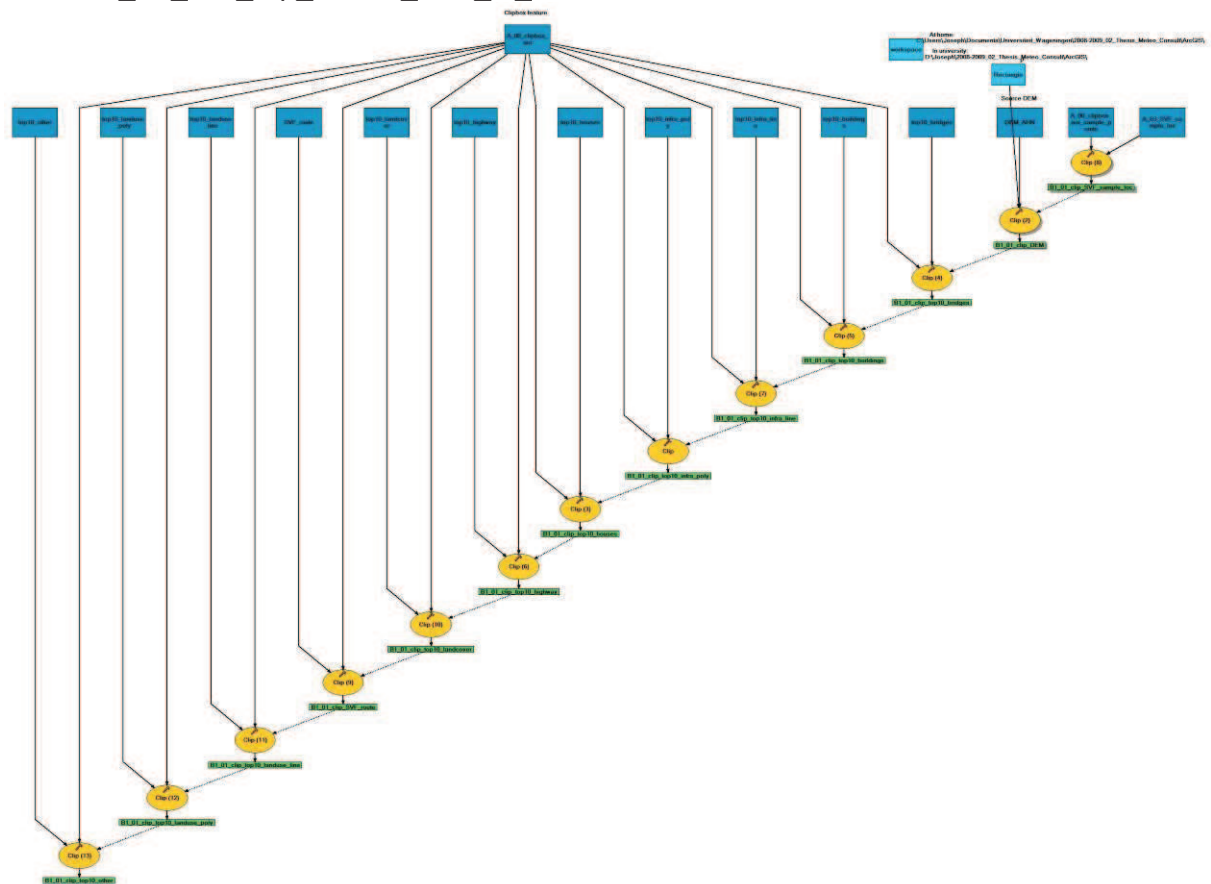




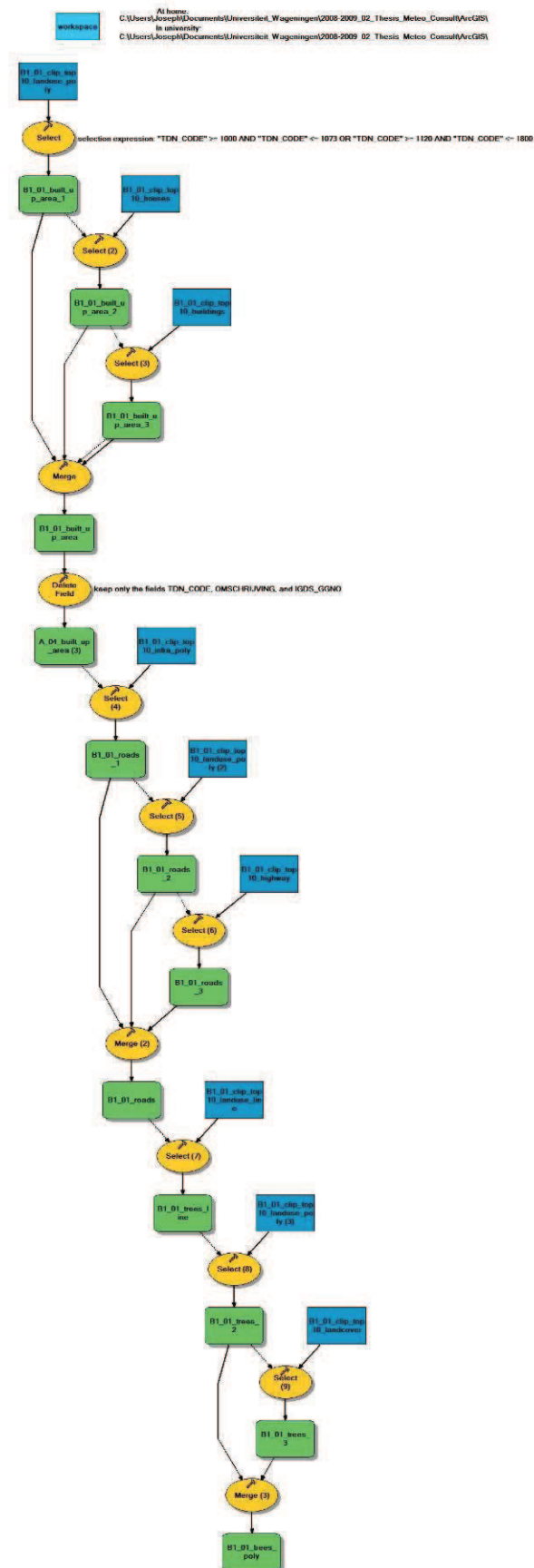
### 1.5: SVF\_A\_05\_create\_raster\_annular\_template



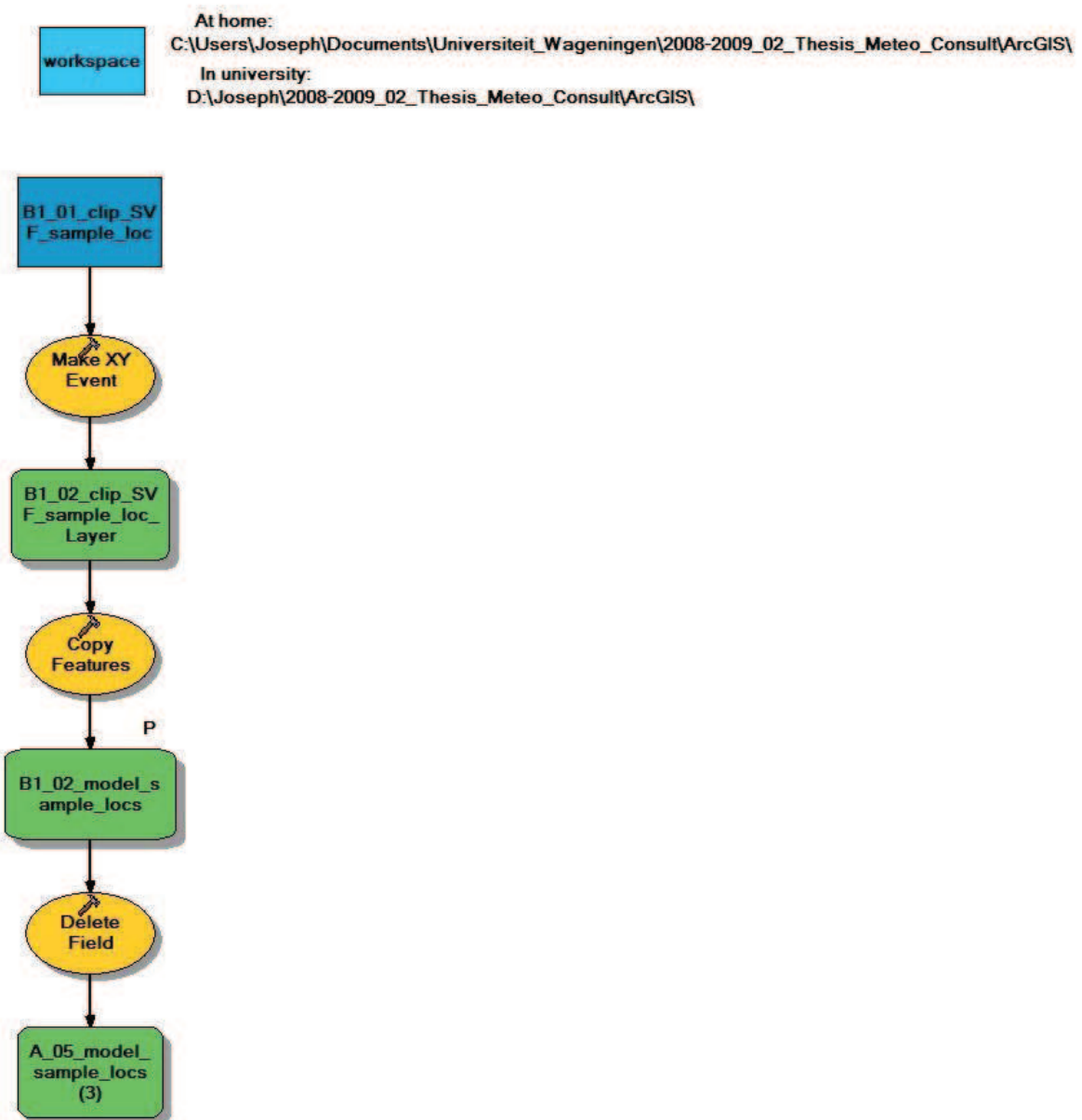
## 1.6: SVF\_B1\_01a\_clip\_source\_data\_to\_aoi



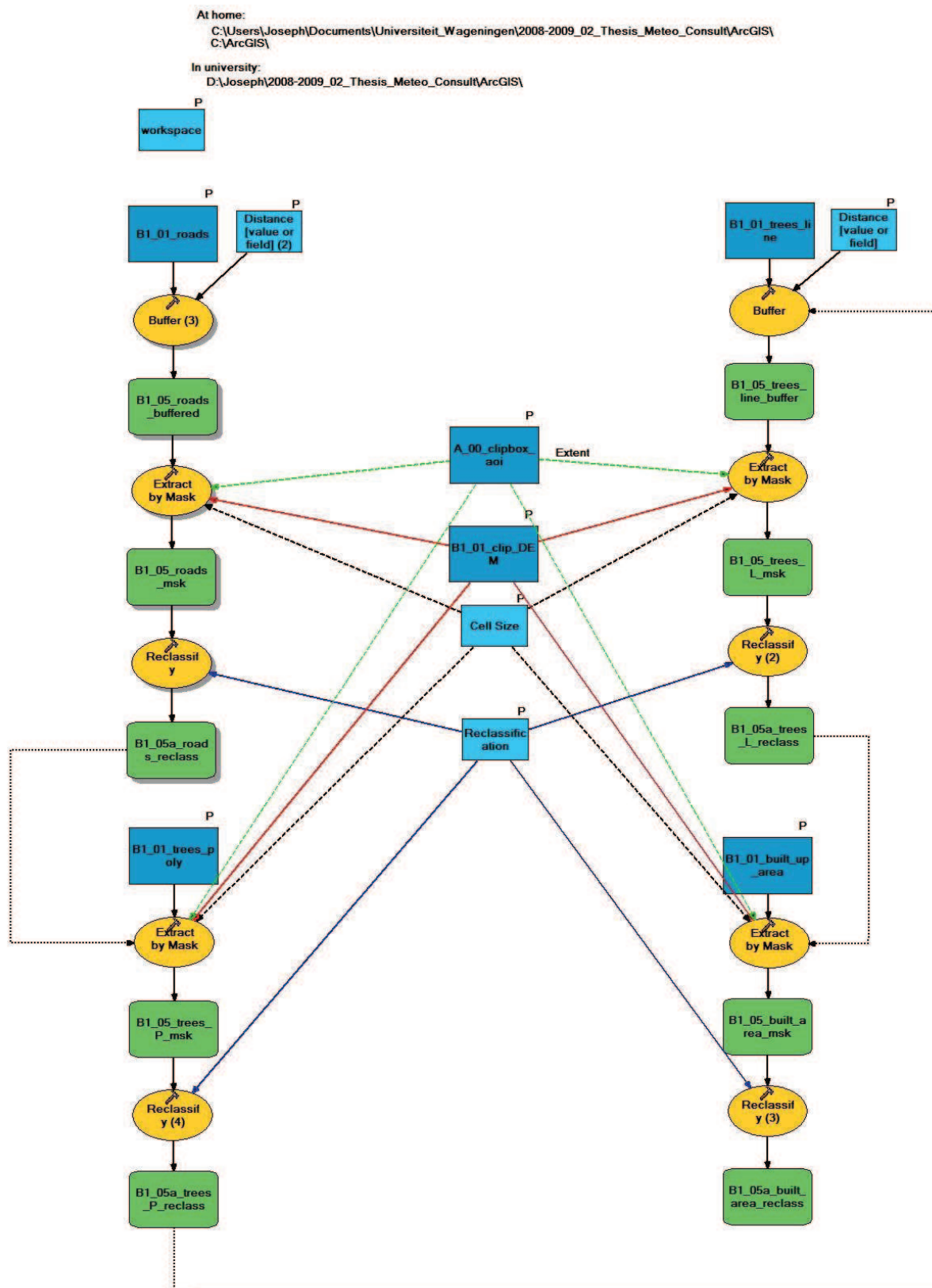
## 1.7: SVF\_B1\_01b\_select\_relevant\_data\_from\_top10\_data



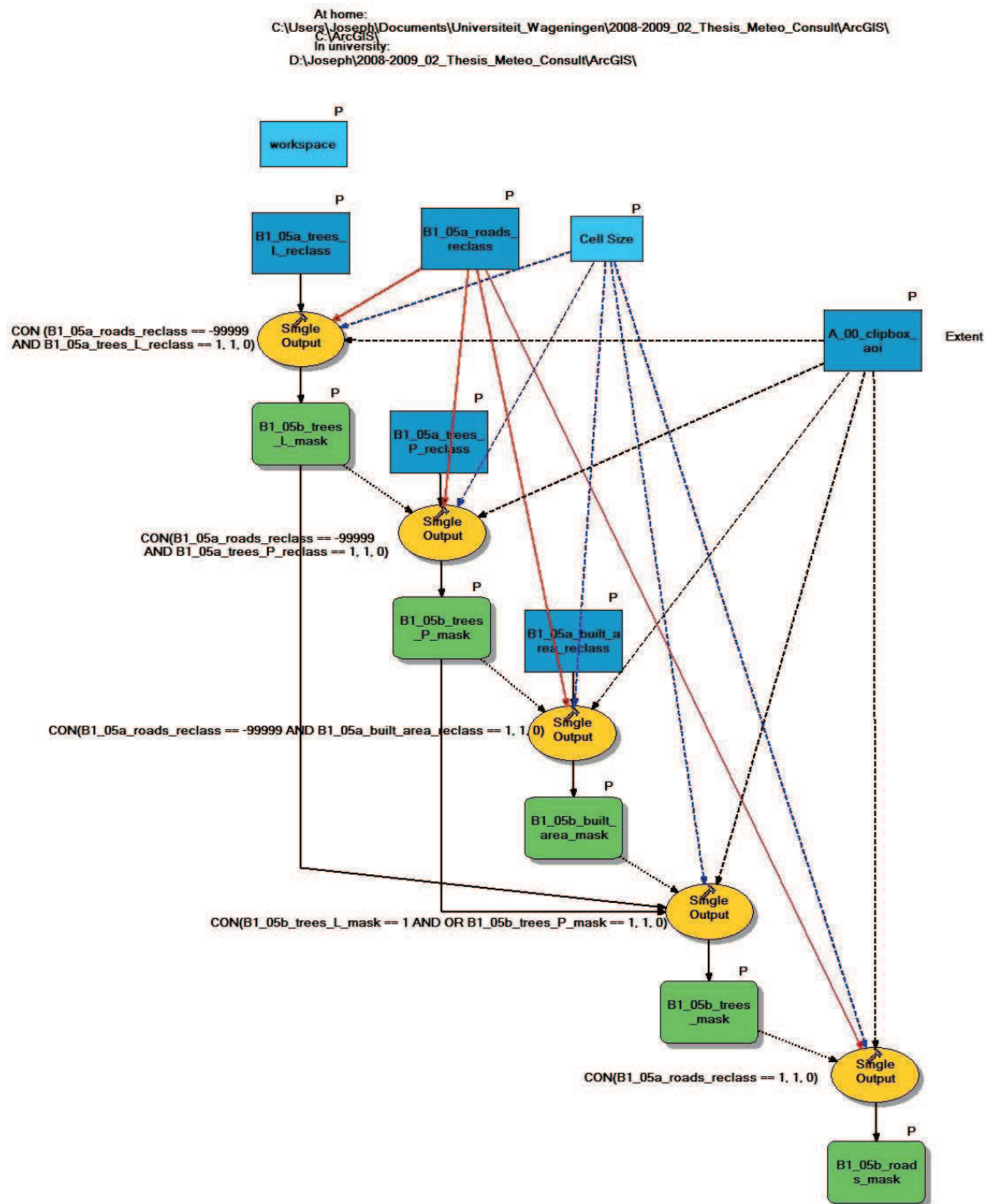
### 1.8: SVF\_B1\_02\_Create\_model\_sampling\_points



## 1.9: SVF\_B1\_05a\_create\_object\_masks\_for\_DEM

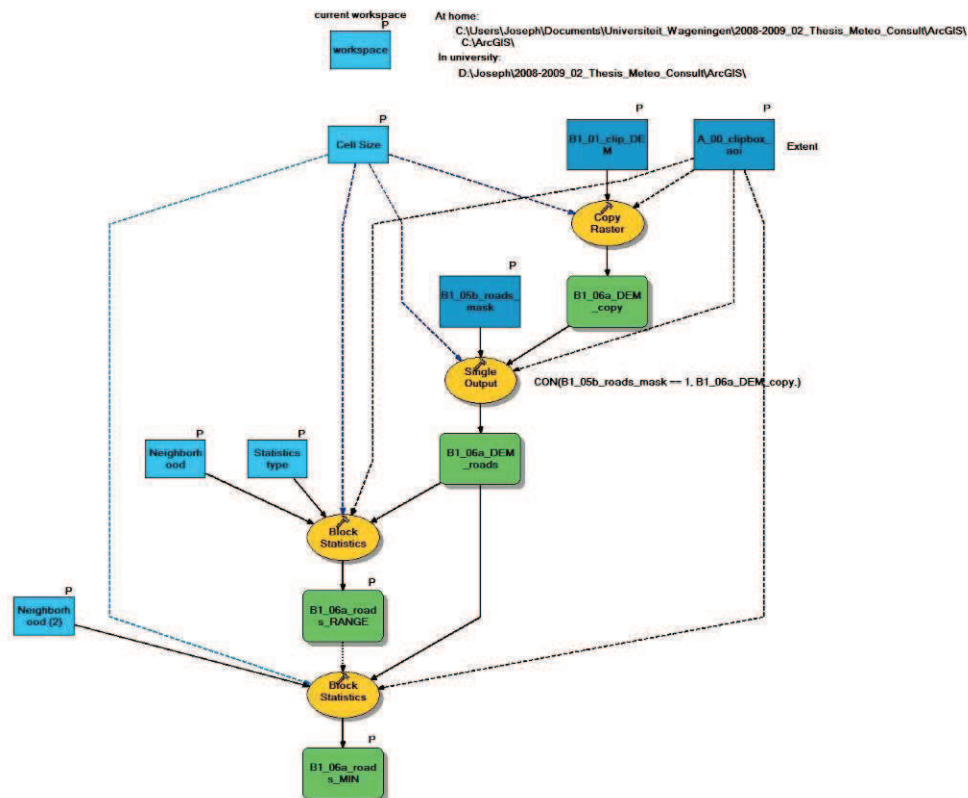


## 1.10: SVF\_B1\_05b\_remove\_road\_pixels\_from\_masks

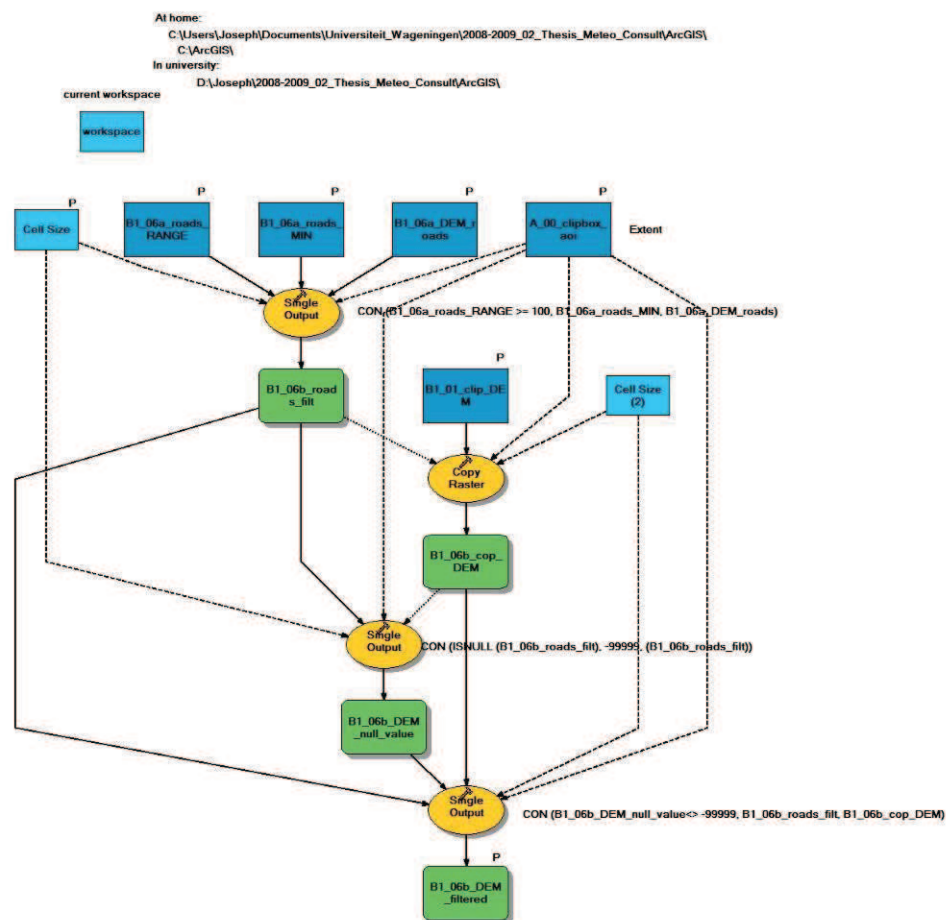




## 1.11: SVF\_B1\_06a\_filter\_trees\_from\_roads\_in\_DEM

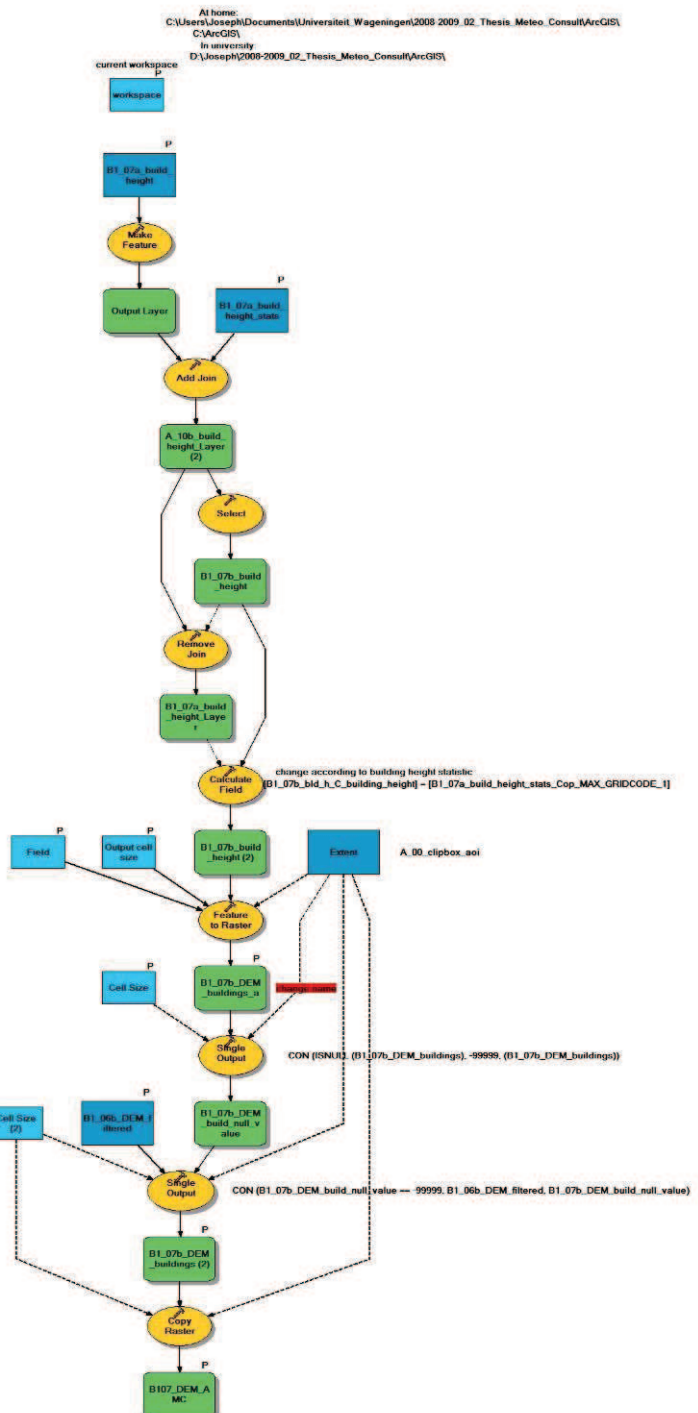
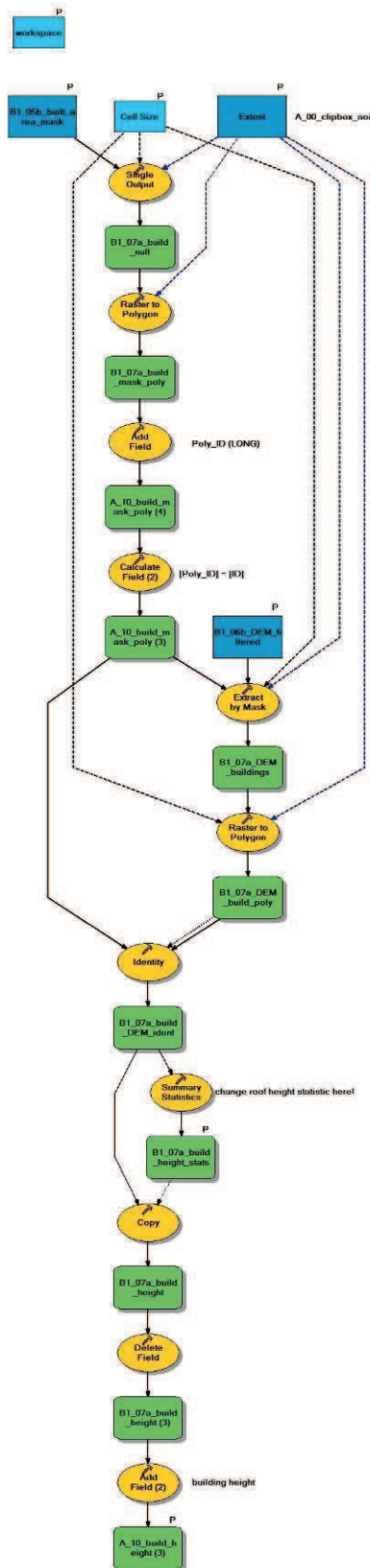


## SVF\_B1\_06b\_filter\_trees\_from\_roads\_in\_DEM

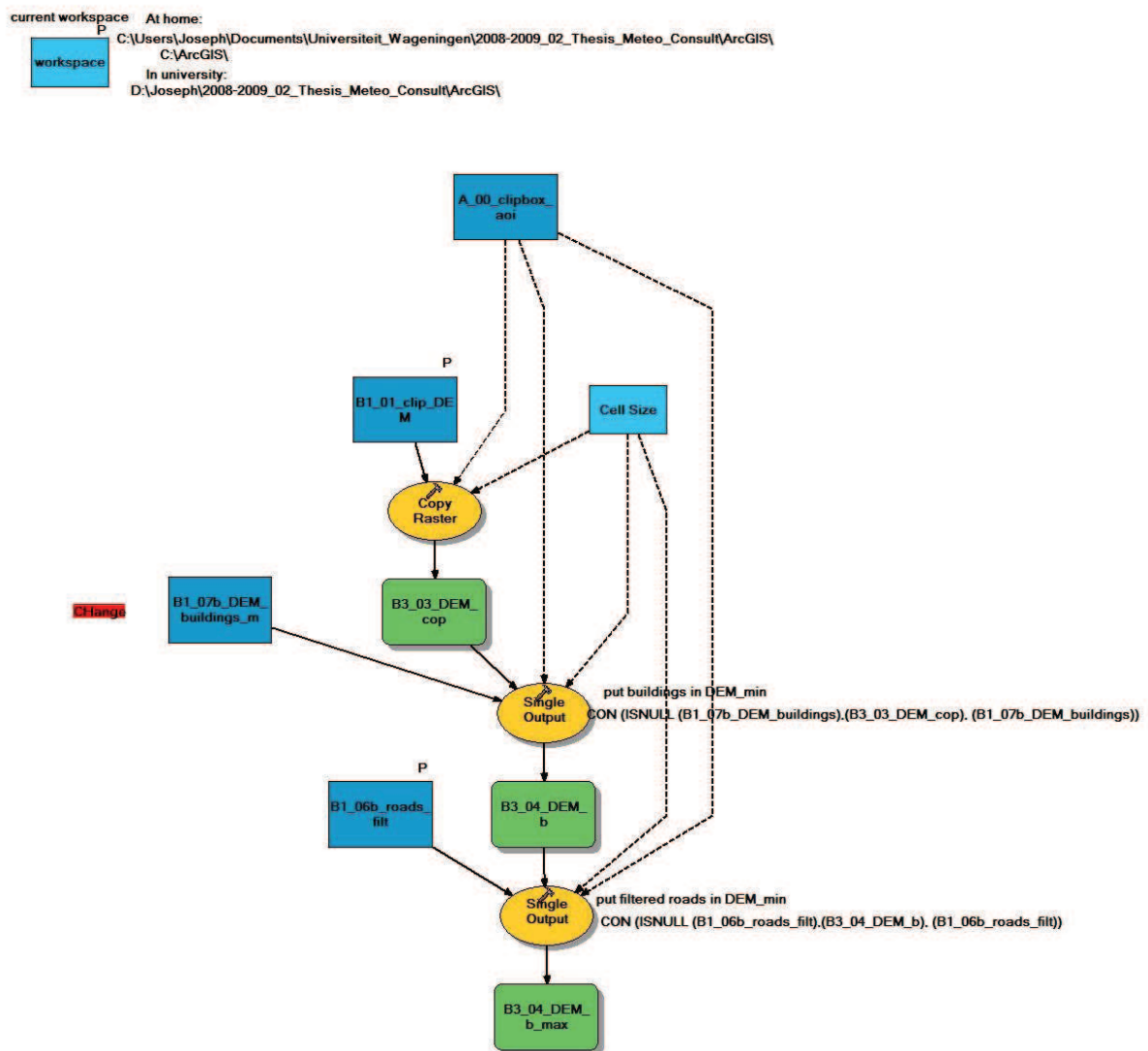


# 1.12: SVF\_B1\_07a\_model\_buildings\_in\_DEM (left) and SVF\_B1\_07b\_model\_buildings\_in\_DEM (right)

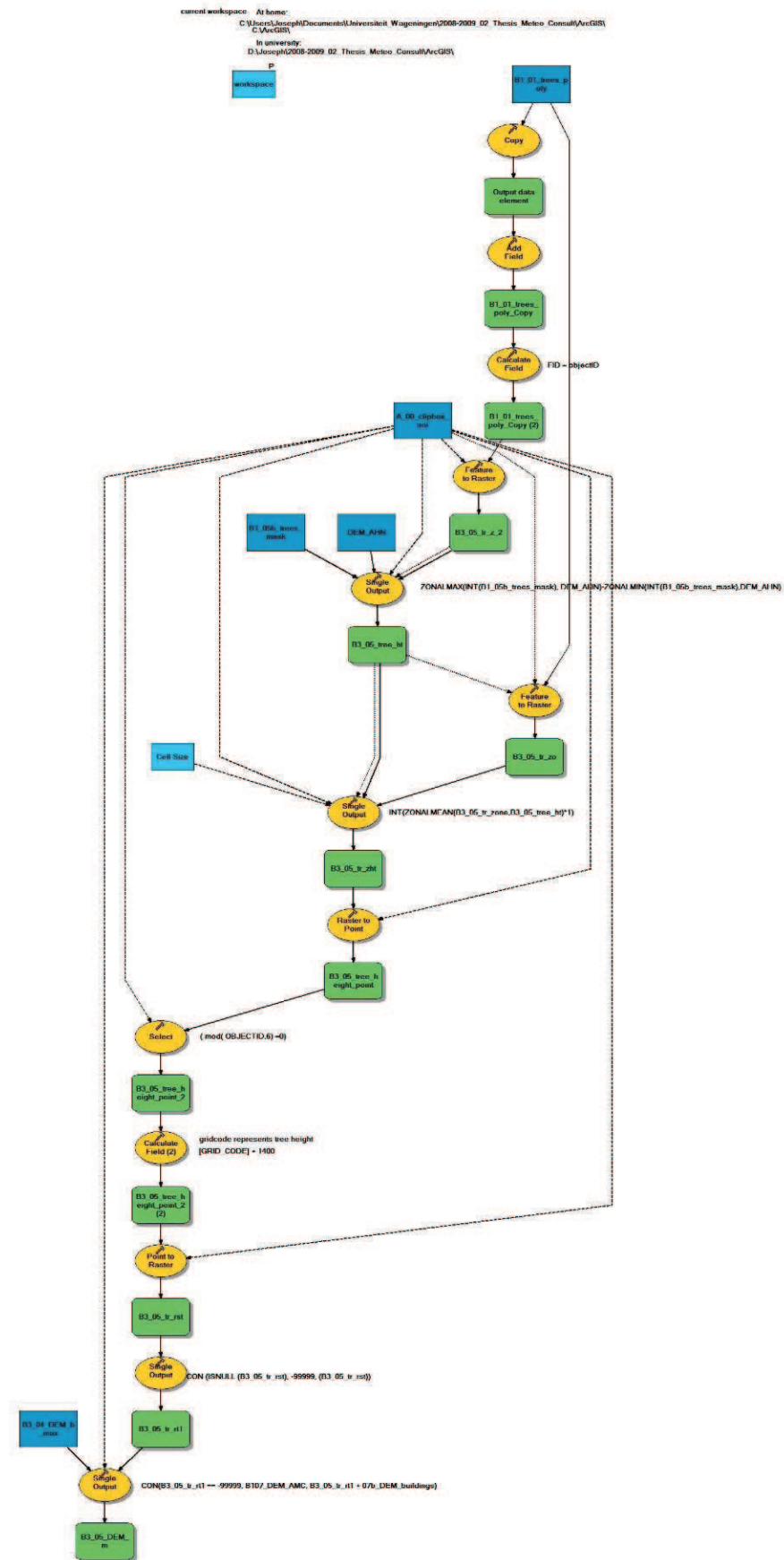
At home:  
C:\Users\Joseph\Documents\Universiteit Wageningen\2008-2009\_02\_Thesis\_Meteorology\ArcGIS\G (ArcGIS)  
current workspace:  
In university:  
D:\Joseph\2008-2009\_02\_Thesis\_Meteorology\ArcGIS\



### 1.13: SVF\_B3\_04\_create\_built\_up\_DEM



## 1.14: SVF\_B3\_05\_insert\_trees\_in\_DEM



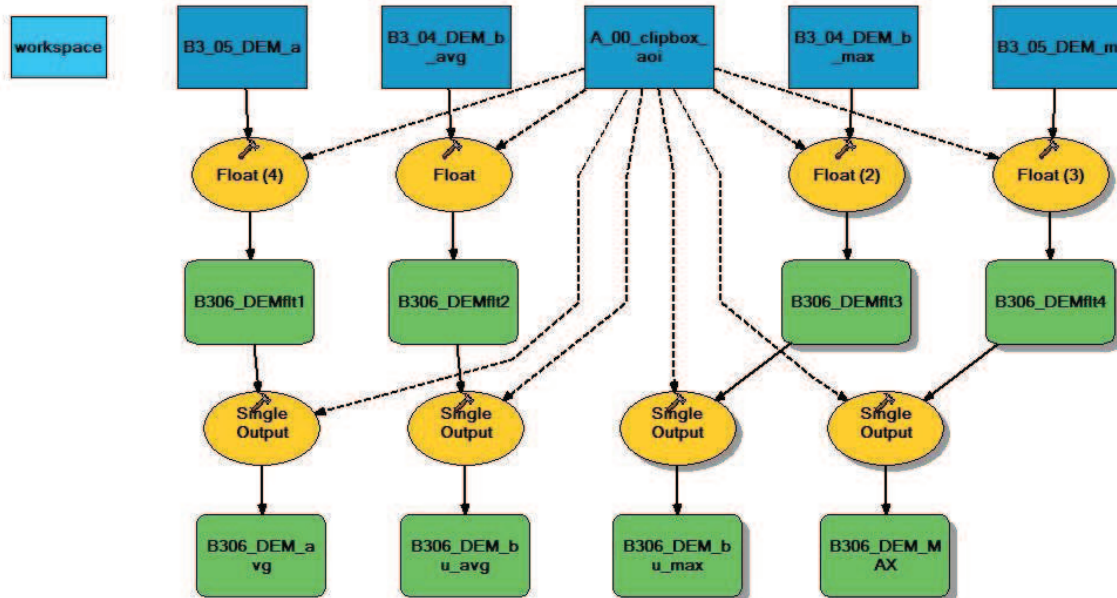
## SVF\_B3\_06\_create\_float\_DEM

current workspace At home:

C:\Users\Joseph\Documents\Universiteit Wageningen\2008-2009\_02\_Thesis\_Meteo\_Consult\ArcGIS\

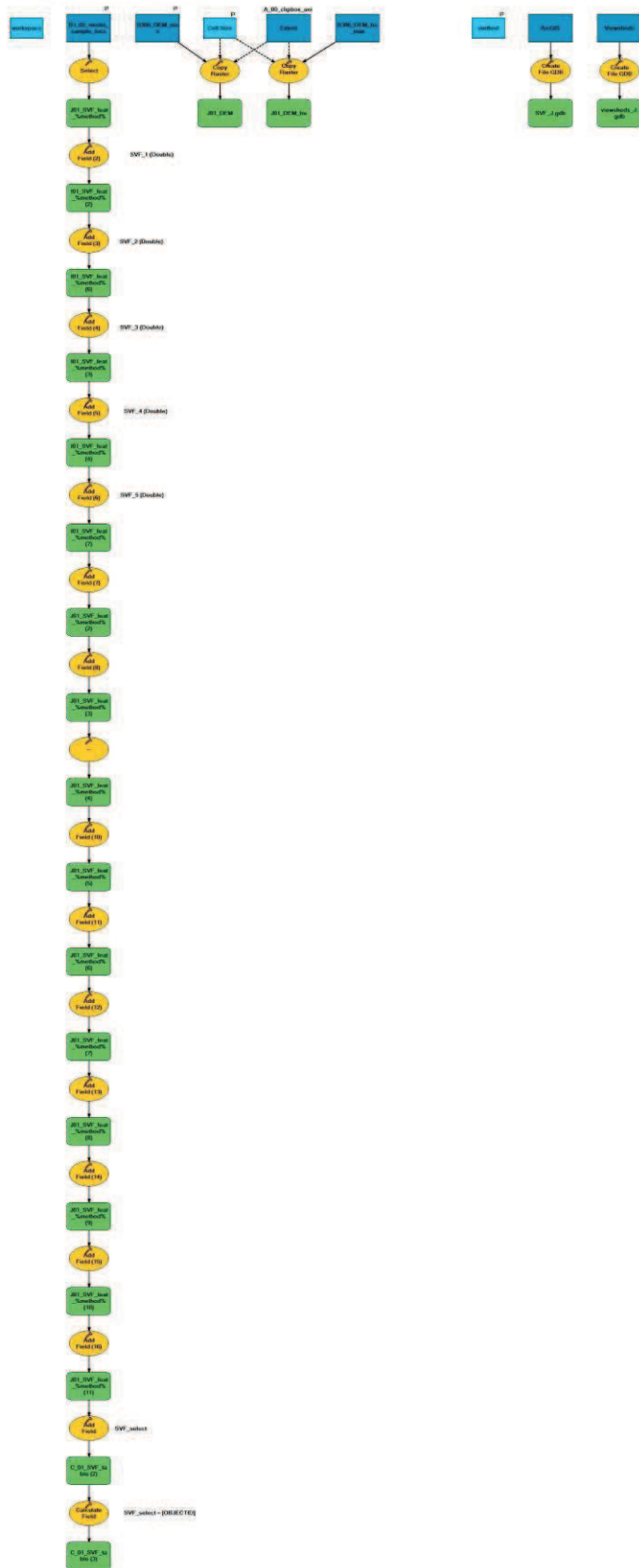
In university:

D:\Joseph\2008-2009\_02\_Thesis\_Meteo\_Consult\ArcGIS\



current workspace: At home  
C:\Users\Joseph\Documents\University\Wageningen\2008-2009\_S2\_Thesis\_Melroe\_Current\ArcGIS  
C:\ArcGIS

In university  
D:\Joseph\2008-2009\_S2\_Thesis\_Melroe\_Current\ArcGIS

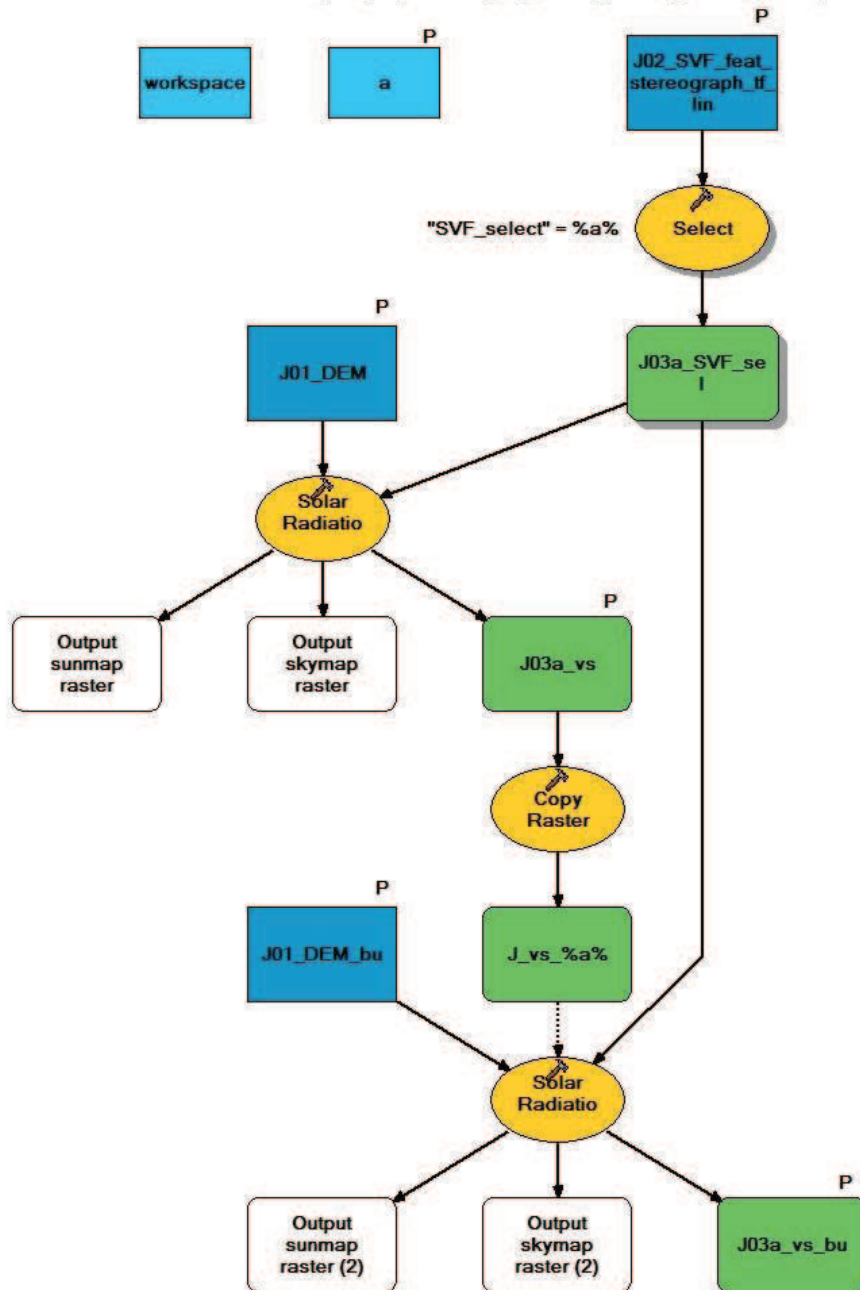




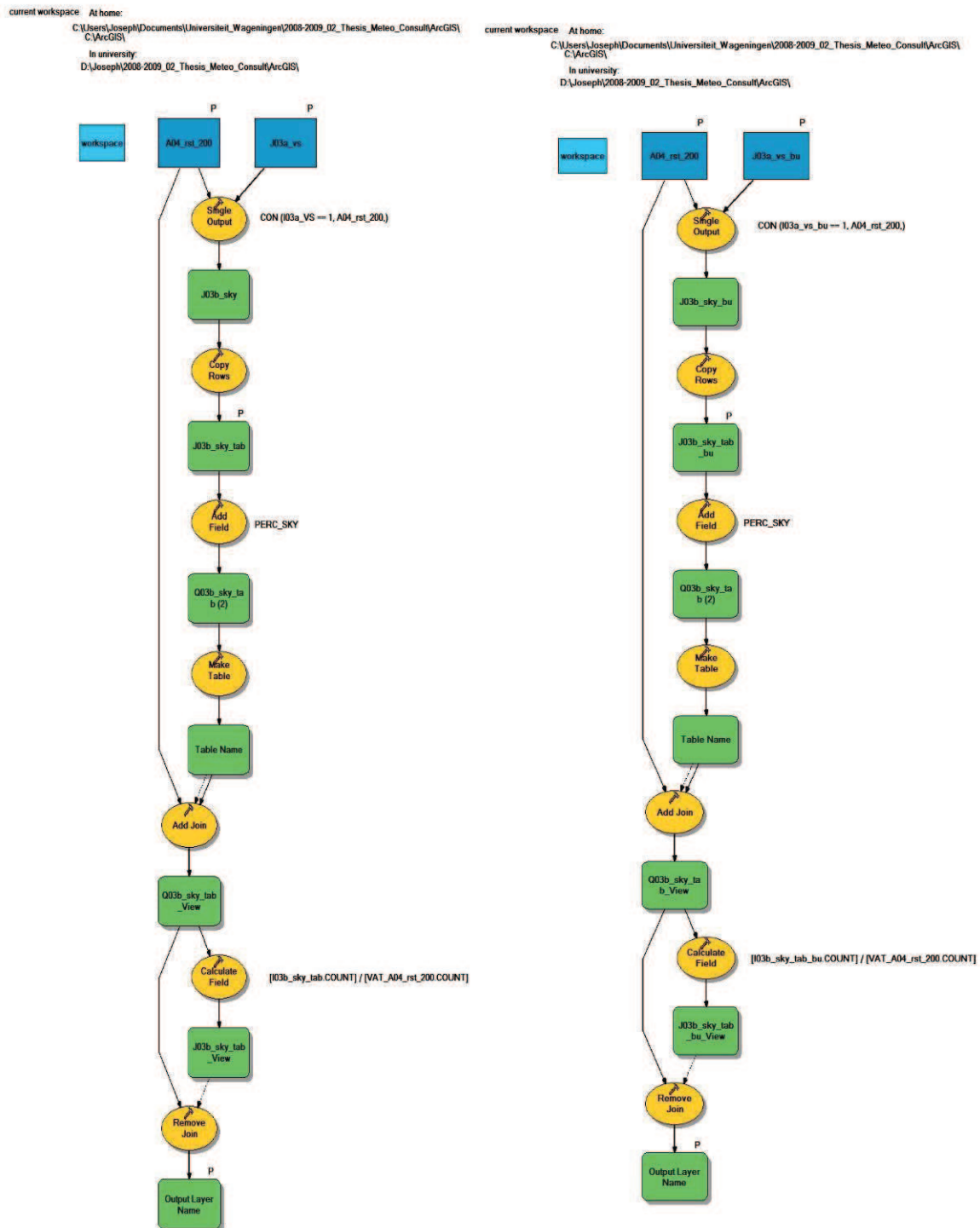
## 1.16: SVF\_J\_03a\_SVF\_computation\_create\_viewsheds

current workspace At home:  
C:\Users\Joseph\Documents\Universiteit Wageningen\2008-2009\_02\_Thesis\_Meteo\_Consult\ArcGIS\

In university:  
D:\Joseph\2008-2009\_02\_Thesis\_Meteo\_Consult\ArcGIS\

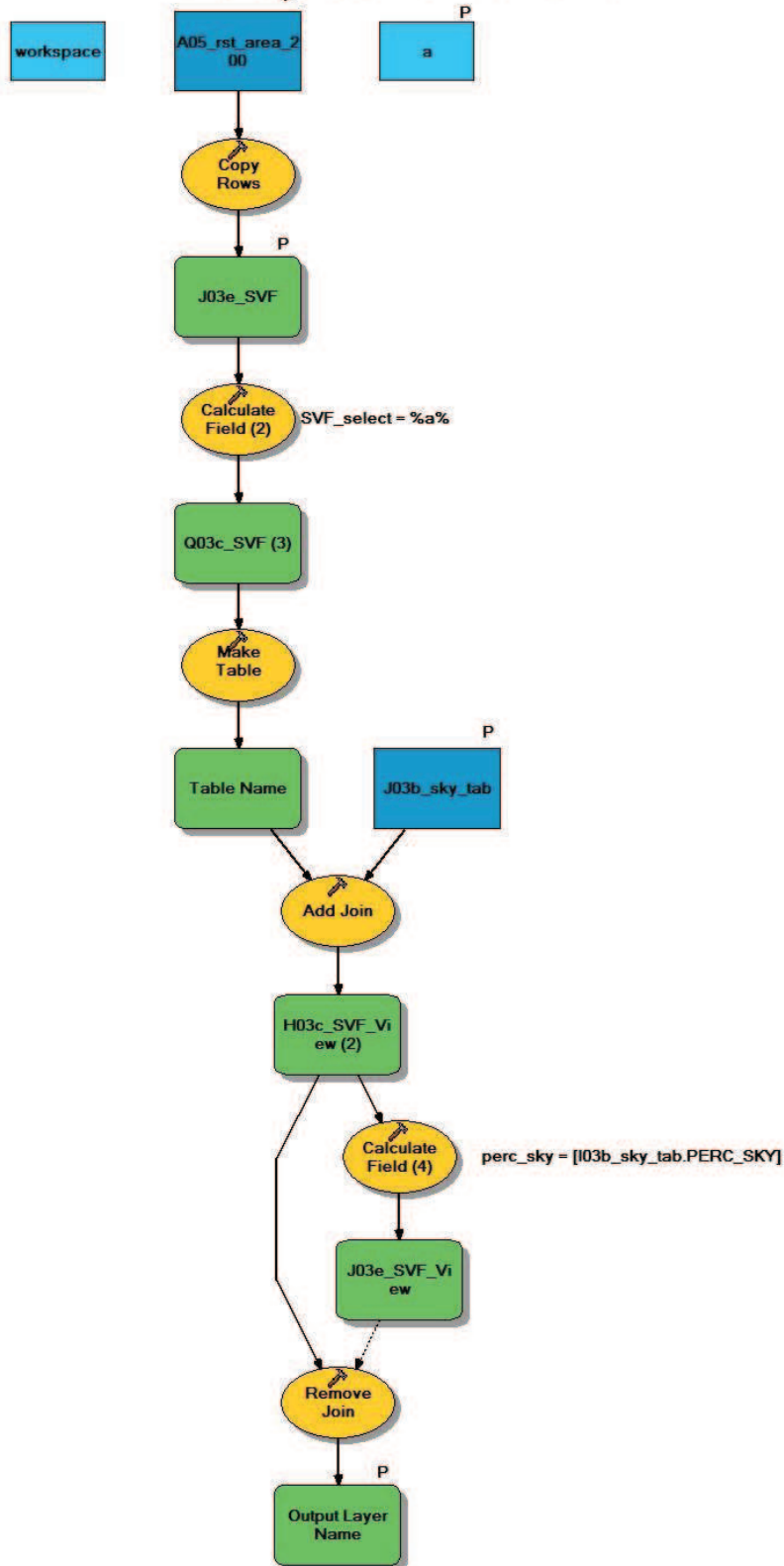


1.17: SVF\_J\_03b\_SVF\_computation\_compute\_sky\_area (left) and SVF\_J\_03c\_SVF\_computation\_compute\_extra\_sky\_area\_building\_method (right)



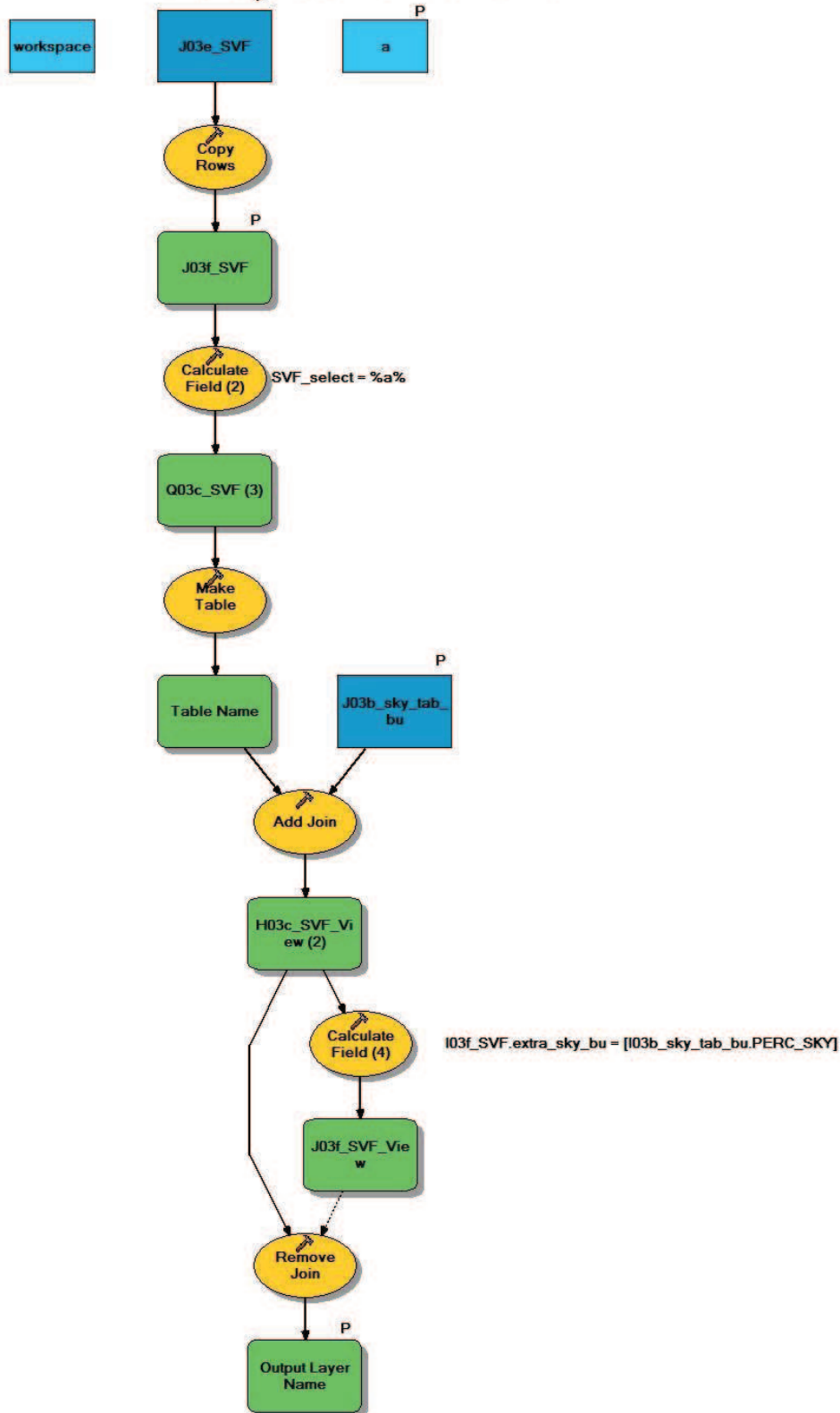
## 1.18: SVF\_J\_03e\_SVF\_computation\_compute\_SVF

current workspace At home:  
 C:\Users\Joseph\Documents\Universiteit Wageningen\2008-2009\_02\_Thesis\_Meteo\_Consult\ArcGIS\  
 C:\ArcGIS\  
 In university:  
 D:\Joseph\2008-2009\_02\_Thesis\_Meteo\_Consult\ArcGIS\  
 P

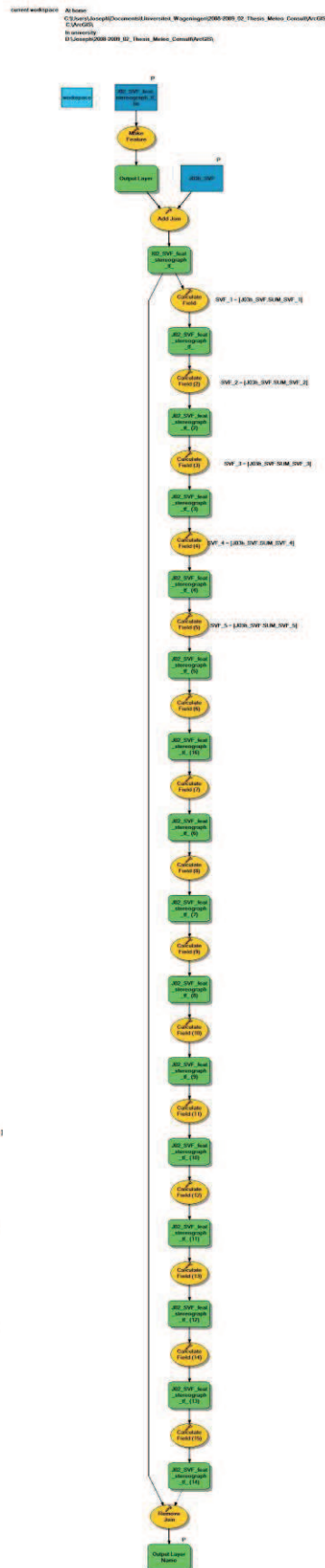
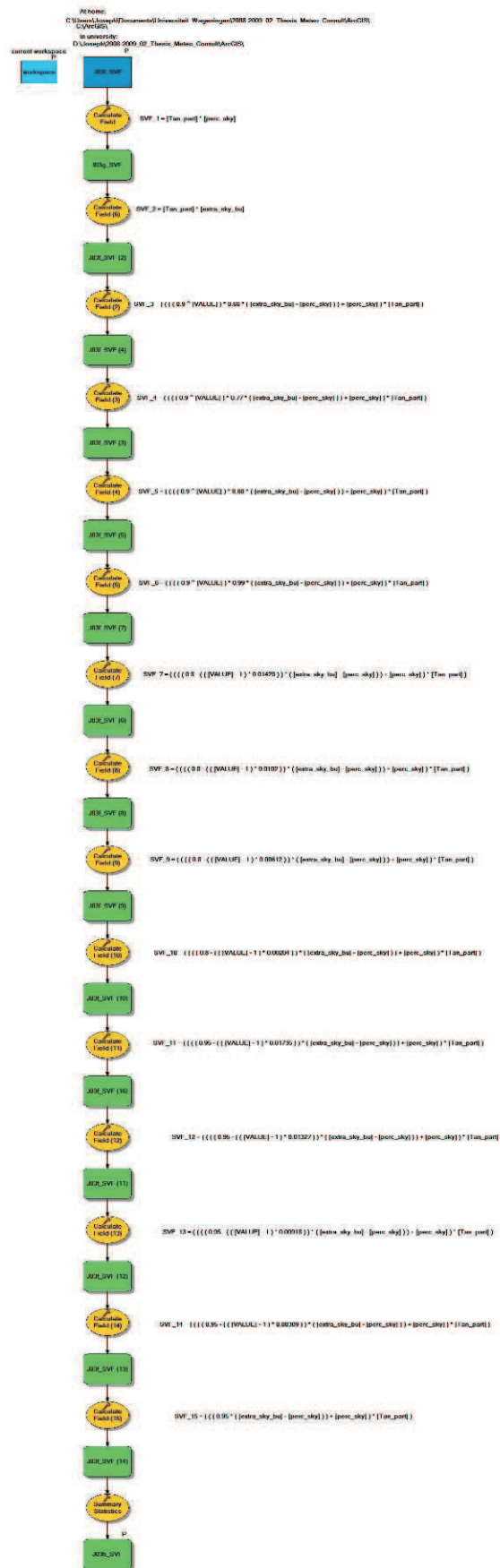


## SVF\_J\_03f\_SVF\_computation\_compute\_SVF

current workspace At home:  
 C:\Users\Joseph\Documents\Universiteit Wageningen\2008-2009\_02\_Thesis\_Meteo\_Consult\ArcGIS\  
 C:\ArcGIS\  
 In university:  
 D:\Joseph\2008-2009\_02\_Thesis\_Meteo\_Consult\ArcGIS\  
 P

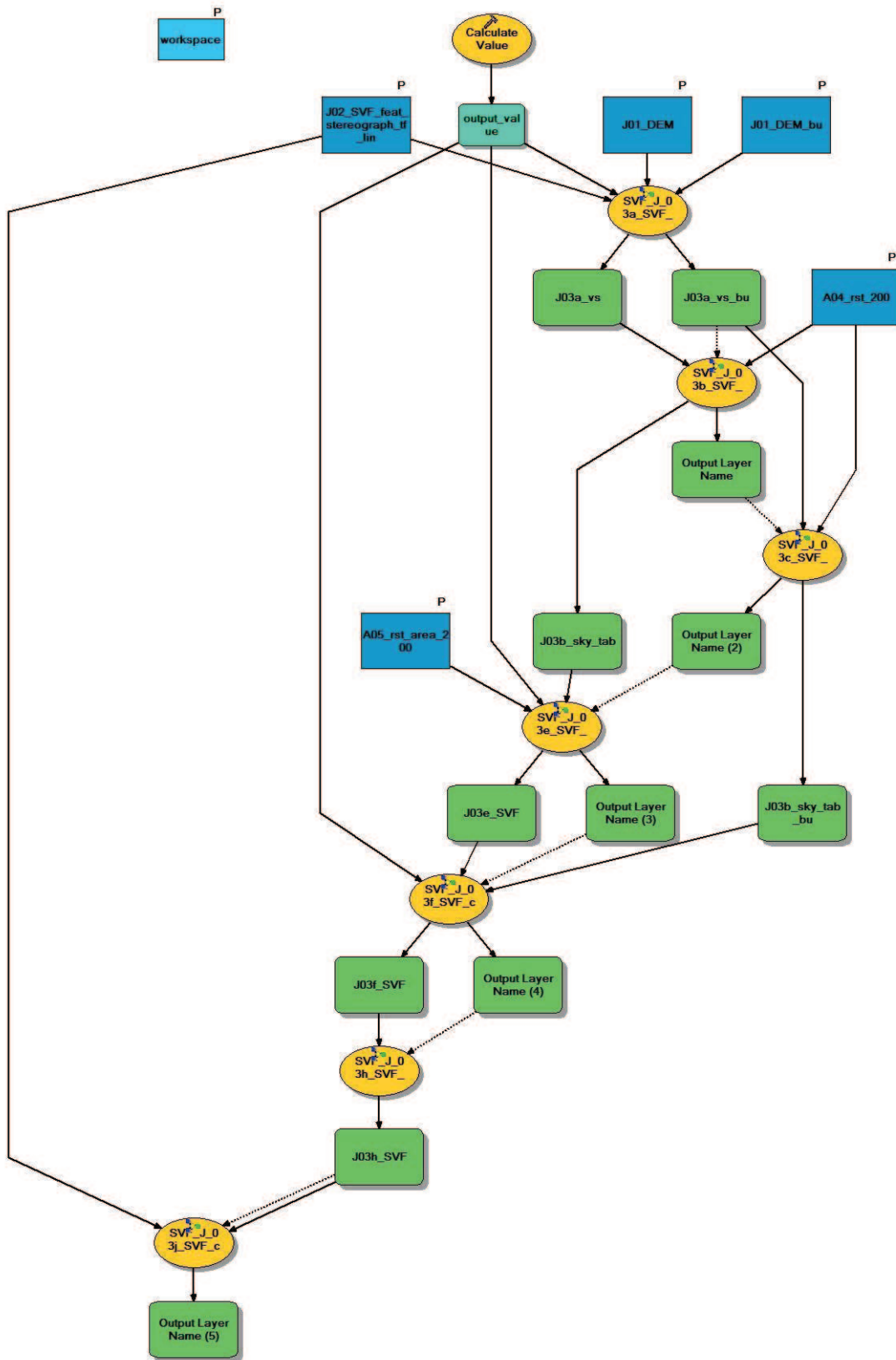


**1.19:** `SVF_J_03h_SVF_computation_compute_all_SVF` (left) and `SVF_J_03j_SVF_computation_add_SVF_to_SVF_feature` (right)



## SVF\_J\_03\_SVF\_computation\_full

current workspace    At home:  
C:\Users\Joseph\Documents\Universiteit Wageningen\2008-2009\_02\_Thesis\_Meteo\_Consult\ArcGIS\ C:\ArcGIS\  
In university:  
D:\Joseph\2008-2009\_02\_Thesis\_Meteo\_Consult\ArcGIS\





## Appendix 2: (TDN-) Code descriptions.

Table 6: Explanation capital letters in toolbox names.

Letter	Indicating:
A	general pre-processing
B	dataset specific pre-processing
C - Z <sup>12</sup>	computation of SVF, each toolset a different computational approach

Table 7: TDN codes used to select relevant information from TOP10vector dataset.

Mask	Selected TDN codes
Road mask	2002, 2203 - 3433, 3533 and 3903
Built-area mask	1000 – 1073, 1120 - 1800
Tree mask deciduous*	5000 – 5063, 5120 – 5131, 5223, 5233 and 5313
Tree mask coniferous	5053

\*In the tree mask used in this research, both deciduous and coniferous trees were selected. No distinction was made because no coniferous trees exist in the area of interest. The distinction can be easily made by excluding coniferous forest (TDN-code 5053) from the deciduous forest mask. For the meaning of the TDN codes in Table 7, see Table 8 (next page)

Mixed forest should be included in the deciduous forest mask, based on the 'better safe than sorry' approach. The ultimate goal of the network model is to predict where the road surface is going to be slippery. The higher the SVF, the higher the risk of slippery roads. In winter deciduous trees do not carry leaves and will therefore cause a higher SVF than equally proportioned coniferous trees. In order to be sure the SVF is not underestimated, mixed forest is added to the deciduous trees mask.

---

<sup>12</sup> Note: not all letters were used

Table 8: Meaning selected TDN-codes

<b>TDN-code</b>	<b>Meaning</b>	<b>TDN - code</b>	<b>Meaning</b>
1000	Building / House	3103	Road other recommendable route > 7m
1010	Built-on plot / Residential block	3142	Local metalled road > 7m
1013	Built-on plot / Residential block	3143	Local metalled road > 7m
1030	High-rise buildings	3202	Road other recommendable route > 4m
1040	Wall	3203	Road other recommendable route > 4m
1070	Department stores	3242	Local metalled road 4-7m
1073	Department stores	3243	Local metalled road 4-7m
1120	City Hall	3302	Local metalled road 2-4m
1370	purification plant / sewage treatment plant	3342	Local metalled road 2-4m
1700	Church without tower	3343	Local metalled road 2-4m
1780	Monument	3402	Other road > 2m
1800	Tower	3403	Other road > 2m
2002	Highway with separated lanes	3413	Partly metalled (tarmac) > 2m
2003	Highway with separated lanes	3432	Unmetalled road > 2m
2103	Highway > 7m	3433	Unmetalled road > 2m
2202	Motorway with separated lanes	3533	Street
2203	Motorway with separated lanes	3903	Car park
2302	Motorway > 7 meter	5000	Solitary Tree
2303	Motorway > 7 meter	5023	Deciduous forest
2342	Motorway with separated lanes	5053	Conifer (pine) forest
2343	Motorway with separated lanes	5063	Mixed forest
2403	Main road between 4-7 meter	5111	Hedge
2802	Main line road with 2 lanes	5120	Line of trees
2803	Main line road with 2 lanes	5121	Line of trees
2873	Main line road with 2 lanes	5131	Line of trees (double)
2903	Main line road > 7m	5223	Orchard
3002	Road other recommendable route with separated	5233	Tree nursery
3003	Road other recommendable route with separated	5313	Fruit tree nursery
3102	Road other recommendable route > 7m		

### Appendix 3: Equations used to compensate for tree transparency.

Table 9: Equations used in the GIS computations to compensate for transparency of the trees (tree filters). The attribute name column contains the name of the attribute which was used to store the SVF computation result in. [VALUE] = annulus number, [extra\_sky\_bu] = fraction of sky visible, based on DEM containing no trees, [perc\_sky] = fraction of visible sky based on full DEM, [Tan\_part] = result of part of SVF equation which can be computed without the need for input data (see paragraph General data pre-processing). SVF\_2 till SVF\_5 are exponential decrease of tree transparency from inner to outer annulus, SVF\_6 till SVF\_13 have a linear decrease of tree transparency from inner to outer annulus.

Attribute name	Equation used in GIS model	Percentage visible sky Inner annulus - outer annulus
SVF_1	$([perc\_sky]) * [Tan\_part]$	0 – 0
SVF_2	$([extra\_sky\_bu] * [Tan\_part])$	0 – 0
SVF_3	$(( ( ( ( 0.9 ^ [VALUE] ) * 0.66 * ([extra\_sky\_bu] - [perc\_sky]) ) ) + [perc\_sky]) * [Tan\_part])$	app. 60 – app. 0
SVF_4	$(( ( ( ( 0.9 ^ [VALUE] ) * 0.77 * ([extra\_sky\_bu] - [perc\_sky]) ) ) + [perc\_sky]) * [Tan\_part])$	app. 70 – app. 0
SVF_5	$(( ( ( ( 0.9 ^ [VALUE] ) * 0.88 * ([extra\_sky\_bu] - [perc\_sky]) ) ) + [perc\_sky]) * [Tan\_part])$	app. 80 – app. 0
SVF_6	$(( ( ( ( 0.9 ^ [VALUE] ) * 0.99 * ([extra\_sky\_bu] - [perc\_sky]) ) ) + [perc\_sky]) * [Tan\_part])$	app. 90 – app. 0
SVF_7	$(( ( ( 0.80 - (( [VALUE] - 1 ) * 0.01429 ) ) * ([extra\_sky\_bu] - [perc\_sky]) ) + [perc\_sky]) * [Tan\_part])$	80 – 10
SVF_8	$(( ( ( 0.80 - (( [VALUE] - 1 ) * 0.01020 ) ) * ([extra\_sky\_bu] - [perc\_sky]) ) + [perc\_sky]) * [Tan\_part])$	80 – 30
SVF_9	$(( ( ( 0.80 - (( [VALUE] - 1 ) * 0.00612 ) ) * ([extra\_sky\_bu] - [perc\_sky]) ) + [perc\_sky]) * [Tan\_part])$	80 – 50
SVF_10	$(( ( ( 0.80 - (( [VALUE] - 1 ) * 0.00204 ) ) * ([extra\_sky\_bu] - [perc\_sky]) ) + [perc\_sky]) * [Tan\_part])$	80 – 70
SVF_11	$(( ( ( 0.95 - (( [VALUE] - 1 ) * 0.01735 ) ) * ([extra\_sky\_bu] - [perc\_sky]) ) + [perc\_sky]) * [Tan\_part])$	95 – 10
SVF_12	$(( ( ( 0.95 - (( [VALUE] - 1 ) * 0.01327 ) ) * ([extra\_sky\_bu] - [perc\_sky]) ) + [perc\_sky]) * [Tan\_part])$	95 – 30
SVF_13	$(( ( ( 0.95 - (( [VALUE] - 1 ) * 0.00918 ) ) * ([extra\_sky\_bu] - [perc\_sky]) ) + [perc\_sky]) * [Tan\_part])$	95 – 50
SVF_14	$(( ( ( 0.95 - (( [VALUE] - 1 ) * 0.00306 ) ) * ([extra\_sky\_bu] - [perc\_sky]) ) + [perc\_sky]) * [Tan\_part])$	95 – 80
SVF_15	$(( ( 0.90 * ([extra\_sky\_bu] - [perc\_sky]) ) + [perc\_sky]) * [Tan\_part])$	90 – 90

## Appendix 4: Tree transparency curves

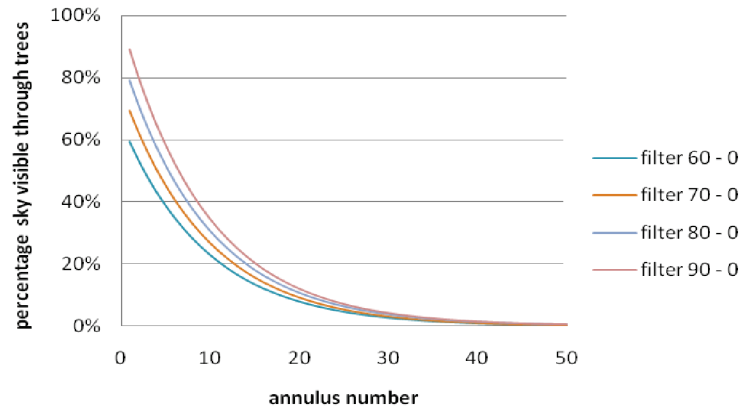


Figure 39: Exponential tree filters with percentage of visible sky ranging from 60 % - 90 % in the inner annulus and 0 % in the outer annulus.

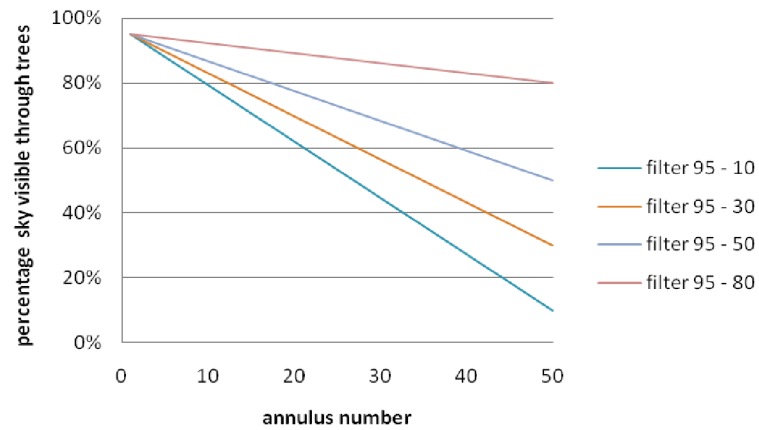


Figure 40: Linear tree filter with a percentage of 95 % of the sky visible through trees in the inner annulus and ranging from 10 % - 80 % in the outer annulus.

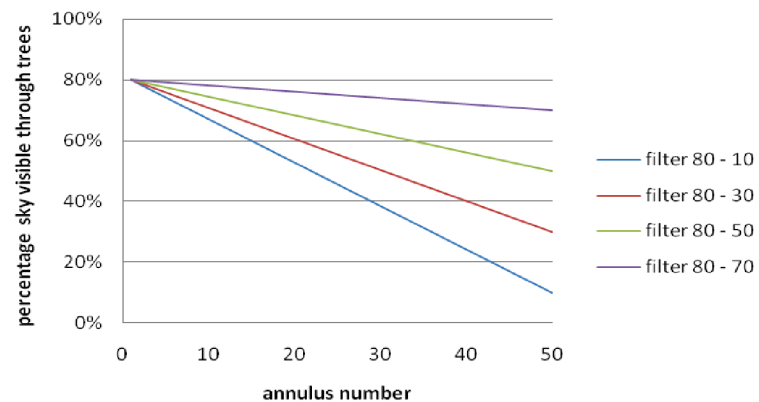


Figure 41: Linear tree filter with a percentage of 80 % of the sky visible through trees in the inner annulus and ranging from 10 % - 70 % in the outer annulus.

## Appendix 5: Scatterplots GIS SVF against reference SVF

Table 10: Scatterplots of the GIS SVF without the application of a tree filter against the reference SVF. The middle column contains the SVF based on trees with a maximum height of approximately 17 meter, the right column contains the SVF based on trees with a maximum height of approximately 20 meter. The first row contains the SVF computed at ground level, the second row the SVF computed 1.5 meter above ground level. Erroneous values of which the cause of the error could be explained were removed from the analysis (22-33 and 123-130), the trend line is forced through (0,0).

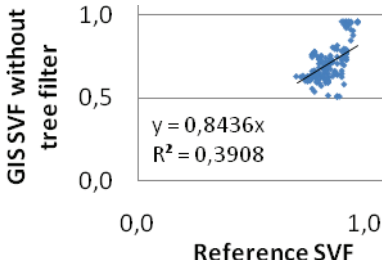
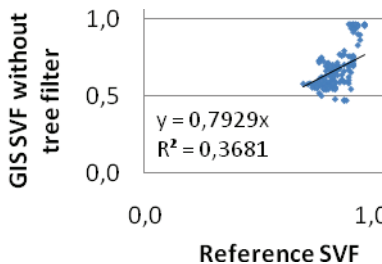
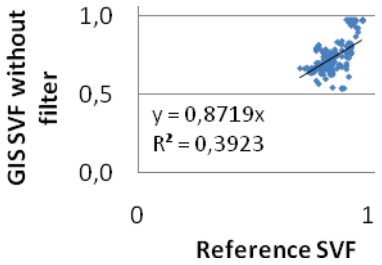
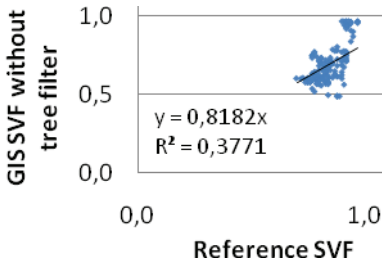
SVF computation height	Trees maximum 17 meter high	Trees maximum 20 meter high
Ground level	 <p>GIS SVF without tree filter</p> <p><math>y = 0,8436x</math> <math>R^2 = 0,3908</math></p> <p>Reference SVF</p>	 <p>GIS SVF without tree filter</p> <p><math>y = 0,7929x</math> <math>R^2 = 0,3681</math></p> <p>Reference SVF</p>
150 cm above ground level	 <p>GIS SVF without filter</p> <p><math>y = 0,8719x</math> <math>R^2 = 0,3923</math></p> <p>Reference SVF</p>	 <p>GIS SVF without tree filter</p> <p><math>y = 0,8182x</math> <math>R^2 = 0,3771</math></p> <p>Reference SVF</p>

Table 11: Comparison of the computed SVF based on a maximum tree height of approximately 17 meter, with the reference SVF. The GIS SVF is shown on the X-axes, the reference SVF on the Y-axis. The GIS SVF was computed at ground level (left column) and 1.5 meter above ground level (right column). Erroneous values of which the cause of the error could be explained were removed from the analysis (22-33 and 123-130), the trend line is forced through (0,0).

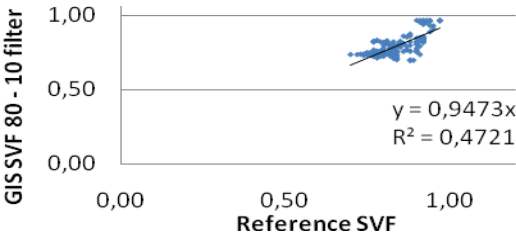

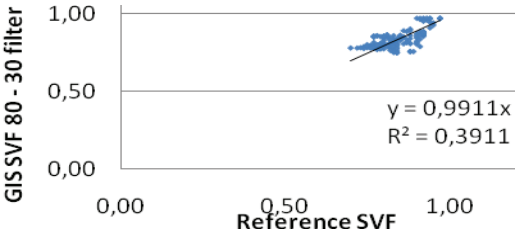
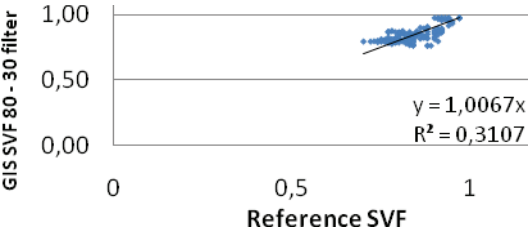
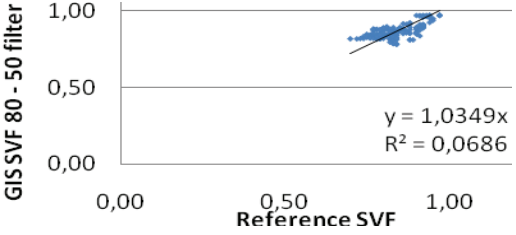
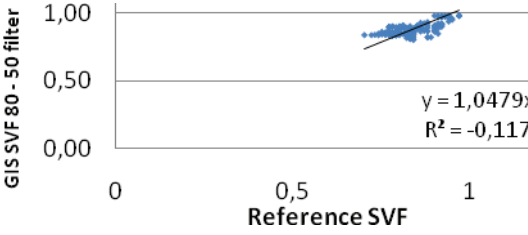
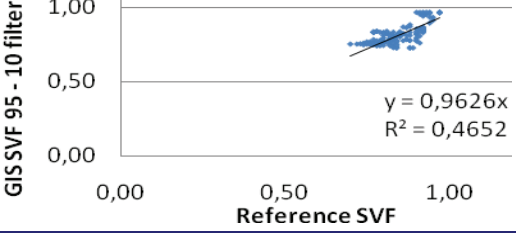
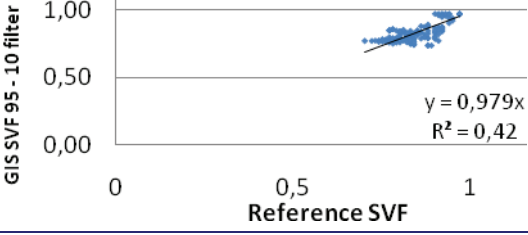
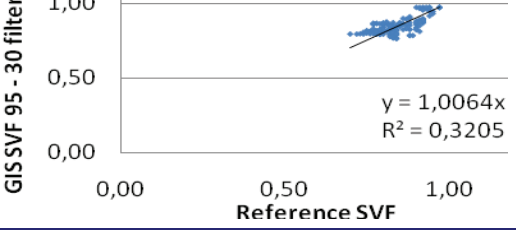
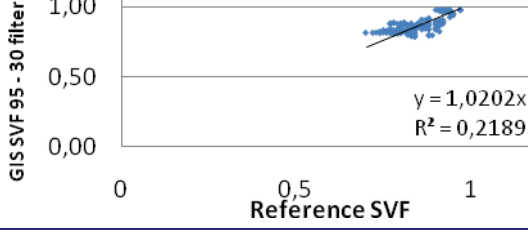
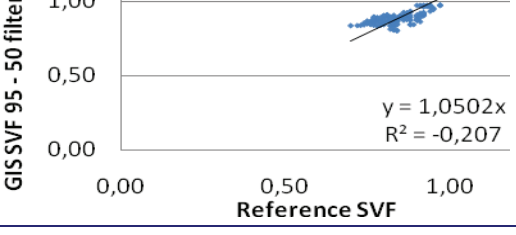
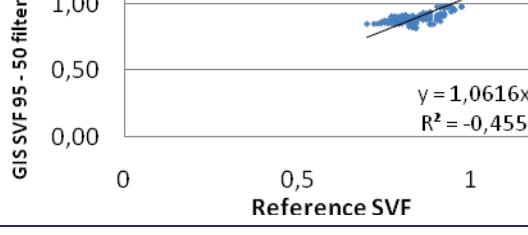
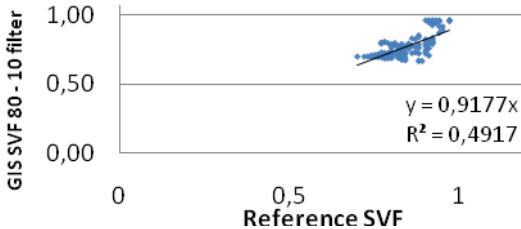
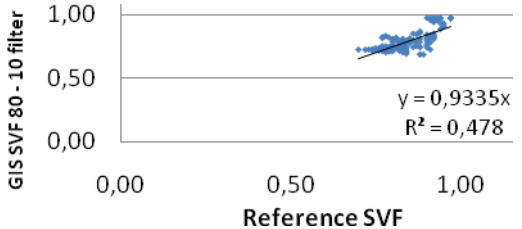
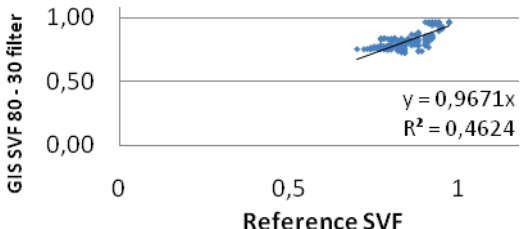
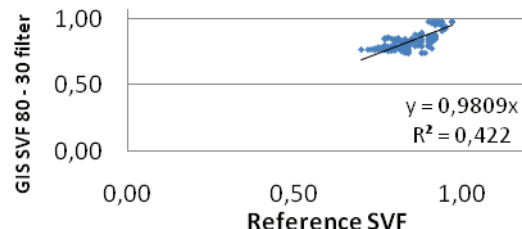

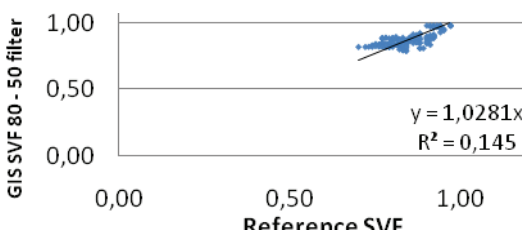

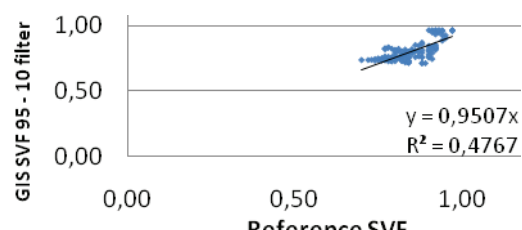

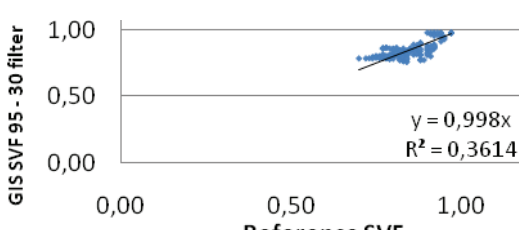
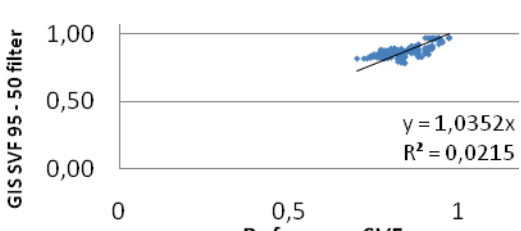
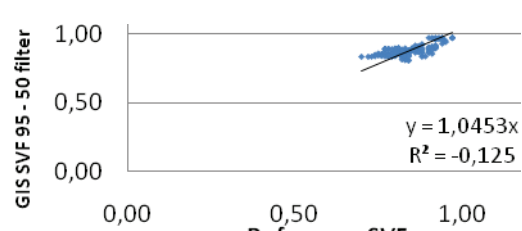
Tree height max 17 meter, ground level		Tree height max 17 meter, ground level + 1.5	
GIS SVF 80 - 10 filter		GIS SVF 80 - 10 filter	
GIS SVF 80 - 30 filter		GIS SVF 80 - 30 filter	
GIS SVF 80 - 50 filter		GIS SVF 80 - 50 filter	
GIS SVF 95 - 10 filter		GIS SVF 95 - 10 filter	
GIS SVF 95 - 30 filter		GIS SVF 95 - 30 filter	
GIS SVF 95 - 50 filter		GIS SVF 95 - 50 filter	



Table 12: Comparison of the computed SVF based on a maximum tree height of approximately 20 meter, with the reference SVF. The GIS SVF is shown on the X-axes, the reference SVF on the Y-axis. The GIS SVF was computed at ground level (left column) and 1.5 meter above ground level (right column). Erroneous values of which the cause of the error could be explained were removed from the analysis (22-33 and 123-130), the trend line is forced through (0,0).

Tree height max 20 meter, ground level		Tree height max 20 meter, ground level + 1.5	
GIS SVF	GIS SVF 80 - 10 filter		
	GIS SVF 80 - 30 filter		
	GIS SVF 80 - 50 filter		
	GIS SVF 95 - 10 filter		
	GIS SVF 95 - 30 filter		
	GIS SVF 95 - 50 filter		

## Appendix 6: SVF graphs linear filters

The four figures below show the full results of the GIS SVF computation. The first 2 graphs are based on a DEM containing trees with a maximum height of approximately 20 meter. The third and fourth graph are based on a maximum tree height of approximately 17 meter.

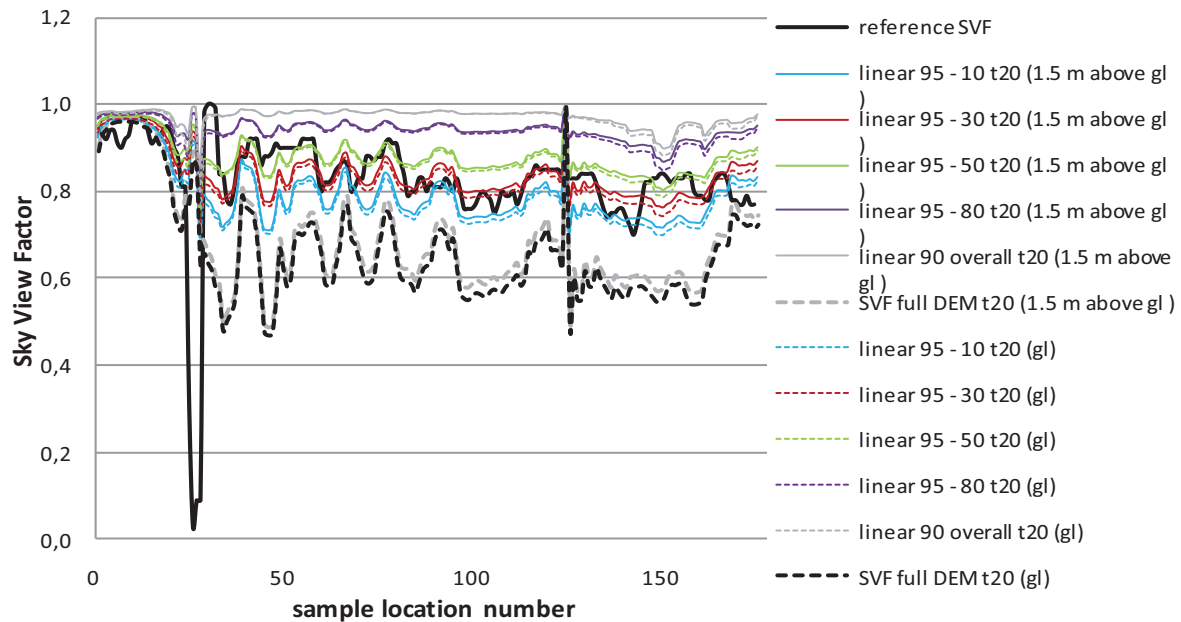


Figure 42: GIS SVF computed using the tree filters with a linear decrease in tree transparency from 95 % in the inner annulus to 10 % - 80 % in the outer annulus). Also, a tree filter with a 90 % tree transparency overall is included in this graph. The SVF was computed at 2 levels, ground level (gl) and 1.5 meter above ground level. The maximum tree height in the DEM used for these computations was approximately 20 meter (t20).

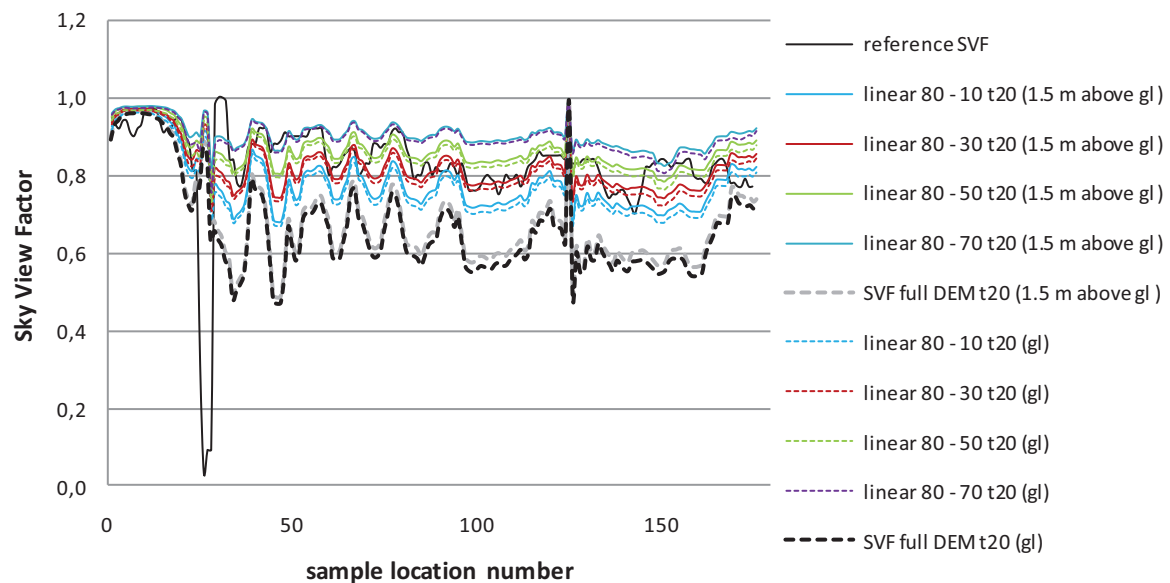


Figure 43: GIS SVF computed using the tree filters with a linear decrease in tree transparency from 80 % in the inner annulus to 10 % - 70 % in the outer annulus). The SVF was computed at 2 levels, ground level (gl) and 1.5 meter above ground level. The maximum tree height in the DEM used for these computations was approximately 20 meter (t20).

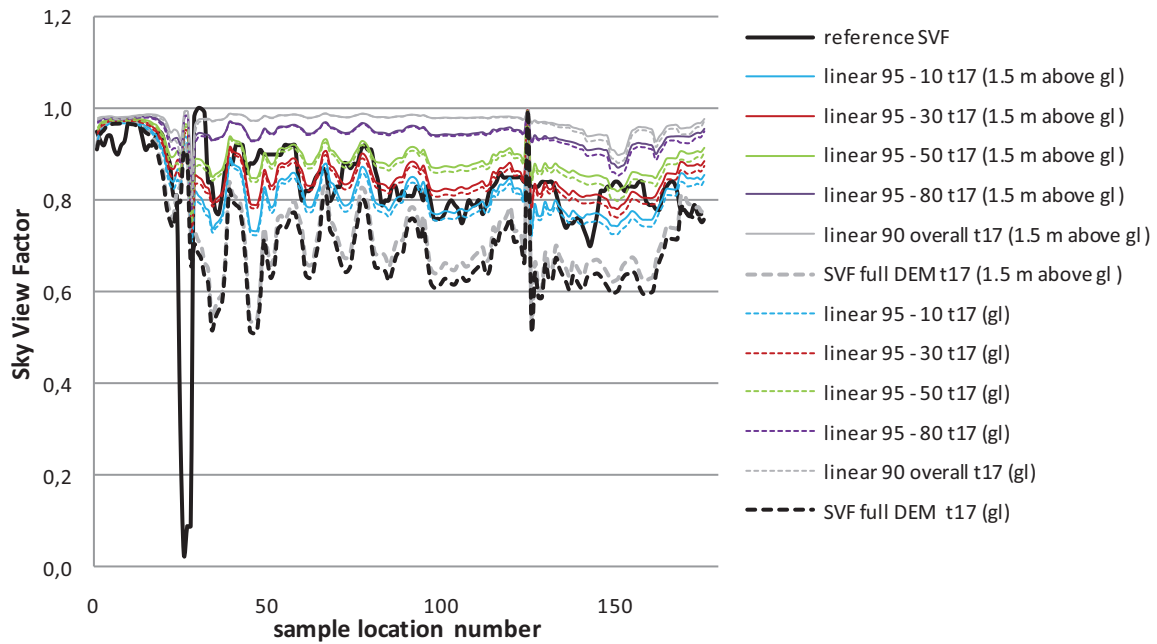


Figure 44: GIS SVF computed using the tree filters with a linear decrease in tree transparency from 95 % in the inner annulus to 10 % - 80 % in the outer annulus). Also, a tree filter with a 90 % tree transparency overall is included in this graph. The SVF was computed at 2 levels, ground level (gl) and 1.5 meter above ground level. The maximum tree height in the DEM used for these computations was approximately 17 meter (t17).

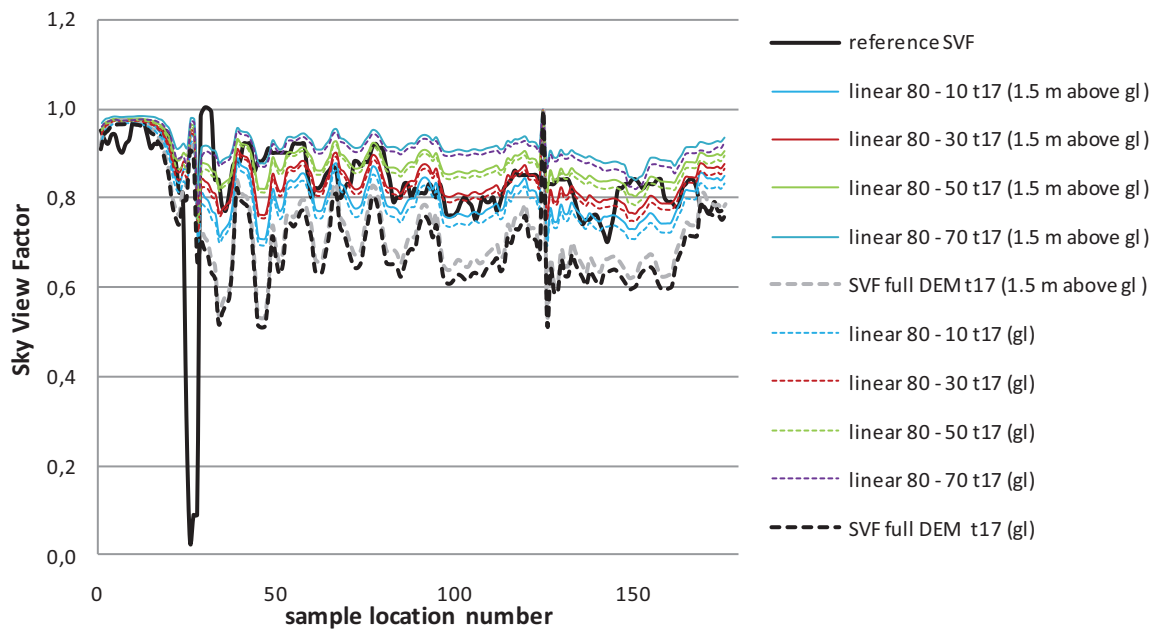
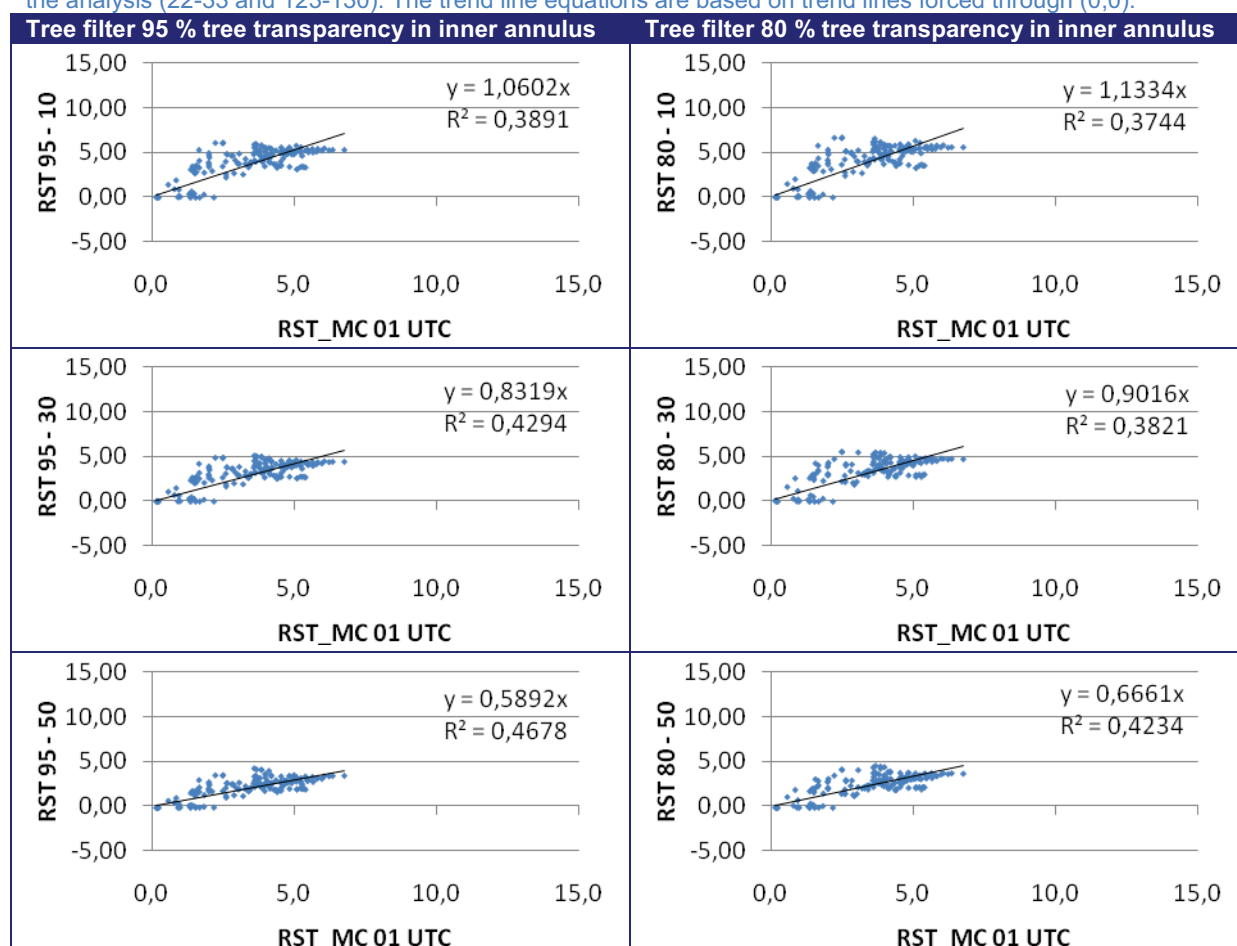


Figure 45: GIS SVF computed using the tree filters with a linear decrease in tree transparency from 80 % in the inner annulus to 10 % - 70 % in the outer annulus). The SVF was computed at 2 levels, ground level (gl) and 1.5 meter above ground level. The maximum tree height in the DEM used for these computations was approximately 17 meter (t17).

## Appendix 7: Scatterplots GIS-based RST forecast against reference SVF-based RST forecast.

Table 13: Scatterplots of the GIS-based RST forecast against the reference SV- based TST forecast for March 14<sup>th</sup>, 2007 01:00 UTC. Erroneous values of which the cause of the error could be explained were excluded from the analysis (22-33 and 123-130). The trend line equations are based on trend lines forced through (0,0).



## Appendix 8: Scatterplots RST forecast against measured RST.

Table 14: forecasted RST based on the GIS SVF plotted against the Actual RST measured between March 13<sup>th</sup> 23:00 UTC and March 14<sup>th</sup> 02:00 UTC. Erroneous values of which the cause of the error could be explained were excluded from the analysis (22-33 and 123-130). The trend line equations are based on trend lines forced through (0,0).

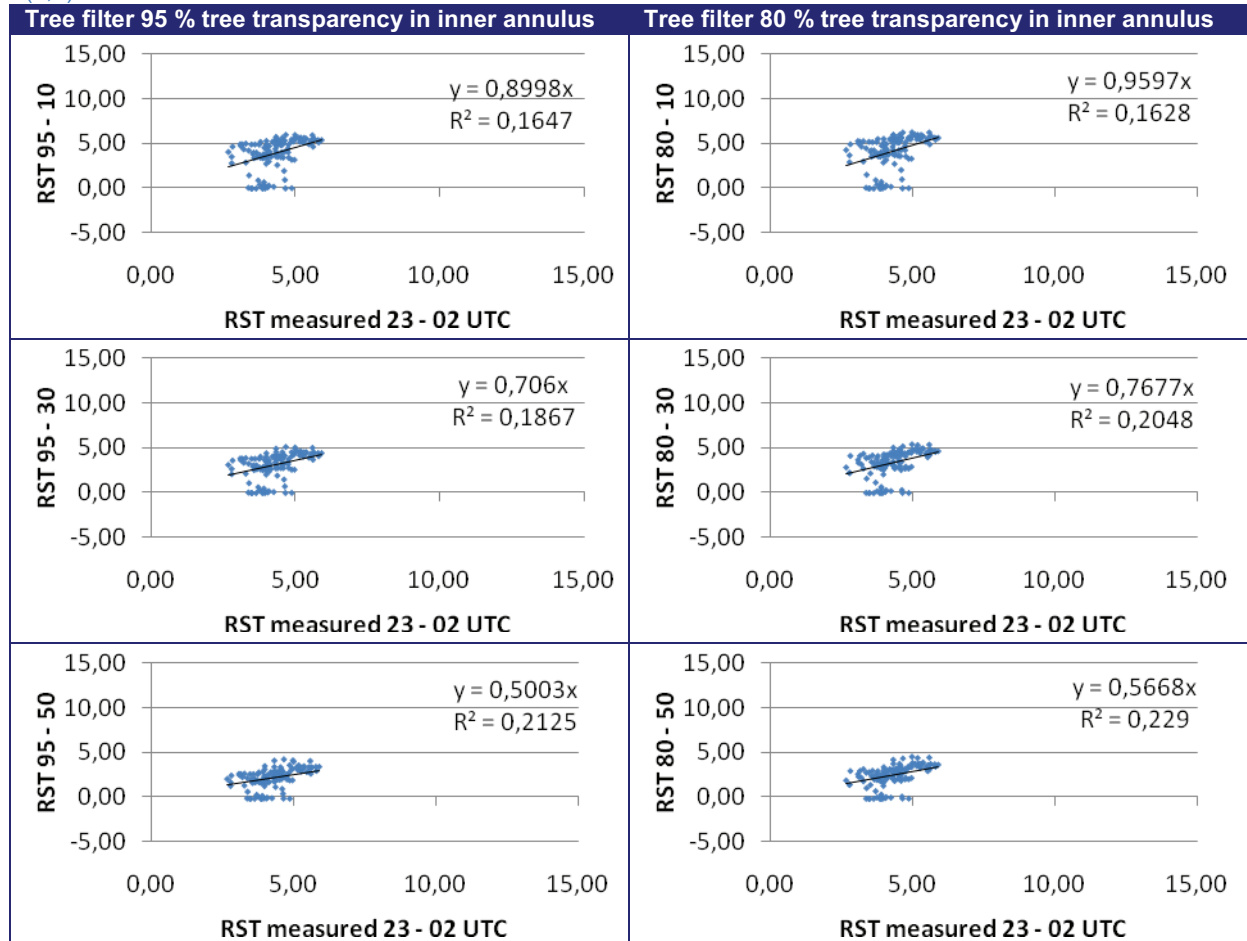
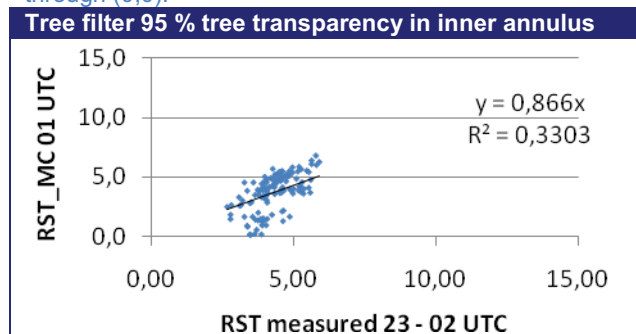


Table 15: forecasted RST based on the reference SVF plotted against the Actual RST measured between March 13<sup>th</sup> 23:00 UTC and March 14<sup>th</sup> 02:00 UTC. Erroneous values of which the cause of the error could be explained were excluded from the analysis (22-33 and 123-130). The trend line equations are based on trend lines forced through (0,0).



## Appendix 9: bug solar radiation graphics tool

The image on the next page (Figure 48) was created in order to demonstrate the current limitations of the Solar Radiation Graphics tool which was used to create the viewsheds. Depending on the number of computation directions and DEM complexity (see Figure 46) the output of this tool varies. During this research project, by coincidence a model run was executed using input raster DEM's with terrain height measured in centimetres.

In this case that resulted for example in trees which seemed to be 500 meter high. In certain situations, this led to erroneous viewsheds (see Figure 48). In case of 'simple' DEM geometry (see Figure 46) no problems occurred, but in more complex situations an increasing number of erroneous viewsheds was created.

As can be seen in Figure 48, using a 'simple' and 'moderately complex' DEM results in a usable viewshed regardless of the number of calculation directions which is used (although accuracy increases with the number of viewshed calculation directions used). The first viewshed in the column of viewsheds based on a DEM with a complex geometry shows an error.

Not only is the generated viewshed not a viewshed, the whole area is given the attribute value of visible air. If this result is used without inspection of the viewshed (e.g. during automated computations), the SVF computation would return a value of (approximately 1), whereas due to the complexity of the DEM actually a lower value (close to 0) would be expected.

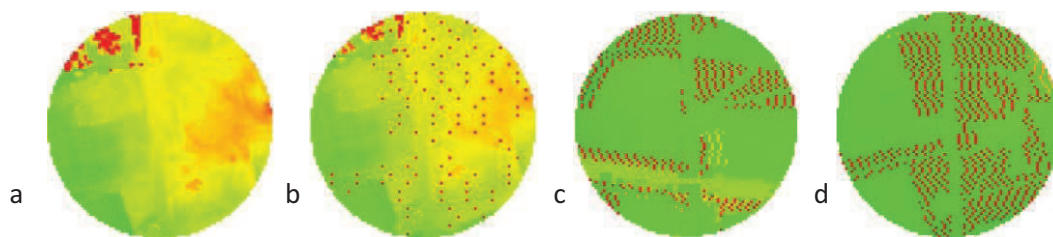


Figure 46: examples of DEM geometry complexity. Simple geometry (a), moderately complex geometry (b), complex geometry (c) and very complex geometry (d). The colour green indicates low terrain height and the colour red high terrain heights. In raster c and d, three height (red dots) was exaggerated for the purpose of demonstrating the limitations of the Solar Radiation Tool, tree height here is approximately 500 meter. These images were created based on the exact locations that were used to created the viewsheds in Figure 48.

This phenomena is even more obviously present at very complex geometries. For some unknown reason a usable viewshed is created using 280 and 320 calculation directions, whereas 360 calculation directions resulted in an erroneous viewshed. This error is also not an incidental random error, it consequentially occurs at the same locations every time the SVF computation procedure is repeated.

Another - often encountered - error within this model run, was the fact that some of the viewsheds contain spaces of invisible sky within the visible sky area (see Figure 47). The cause of this error is unknown. The consequence of this error is an underestimation of the actual SVF. In order to be able to actually notice this error during automated SVF computations, is to inspect every single viewshed visually.

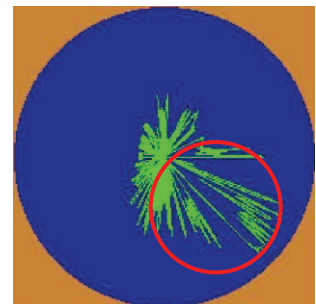


Figure 47: viewshed 89, showing a large part of invisible sky within the visible sky area.



Because the ultimate goal of Meteo Consult is to make the Network model applicable in all of Europe, the extent of these errors has to be researched to greater depth. Because although such extreme differences in terrain height as mentioned above might not exist in the Netherlands, in other large cities in Europe sky scrapers might be present, or roads in mountainous areas might be located at the bottom of a cliff or a ravine, thus creating potentially very large terrain height fluctuations over a short distance.

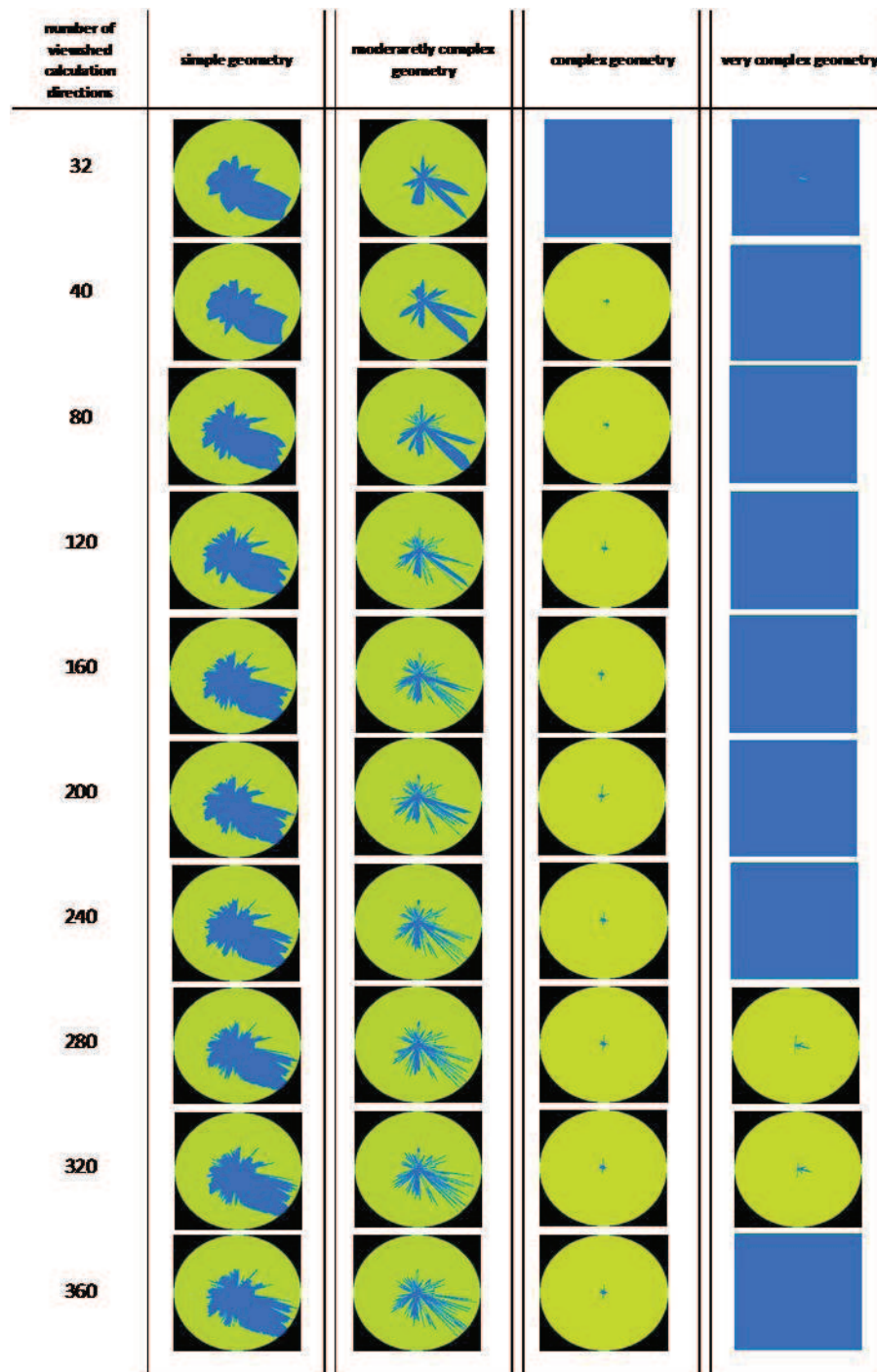


Figure 48: example of viewsheds created based on DEM's with different complexity (see Figure 46) and different number of computation directions. The circular area is the actual viewshed. Black colour indicates nodata, blue colour is visible part of the sky and green colour is the invisible part of the sky.